Study of the Ballistic Capabilities of a Tethered Satellite System

by

Jennifer Marie Grant

A thesis submitted to the Graduate Faculty of
Auburn University
in partial fulfillment of the
requirements for the Degree of
Master of Science

Auburn, Alabama
August 4, 2012

Approved by

David Cicci, Chair, Professor of Aerospace Engineering
Andrew Sinclair, Associate Professor of Aerospace Engineering
George Flowers, Professor of Mechanical Engineering and Dean of the Graduate School

Abstract

This thesis is an investigation into the ballistic capabilities of a Tethered Satellite System (TSS) when the sub-satellite is released from the system. This topic is of particular interest because TSS could be potentially used as threats, or weapons. There is a need to determine the velocity change or angular velocity that is required to cause a sub-satellite to enter an impact trajectory. Once the sub-satellite enters an impact trajectory, the ground range covered by the new trajectory and the time to impact are determined. A simple dumbbell model is used to represent the TSS in a dynamical simulation. Changes to the velocity of the system were introduced at release point in the orbit in order to cause the sub-satellite to enter an impact trajectory toward the Earth after release from the TSS. The parameters of the TSS that affect the impact trajectories are the altitude, tether length, and release point. A comparison is then done for changes in these parameters in order to determine the maximum and minimum ground range and time to impact for the various cases studied. An analytical solution is also developed to determine the maximum and minimum ranges when given a range of changes in velocity and to find the angular velocity and velocity change necessary for a given a set of initial conditions and desired impact trajectories.

Acknowledgments

I would like to thank my advisor, Dr. Cicci, for helping me to get through graduate school and complete this thesis. I would also like to thank Dr. Cicci and Dr. Gross for their support during the more stressful times of my college education. Without their support I might have given up due to all the ups and downs in life.

I would also like to thank my father, Richard K. Grant, for his continued support and his encouragement for me to pursue an engineering degree. I will always remember those late night calls where he is trying to help me solve homework problems, telling me that I can complete my thesis, and telling me to remember to relax and say a little prayer. I also appreciate the support my step-mother, Patty Caldwell Grant, gave me after she married my father.

Finally, I would like to dedicate this thesis to my mother, Maria T. Grant. She never got to see her daughter graduate with a Bachelor's degree in Aerospace Engineering and go after a Master's Degree in Aerospace Engineering; however, without her I would never have considered going for a Masters. Thanks to her I have followed my dreams and now they have come true.

Table of Contents

Abstract ii

Acknowledgments iii

List of Tables vii

List of Figures x

Nomenclature xv

1. Introduction 1

1.1 Historical Background 1

1.2 TSS Applications 5

1.3 Previous Research 7

1.4 Problem Description 13

2. Relevant Theory Used in TSS Analysis 16

2.1 Tethered Satellite System Dynamics 16

2.1.1 Equations of Motion 21

2.2 Attitude Dynamics Using Euler Parameters 23

2.3 Rigid Body Dynamics 26

2.4 Orbital Elements of a Trajectory 29

2.5 Numerical Integration Using a 4^{th} Order Runge Kutta 35

2.6 Analytical Approach 37

3: Model and Problem Formulation 39

3.1 Problem Set-up of the TSS 40

3.2 Changes Applied to the System to Create Impact of Sub-Satellite 50

3.3 Variations to the Problem Set-up 51

3.4 Analytical Solutions 53

3.4.1 Equations to Find the Range and Time to Impact 55

3.4.2 Algorithm to Find the Range and Time to Impact 59

3.4.3 Equations to Find the Velocity Change and Angular Velocity..... 64

3.4.4 Algorithm to Find the Velocity Change and Angular Velocity 66

4: Results for Analytical Solutions 68

4.1 Analytical Results for the Range and Time to Impact..... 68

4.1.1 Case A Results..... 69

4.1.2 Case B Results 72

4.1.3 Case C Results 75

4.1.4 Case D Results..... 78

4.2 Analytical Results for the Impulsive Velocity Change and the Angular Velocity . 80

4.2.1 Ground Range of 1500 km and $\nu_{imp} = 240°$..... 81

4.2.2 Ground Range of 3000 km and $\nu_{imp} = 240°$..... 87

5: Results for Numerical Integration Simulation 95

5.1 Results for First Configuration or Case 1 96

5.1.1 Impulsive Velocity Change of 1.0 km/s in the Positive Y - Direction 96

5.1.2 Impulsive Velocity Change of 1.0 km/s in the Positive Z - Direction..... 104

5.1.3 Impulsive Velocity Change of 3.0 km/s in the Negative Z - Direction ... 113

5.1.4 Comparison between Velocity Changes for First Configuration..... 121

5.2 Results for Second Configuration or Case 2 122

5.2.1 Impulsive Velocity Change of 1.0 km/s in the Positive Z- Direction..... 123

5.2.2 Impulsive Velocity Change of 1.5 km/s in the Negative Z - Direction ... 132

5.2.3 Impulsive Velocity Change of 1.0 km/s in the Positive Y - Direction 140

5.2.4 Comparison between Velocity Changes for Second Configuration 149

5.3 Comparison between the Analytical Results and the Simulation Results 150

6: Conclusions and Future Work 155

References 157

Appendix A: Sample Results from Numerical Integration 161

Appendix B: Sample Results from Analytical Solutions 164

List of Tables

Table 3.1: Sub-satellite Position Components for Cases A - D 54

Table 4.1: Minimum Impulsive Velocity Change Needed for Case A 70

Table 4.2: Maximum Ground Range and Time to Impact for Case A 71

Table 4.3: Minimum Ground Range and Time to Impact for Case A 71

Table 4.4: Minimum Impulsive Velocity Change Needed for Case B 74

Table 4.5: Maximum Ground Range and Time to Impact for Case B 74

Table 4.6: Minimum Ground Range and Time to Impact for Case B 75

Table 4.7: Minimum Impulsive Velocity Change Needed for Case C 77

Table 4.8: Maximum Ground Range and Time to Impact for Case C 77

Table 4.9: Minimum Ground Range and Time to Impact for Case C 77

Table 4.10: Minimum Impulsive Velocity Change Needed for Case D 79

Table 4.11: Maximum Ground Range and Time to Impact for Case D 80

Table 4.12: Minimum Ground Range and Time to Impact for Case D 80

Table 4.13: Impulsive Velocity Change and Angular Velocity for Case A and B at Three Altitudes When R = 1500 km and θ_{imp} = 270° 83

Table 4.14: Impulsive Velocity Change and Angular Velocity for Case A and B at Three Tether Lengths When R = 1500 km and θ_{imp} = 270° 85

Table 4.15: Impulsive Velocity Change and Angular Velocity for Case C and D at Three Altitudes When R = 1500 km and θ_{imp} = 270° 86

Table 4.16: Impulsive Velocity Change and Angular Velocity for Case C and D at Three Tether Lengths When R = 1500 km and θ_{imp} = 270° 87

Table 4.17: Impulsive Velocity Change and Angular Velocity for Case A and B at Three Altitudes When R = 3000 km and θ_{imp} = 270° 89

Table 4.18: Impulsive Velocity Change and Angular Velocity for Case A and B at Three Tether Lengths When R = 3000 km and θ_{imp} = 270° 91

Table 4.19: Impulsive Velocity Change and Angular Velocity for Case C and D at Three Altitudes When R = 3000 km and θ_{imp} = 270° 92

Table 4.20: ImpulsiveVelocity Change and Angular Velocity for Case C and D at Three Tether Lengths When R = 3000 km and θ_{imp} = 270° 94

Table 5.1: Impulsive Velocity Changes for Case 1 96

Table 5.2: Range and Impact Time for $\Delta V_{1y} = 1.0$ km/s at Three Altitudes for Case 1 97

Table 5.3: Range and Impact Time for $\Delta V_{1y} = 1.0$ km/s at Three Tether Lengths for Case 1 101

Table 5.4: Maximum and Minimum Values as $+\Delta V_{1y}$ Increases for Case 1 104

Table 5.5: Range and Impact Time for $\Delta V_{1z} = 1.0$ km/s at Three Altitudes for Case 1 106

Table 5.6: Range and Impact for $\Delta V_{1z} = 1.0$ km/s at Three Tether Lengths for Case 1 109

Table 5.7: Maximum and Minimum Values as $+\Delta V_{1z}$ Increases for Case 1 113

Table 5.8: Range and Impact Time for $\Delta V_{1z} = -3.0$ km/s at Three Altitudes Case 1 114

Table 5.9: Range and Impact Time for $\Delta V_{1z} = -3.0$ km/s at Three Tether Lengths for Case 1 118

Table 5.10: Maximum and Minimum Values as $-\Delta V_{1z}$ Increases for Case 1 121

Table 5.11: Impulsive Velocity Changes for Case 2 123

Table 5.12: Range and Impact Time for $\Delta V_{1z} = 1.0$ km/s at Three Altitudes for Case 2 125

Table 5.13: Range and Impact Time for $\Delta V_{1z} = 1.0$ km/s at Three Tether Lengths for Case 2 128

Table 5.14: Maximum and Minimum Values as $+\Delta V_{1z}$ Increases for Case 2 132

Table 5.15: Range and Impact Time for $\Delta V_{1z} = -1.5$ km/s at Three Altitudes for Case 2 133

Table 5.16: Range and Impact Time for $\Delta V_{1z} = -1.5$ km/s at Three Tether Lengths for Case 2 137

Table 5.17: Maximum and Minimum Values as $-\Delta V_{1z}$ Increases for Case 2 140

Table 5.18: Range and Impact Time for $\Delta V_{1y} = 1.0$ km/s at Three Altitudes for Case 2..... 141

Table 5.19: Range and Impact Time for $\Delta V_{1y} = 1.0$ km/s at Three Tether Lengths for Case 2 145

Table 5.20: Maximum and Minimum Values as $+\Delta V_{1y}$ Increases for Case 2 148

Table 5.21: Results for Configuration 1 and Case B with $\Delta V_{1y} = 1.0$ km/s..... 150

Table 5.22: Comparison of Results for Configuration 1 and Case B with $\Delta V_{1y} = 1.0$ km/s... 151

Table 5.23: Results for Configuration 1 and Case B with $\Delta V_{1y} = 6.0$ km/s..... 151

Table 5.24: Comparison of Results for Configuration 1 and Case B with $\Delta V_{1y} = 6.0$ km/s... 152

Table 5.25: Results for Configuration 2 and Case A with $\Delta V_{1y} = 1.0$ km/s..... 152

Table 5.26: Comparison of Results for Configuration 2 and Case A with $\Delta V_{1y} = 1.0$ km/s... 152

Table 5.27: Results for Configuration 2 and Case A with $\Delta V_{1y} = 6.0$ km/s..... 153

Table 5.28: Comparison of Results for Configuration 2 and Case A with $\Delta V_{1y} = 6.0$ km/s... 153

Table A.1: Simulation Results as Altitude Increases for Case 1 at $\Delta V_{1y} = 1.0$ km/s 161

Table A.2: Simulation Results as Tether Length Increases for Case 1 at $\Delta V_{1y} = 1.0$ km/s..... 162

Table A.3: Simulation Results as $+\Delta V_{1y}$ Increases for Case 1..... 163

Table B.1: Analytical Results as Altitude Increases for Case A When R = 1500 km and $\theta_{imp} = 240°$ 164

Table B.2: Analytical Results as Tether Length Increases for Case A When R = 1500 km and $\theta_{imp} = 240°$ 165

Table B.3: Analytical Results as ΔV_{1y} Increases for Case A When H = 500 km and L_t = 4 km..... 166

List of Figures

Figure 2.1: Tethered Satellite System Model 17

Figure 2.2: Geocentric Equatorial Coordinate System 19

Figure 2.3: Body Fixed Coordinate System for a Negative φ 21

Figure 2.4: Orbital Elements of a Trajectory 30

Figure 3.1: Initial Set-up of the TSS for a Negative φ 40

Figure 3.2: Analytical Cases 54

Figure 4.1: Ground Range vs. $+\Delta V_{1y}$ for Case A 69

Figure 4.2: Time to Impact vs. $+\Delta V_{1y}$ for Case A 70

Figure 4.3: Ground Range vs. $+\Delta V_{1y}$ for Case B 73

Figure 4.4: Time to Impact vs. $+\Delta V_{1y}$ for Case B 73

Figure 4.5: Ground Range vs. $+\Delta V_{1y}$ for Case C 76

Figure 4.6: Time to Impact vs. $+\Delta V_{1y}$ for Case C 76

Figure 4.7: Ground Range vs. $+\Delta V_{1y}$ for Case D 78

Figure 4.8: Time to Impact vs. $+\Delta V_{1y}$ for Case D 79

Figure 4.9: Velocity Change vs. Altitude for Case A and B; R = 1500 km and θ_{imp} = 240° 82

Figure 4.10: Angular Velocity vs. Altitude for Case A and B; R = 1500 km and θ_{imp} = 240° 82

Figure 4.11: Velocity Change vs. Tether Length for Case A and B; R = 1500 km and θ_{imp} = 240° 84

Figure 4.12: Angular Velocity vs. Tether Length for Case A and B; R = 1500 km and θ_{imp} = 240° 84

Figure 4.13: Velocity Change vs. Altitude for Case C and D; R = 1500 km and θ_{imp} = 240° 86

Figure 4.14: Velocity Change vs. Tether Length for Case C and D; R = 1500 km and θ_{imp} = 240° 87

Figure 4.15: Velocity Change vs. Altitude for Case A and B; R = 3000 km and θ_{imp} = 240° 88

Figure 4.16: Angular Velocity vs. Altitude for Case A and B; R = 3000 km and θ_{imp} = 240° 88

Figure 4.17: Velocity Change vs. Tether Length for Case A and B; R = 3000 km and θ_{imp} = 240° 90

Figure 4.18: Angular Velocity vs. Tether Length for Case A and B; R = 3000 km and θ_{imp} = 240° 90

Figure 4.19: Velocity Change vs. Altitude for Case C and D; R = 3000 km and θ_{imp} = 240° 92

Figure 4.20: Velocity Change vs. Tether Length for Case C and D; R = 3000 km and θ_{imp} = 240° 93

Figure 5.1: Ground Range vs. Altitude for $\Delta V_{1y} = 1.0$ km/s in Case 1 96

Figure 5.2: Time to Impact vs. Altitude for $\Delta V_{1y} = 1.0$ km/s in Case 1 97

Figure 5.3: Trajectory at 500 km Altitude for $\Delta V_{1y} = 1.0$ km/s in Case 1 98

Figure 5.4: Trajectory at 1000 km Altitude for $\Delta V_{1y} = 1.0$ km/s in Case 1 99

Figure 5.5: Trajectory at 1500 km Altitude for $\Delta V_{1y} = 1.0$ km/s in Case 1 99

Figure 5.6: Ground Range vs. Tether Length for $\Delta V_{1y} = 1.0$ km/s in Case 1 100

Figure 5.7: Time to Impact vs. Tether Length for $\Delta V_{1y} = 1.0$ km/s in Case 1 100

Figure 5.8: Trajectory at 55 km Tether Length for $\Delta V_{1y} = 1.0$ km/s in Case 1 102

Figure 5.9: Trajectory at 100 km Tether Length for $\Delta V_{1y} = 1.0$ km/s in Case 1 102

Figure 5.10: Ground Range vs. $+\Delta V_{1y}$ for Case 1 103

Figure 5.11: Time to Impact vs. $+\Delta V_{1y}$ for Case 1 103

Figure 5.12: Ground Range vs. Altitude for $\Delta V_{1z} = 1.0$ km/s in Case 1 105

Figure 5.13: Time to Impact vs. Altitude for $\Delta V_{1z} = 1.0$ km/s in Case 1 105

Figure 5.14: Trajectory at 500 km Altitude for $\Delta V_{1z} = 1.0$ km/s in Case 1 106

Figure 5.15: Trajectory at 650 km Altitude for $\Delta V_{1z} = 1.0$ km/s in Case 1 107

Figure 5.16: Trajectory at 850 km Altitude for $\Delta V_{1z} = 1.0$ km/s in Case 1 107

Figure 5.17: Ground Range vs. Tether Length for $\Delta V_{1z} = 1.0$ km/s in Case 1 108

Figure 5.18: Time to Impact vs. Tether Length for $\Delta V_{1z} = 1.0$ km/s in Case 1 109

Figure 5.19: Trajectory at 55 km Tether Length for $\Delta V_{1z} = 1.0$ km/s in Case 1 110

Figure 5.20: Trajectory at 100 km Tether Length for $\Delta V_{1z} = 1.0$ km/s in Case 1 110

Figure 5.21: Ground Range vs. $+\Delta V_{1z}$ for Case 1 111

Figure 5.22: Time to Impact vs. $+\Delta V_{1z}$ for Case 1 111

Figure 5.23: Lofted Trajectory at $\Delta V_{1z} = 3.0$ km/s for Case 1 112

Figure 5.24: Ground Range vs. Altitude for $\Delta V_{1z} = -3.0$ km/s in Case 1 114

Figure 5.25: Time to Impact vs. Altitude for $\Delta V_{1z} = -3.0$ km/s in Case 1 114

Figure 5.26: Trajectory at 500 km Altitude for $\Delta V_{1z} = -3.0$ km/s in Case 1 115

Figure 5.27: Trajectory at 1000 km Altitude for $\Delta V_{1z} = -3.0$ km/s in Case 1 116

Figure 5.28: Trajectory at 1500 km Altitude for $\Delta V_{1z} = -3.0$ km/s in Case 1 116

Figure 5.29: Ground Range vs. Tether Length for $\Delta V_{1z} = -3.0$ km/s in Case 1 117

Figure 5.30: Time to Impact vs. Tether Length for $\Delta V_{1z} = -3.0$ km/s in Case 1 117

Figure 5.31: Trajectory at 55 km Tether Length for $\Delta V_{1z} = -3.0$ km/s in Case 1 118

Figure 5.32: Trajectory at 100 km Tether Length for $\Delta V_{1z} = -3.0$ km/s in Case 1 119

Figure 5.33: Ground Range vs. $-\Delta V_{1z}$ for Case 1 120

Figure 5.34: Time to Impact vs. $-\Delta V_{1z}$ for Case 1 120

Figure 5.35: Ground Range vs. Altitude for $\Delta V_{1z} = 1.0$ km/s in Case 2 124

Figure 5.36: Time to Impact vs. Altitude for $\Delta V_{1z} = 1.0$ km/s in Case 2 124

Figure 5.37: Trajectory at 500 km Altitude for $\Delta V_{1z} = 1.0$ km/s in Case 2 127

Figure 5.38: Trajectory at 650 km Altitude for $\Delta V_{1z} = 1.0$ km/s in Case 2 126

Figure 5.39: Trajectory at 850 km Altitude for $\Delta V_{1z} = 1.0$ km/s in Case 2 126

Figure 5.40: Ground Range vs. Tether Length for $\Delta V_{1z} = 1.0$ km/s in Case 2 127

Figure 5.41: Time to Impact vs. Tether Length for $\Delta V_{1z} = 1.0$ km/s in Case 2 128

Figure 5.42: Trajectory at 55 km Tether Length for $\Delta V_{1z} = 1.0$ km/s in Case 2 129

Figure 5.43: Trajectory at 100 km Tether Length for $\Delta V_{1z} = 1.0$ km/s in Case 2 129

Figure 5.44: Ground Range vs. $+\Delta V_{1z}$ for Case 2 130

Figure 5.45: Time to Impact vs. $+\Delta V_{1z}$ for Case 2 130

Figure 5.46: Lofted Trajectory at $\Delta V_{1Z} = 1.0$ km/s for Case 2 131

Figure 5.47: Ground Range vs. Altitude for $\Delta V_{1z} = -1.5$ km/s in Case 2 132

Figure 5.48: Time to Impact vs. Altitude for $\Delta V_{1z} = -1.5$ km/s in Case 2 133

Figure 5.49: Trajectory at 500 km Altitude for $\Delta V_{1z} = -1.5$ km/s in Case 2 134

Figure 5.50: Trajectory at 1000 km Altitude for $\Delta V_{1z} = -1.5$ km/s in Case 2 134

Figure 5.51: Trajectory at 1300 km Altitude for $\Delta V_{1z} = -1.5$ km/s in Case 2 135

Figure 5.52: Ground Range vs. Tether Length for $\Delta V_{1z} = -1.5$ km/s in Case 2 136

Figure 5.53: Time to Impact vs. Tether Length for $\Delta V_{1z} = -1.5$ km/s in Case 2 136

Figure 5.54: Trajectory at 55 km Tether Length for $\Delta V_{1z} = -1.5$ km/s in Case 2 137

Figure 5.55: Trajectory at 100 km Tether Length for $\Delta V_{1z} = -1.5$ km/s in Case 2 138

Figure 5.56: Ground Range vs. $-\Delta V_{1z}$ for Case 2 139

Figure 5.57: Time to Impact vs. $-\Delta V_{1z}$ for Case 2 139

Figure 5.58: Ground Range vs. Altitude for $\Delta V_{1y} = 1.0$ km/s in Case 2 140

Figure 5.59: Time to Impact vs. Altitude for $\Delta V_{1y} = 1.0$ km/s in Case 2 141

Figure 5.60: Trajectory at 500 km Altitude for $\Delta V_{1y} = 1.0$ km/s in Case 2 142

Figure 5.61: Trajectory at 1000 km Altitude for $\Delta V_{1y} = 1.0$ km/s in Case 2 142

Figure 5.62: Trajectory at 1500 km Altitude for $\Delta V_{1y} = 1.0$ km/s in Case 2 143

Figure 5.63: Ground Range vs. Tether Length for $\Delta V_{1y} = 1.0$ km/s in Case 2 144

Figure 5.64: Time to Impact vs. Tether Length for $\Delta V_{1y} = 1.0$ km/s in Case 2 144

Figure 5.65: Trajectory at 55 km Tether Length for $\Delta V_{1y} = 1.0$ km/s in Case 2 146

Figure 5.66: Trajectory at 100 km Tether Length for $\Delta V_{1y} = 1.0$ km/s in Case 2 146

Figure 5.67: Ground Range vs. $+\Delta V_{1y}$ for Case 2 147

Figure 5.68: Time to Impact vs. $+\Delta V_{1y}$ for Case 2 148

Nomenclature

ATEx	Advanced Tether Experiment
a	Semi-major axis
a_1	First value in the principal axis vector
a_2	Second value in the principal axis vector
a_3	Third value in the principal axis vector
$\bar{a}$	Acceleration vector, Principal axis
$\bar{a}_1$	Acceleration vector of the sub-satellite
$\bar{a}_{cm}$	Acceleration vector of the center of mass
C	Direction cosine matrix
C_{ij}	Direction cosine matrix element from the ith row and jth column
E	Energy, Eccentric anomaly
e	Eccentricity
e_x	X-component of the eccentricity vector
e_y	Y-component of the eccentricity vector
e_z	Z-component of the eccentricity vector
$\bar{e}$	Eccentricity vector
$\bar{F}$	Force Vector
$\bar{F_g}$	Gravitational Force
f	Function for the fourth order Runge Kutta

G	Universal gravitational constant
H	Altitude
$\bar{h}$	Angular momentum vector
h	Magnitude of the angular momentum vector
h_i	X-component of the angular momentum vector
h_j	Y-component of the angular momentum vector
h_k	Z-component of the angular momentum vector
$\bar{I}$	Unit vector for the X axis in the geocentric equatorial coordinate system
$\bar{I}_2$	Unit vector for the X_2 axis in the body fixed coordinate system
i	Inclination
$\bar{J}$	Unit vector for the Y axis in the geocentric equatorial coordinate system
$\bar{J}_2$	Unit vector for the Y_2 axis in the body fixed coordinate system
$\bar{K}$	Unit vector for the Z axis in the geocentric equatorial coordinate system
$\bar{K}_2$	Unit vector for the Z_2 axis in the body fixed coordinate system
k_1	First step in the fourth order Runge Kutta
k_2	Second step in the fourth order Runge Kutta
k_3	Third step in the fourth order Runge Kutta
k_4	Fourth step in the fourth order Runge Kutta
L_t	Magnitude of the tether length vector
$\bar{L}_t$	Tether length vector, position of m_1 relative to m_2
L_{t1}	Magnitude of the position vector of m_1 relative to the center of mass of the system
$\bar{L}_{t1}$	Position vector of m_1 relative to the center of mass of the system
L_{t2}	Magnitude of the position vector of m_2 relative to the center of mass of the system

$\bar{L}_{t2}$	Position vector of m_2 relative to the center of mass of the system
M	total mass of a TSS; Mean anomaly
M_E	Mass of the Earth
M_2	Secondary mass, usually of a planet in a two-body problem
m_1	Sub-satellite mass
m_2	Main satellite mass
NORAD	North American Aerospace Defense Command
N	Magnitude of the node vector
N_j	Y-component of the node vector
$\bar{N}$	Node vector
n	Mean motion
n_{cm}	Mean motion of the center of mass
PMG	Plasma Motor Generator
ProSEDS	Propulsive Small Expendable Deployer System
R	Ground range covered by the sub-satellite after release
R_e	Radius of the Earth
r_{cm}	Position Magnitude of the center of mass
r_{cmx}	X-component of the position of the center of mass of the TSS
r_{cmy}	Y-component of the position of the center of mass of the TSS
r_{cmz}	Z-component of the position of the center of mass of the TSS
$\bar{r}_{cm}$	Position vector of the center of mass
$\dot{\bar{r}}_{cm}$	First derivative of the position vector of the center of mass
$\ddot{\bar{r}}_{cm}$	Second derivative of the position vector of the center of mass

r	Magnitude of the position vector
r_p	Position magnitude at perigee
r_x	X component of the position vector
r_y	Y component of the position vector
r_z	Z component of the position vector
$\bar{r}$	Position vector
r_1	Position magnitude of the sub-satellite
r_{1x}	X-component of the position of the sub-satellite
r_{1y}	Y-component of the position of the sub-satellite
r_{1z}	Z-component of the position of the sub-satellite
$\bar{r}_1$	Position vector of the sub-satellite
r_2	Position magnitude of the main satellite
$\bar{r}_2$	Position vector of the main satellite
SEDS	Small Expendable Deployment System
TiPS	Tether Physics and Survivability Experiment
TSS	Tethered Satellite System
t_{imp}	Time at sub-satellite impact
t_{impact}	Time to impact from release
t_f	Final time
t_o	Initial time
t_{rel}	Time at sub-satellite release
V	Magnitude of the velocity vector
$\bar{V}$	Velocity vector

V_{cm}	Velocity magnitude of the center of mass
V_x	X component of the velocity vector
V_y	Y component of the velocity vector
V_z	Z component of the velocity vector
$\bar{V}_{cm}$	Velocity vector of the center of mass
V_{cmc}	Circular velocity of the center of mass
V_{cmx}	Velocity of the center of mass in the X-direction
V_{cmy}	Velocity of the center of mass in the Y-direction
V_{cmz}	Velocity of the center of mass in the Z-direction
V_1	Velocity magnitude of the sub-satellite
$\bar{V}_1$	Velocity vector of the sub-satellite
$\bar{V}_{1rel}$	Velocity vector of the sub-satellite at release
V_{1relx}	Velocity magnitude of the sub-satellite in the X-direction
V_{1rely}	Velocity magnitude of the sub-satellite in the Y-direction
V_{1relz}	Velocity magnitude of the sub-satellite in the Z-direction
$\bar{V}_{1/cm}$	Relative velocity of m_1 with respect to the center of mass
V_{1c}	Circular velocity of the sub-satellite
V_2	Velocity magnitude of the main satellite
$\bar{V}_2$	Velocity vector of the main satellite
$\bar{V}_{2/cm}$	Relative velocity of m_2 with respect to the center of mass
V_{2c}	Circular velocity of the main satellite
$\bar{X}$	State Matrix
$\dot{\bar{X}}$	First derivative of the state matrix

X, Y, Z	Axes for the geocentric equatorial coordinate system
X_2, Y_2, Z_2	Axes for the body fixed coordinate system.
x_1	X-position of the sub-satellite
$\ddot{x}_1$	X-acceleration of the sub-satellite
y_1	Y-position of the sub-satellite
$\ddot{y}_1$	Y-acceleration of the sub-satellite
z_1	Z-position of the sub-satellite
$\ddot{z}_1$	Z-acceleration of the sub-satellite
x_{cm}	X-position of the center of mass
$\ddot{x}_{cm}$	X-acceleration of the center of mass
y_{cm}	Y-position of the center of mass
$\ddot{y}_{cm}$	Y-acceleration of the center of mass
z_{cm}	Z-position of the center of mass
$\ddot{z}_{cm}$	Z-acceleration of the center of mass
Δt	Time step
ΔV_{cmx}	Velocity change of the center of mass in the X-direction
ΔV_{cmy}	Velocity change of the center of mass in the Y-direction
ΔV_{cmz}	Velocity change of the center of mass in the Z-direction
$\bar{\alpha}$	Angular acceleration vector
β_o	Fourth Euler parameter
β_1	First Euler parameter
β_2	Second Euler parameter
β_3	Third Euler parameter

$\dot{\beta}_o$	First derivative of the fourth Euler parameter
$\dot{\beta}_1$	First derivative of the first Euler parameter
$\dot{\beta}_2$	First derivative of the second Euler parameter
$\dot{\beta}_3$	First derivative of the third Euler parameter
γ	Angle between the position and velocity vector
θ	True anomaly
θ_{imp}	True anomaly at sub-satellite impact
θ_{rel}	True anomaly at sub-satellite release
μ	Gravitational parameter
ν	True anomaly
φ	Rotation angle, Principal angle
Ω	Longitude of the ascending node
ω	Argument of periapsis
$\bar{\omega}$	Angular velocity vector
ω_1	X-component of the Angular Velocity
ω_2	Y-component of the Angular Velocity
ω_3	Z-component of the Angular Velocity

Chapter 1: Introduction

This research is a conceptual study to evaluate the possible ballistic capabilities of a satellite that is launched from a space based platform. While any space based platform could be used, the platform chosen for this study is a Tethered Satellite System (TSS). A TSS is used as the platform because different release point configurations can be created having different velocities. The sub-satellite of the TSS will be the object that is launched or released from the system. The sub-satellite will be released from the TSS after a velocity change is placed on the sub-satellite. This velocity change could be the result of an impulsive velocity change maneuver done by the sub-satellite or it could be the result of an increase in the angular velocity of the TSS. The ballistic capabilities that will be studied are the ground range and time to impact after the sub-satellite is released from the system. Different release point configurations and changes in the TSS parameters will be analyzed to determine the options in the available ground ranges and times to impact. This chapter will discuss the history and applications of a TSS, the previous work done on TSS, and a more detailed problem description for this study.

1.1 Historical Background

A Tethered Satellite System (TSS) is made up of two satellites connected by a cord or tether. The two end bodies are called the main satellite and the sub-satellite. The sub-satellite is in a lower orbit than the main satellite and is deployed from the main satellite using the tether. The main satellite can be a larger satellite than the sub-satellite or even a shuttle-type orbiter. The idea of a TSS was first introduced in 1895 by a Russian scientist by the name of Tsiolkoskii,

who presented the concept of a "space tower" or a space elevator. Tsiolkoskii's idea of a space tower was to have a system that would be attached to the surface of the Earth with the other end being in a geosynchronous orbit about the Earth. The objective of the space tower was to allow an object to travel up the tower and be released once it reached the top. At the top of the tower the object would be released into a geosynchronous orbit. The idea of a space tether is attributed to Tsiolkovskii because of his proposal for the space tower.[7]

In 1965 the idea of a TSS was put to the test by NASA during the Gemini XI and Gemini XII missions. In Gemini XI, the sub-satellite was connected to the upper stage and both the sub-satellite and the upper stage swung around the center of mass of the system and generated an artificial gravity.[7] The Gemini XII mission was designed to test the gravity-gradient stabilization of a TSS.[17] Both the Gemini XI and Gemini XII missions verified the assumptions and calculations done by scientists thereby, proving that tethered satellites could be useful. Issac Artsutanov, was the first person to propose a nonsynchronous sky hook. This sky hook was a rotation tethered system that would approach Earth's surface with a zero relative velocity at the perigee of the tethered system's orbit.[3]

Despite the missions and the ideas presented in the 1960s the "Era of TSS" did not begin until the 1970s when Mario Grossi and Giuseppe Colombo proposed their idea for a skyhook to NASA and the Italian Space Agency.[7] Grossi was from the Smithsonian Astrophysical Observatory and Colombo was working at the University of Padua in Italy. The skyhook proposal involved a small satellite that could be deployed from a shuttle orbiter along a twenty to one hundred kilometer tether. The small satellite could then help with exploration and data collection of the Earth's upper atmosphere.[18] This proposal by Grossi and Colombo generated interest in TSS for NASA and the Italian Space Agency.

The interest generated by the proposal by Grossi and Colombo resulted in NASA and the Italian Space Agency formally agreeing to collaborate on TSS projects. While several short tethered experiments were conducted on the shuttle during the 1980s, it was not until 1992 that the first major joint project between the two agencies was launched.[18] The satellite was called the TSS-1 and was launched from the Atlantis orbiter. The TSS-1 was the first test of a TSS in space.[7] The purpose of the TSS-1 mission was to study the electro-dynamic properties of the Earth's ionosphere. This required that the tether be made of an electrically conducting material.[18] However, during the mission the reeling mechanism for the tether and sub-satellite malfunctioned. This caused the tether to stop its deployment. In other words the tether did not deploy from the shuttle to its full length.[7] Despite this malfunction the TSS-1 mission proved that a satellite could be deployed and controlled. The mission also showed that a TSS could be easily controlled and showed that the system was more stable than predicted.[5]

The Small Expendable Deployment System 1 (SEDS-1) and the Plasma Motor Generator (PMG) missions were conducted during 1993. The SEDS-1 successfully demonstrated the downward free-reeling deployment of the sub-satellite in a TSS. The PMG's mission was to investigate the possibility of using an electrically conducting tether to generate power that could be used to create thrust for the TSS. This was the first example of propulsion for a system that did not require any propellant. A year later the SEDS-2 was deployed and remained in orbit for five days until space debris or a micro-meteorite severed the tether.[7] The purpose for deploying the SEDS-2 was to study long term tether dynamics.[18] Even though the tether was severed, the SEDS-2 mission collected useful data.

In 1995 and 1996 three more missions were launched to further study the dynamics and applications of TSS. These missions were the OEDIPUS-C, the TSS-1R, and the Tether Physics

and Survivability Experiment (TiPS). The OEDIPUS-C system was made up of two rocket payloads and was launched in 1995. After the system reached the apogee of the TSS orbit, the tether was intentionally cut in order to study a post-apogee trajectory.[18] The TSS-1R and TiPS systems were launched in 1996. The TSS-1R is named because it is the re-launch of the TSS-1 mission. During this launch the tether was not severed and the mission was able to prove that a tether could be used to create a high voltage charge as it passes through the Earth's ionosphere.[7] The TiPS satellite was launched by the Naval Research Laboratory.[18] The system consisted of two small satellites rather than a shuttle orbiter and satellite combination. The TiPS satellite remained in space for several years and provided enough data to further study tether satellite dynamics and orbital motion.[7]

The last TSS mission launched in the 1990s was the Advanced Tether Experiment (ATEx). The Naval Research Laboratory launched the ATEx system with a goal to demonstrate TSS stability, control, and attitude determination of the two end bodies. The plan behind the mission was to deploy the sub-satellite and tether out to 6 km over the course of three and a half days; however, after only eighteen minutes of deployment the ATEx system was jettisoned from the main satellite. The reason behind the jettison of the ATEx was because the tether angle sensor detected that an out-of-limits condition had been reached and automatically jettisoned the system. It is believed that the condition was detected due to a thermal expansion of the tether.[7,18]

Very few tether missions have been launched in the 21st century. Some missions were proposed but later cancelled. One successful launch was the PICOSat in 2001. The PICOSat consisted of a small TSS that had a mass less than a kilogram. In 2002 the Propulsive Small Expendable Deployer System (ProSEDS) was proposed. This system was a propulsive experiment that was designed to test the ability of a TSS to draw energy from the magnetic field

of the Earth and then use that energy as an electric thruster to raise or lower the TSS's orbit.[7] Work was done on the ProSEDS until NASA cancelled the project due to the fact that key parameters in the performance of the TSS could not be met.[27]

1.2 TSS Applications

TSS applications can be broken into three categories: space transportation, electrically conducting tethers, and atmospheric exploration. The first application that will be discussed is the space transportation category, which focuses on the movement of the satellite system. A TSS can be used to put a satellite into a higher or lower orbit than the original orbit without the use of boosters. The system can also be used to return a discarded payload to the Earth and help during the docking process of a shuttle to a space station. These applications can be done because energy and momentum exchange occurs between the main satellite and the sub-satellite during the deployment of the sub-satellite. This same momentum and energy exchange can also help with controlling the attitude of the main satellite.[18] A TSS could be used to perform aero-braking when approaching a planet. Aero-breaking occurs when the sub-satellite is deployed into the planet's atmosphere where atmospheric drag would affect the satellite. When aerodynamic drag is exerted on the sub-satellite, the system will theoretically decrease to a capture speed from the approach speed before deployment. This decrease in the satellite speed is caused by the tension in the tether instead of using a propulsive maneuver to slow down the satellite.[7]

Since the space transportation application for TSS deals with movement of all or part of the system, fuel savings and artificial gravity could be a result.[18] The fuel savings are beneficial for obvious reasons. The benefit from artificial gravity may not be as obvious. Artificial gravity is created by the spin rate of a spacecraft rotating about its center of mass. However, in order for

a shuttle orbiter to generate enough artificial gravity the required spin rate would be too high for the crew of the shuttle to withstand. When a TSS is used to create an artificial gravity, the spin rate of the system is at an acceptable level for the crew.[7]

The second category of TSS applications is electrically conducting tethers, which allows for the transportation of energy. In this case the energy is in the form of electricity that is generated from the Earth's magnetic field. The electricity will produce a current along the tether which will create a force that can move the TSS into a higher or lower orbit. In other words the force generated by the electric current can be used instead of propellant in a propulsive maneuver to change the trajectory of the TSS. If the tether can conduct electricity, it can also be used as an antenna for the system, which can transmit electromagnetic waves in the direction that the tether is pointed.[18] There are two main benefits to using a conducting tether. The first one is reduced cost. If the conducting tether can provide a force to move the satellite system, the amount of fuel needed for the mission is reduced and the fuel cost will be reduced as well. The second benefit is that there is a reduced risk of a chemical propellant contaminating any external part of the TSS.[7] While fuel will always be needed on the TSS, a conducting tether can reduce the amount the system carries; thereby, decreasing the risk and cost of the mission.

The final category of tether applications is atmospheric exploration. In atmospheric exploration an instrument is deployed into the Earth's atmosphere from a large spacecraft, like the shuttle orbiter. A TSS is a great system for atmospheric exploration because the tether can be extended into areas of the upper atmosphere that are too "rarified" for the aircraft and too dense for shuttle orbiters or other large spacecraft. One use of tethers for atmospheric exploration is the gathering of physical, meteorological, and environmental data over a long course of time. The tethers could also be used for surveillance and measurements of the Earth's magnetic and

electric fields. Perhaps the most useful application for tethers in atmospheric exploration is the lowering of a model into the atmosphere for high-speed and high altitude aircraft. Wind tunnels are normally used to determine the characteristics of an aircraft design; however, high altitudes and high speeds are harder to replicate inside a wind tunnel. Overall, the tether can be used to collect data for a variety of experiments in atmospheric exploration.[18]

Atmospheric exploration is an area of great interest, especially when it comes to how the sun interacts with the Earth's atmosphere. The peak area for this interaction occurs anywhere at or below a four hundred kilometer altitude above the Earth. This region contains the maximum gradient in electron content and temperature in the Earth's atmosphere. The higher areas of this segment are hard to reach with an aircraft and difficult to maintain for long periods of time for a large spacecraft. By extending a tether into this region long term data can be collected. It's important to note that once the scientific community has an understanding on how to use TSS to study the Earth's atmosphere this application can be extended to other planets.[7]

1.3 Previous Research

TSS research has mainly focused on the orbit determination and the identification of TSS throughout the years. Some researchers have studied the dynamics and attitude of tethered satellites and there has been some research done that looks at the impact trajectory of the sub-satellite and the new orbital elements of the trajectory for the sub-satellite once it has been released from the system; however, there has not been an effort, to this writer's knowledge, to determine what can cause an impact trajectory and what will lead to a maximum range with the best time to impact for the sub-satellite. That being said this section will still discuss some previous research that has helped to formulate the problem and model development for this research as well as for research studying impacting trajectories.

In 1983 Hoots, Roehrich, and Szebehely published a study that focused on TSS analysis and the effect of the tether on both satellites. The authors discussed the effect of the tether on the speed of the satellites in the system. The tether causes the sub-satellite to have a lower velocity than its expected circular velocity without the tether and the main satellite actually has a higher velocity than its circular velocity without the tether. Hoots, Roehrich, and Szebehely also determined the conditions for impact after the sub-satellite is released from the TSS and define how to modify the gravitational constant in order to make the Keplerian acceleration valid while the tether remains intact. The authors also pointed out the problem of detecting a TSS system and what it does to detection programs, such as the one used by North American Aerospace Defense Command, NORAD.[13]

Several papers have also been published concerning the modeling, orbit determination, and quick identification of TSS. Qualls and Cicci[24] published a paper in 2007 that studied the modifications of classic preliminary orbit determination methods to distinguish between a tethered satellite and an untethered satellite. It was determined that the Herrick – Gibbs Method and the true anomaly iteration technique provided the most accurate results in determining if the object in question was tethered or not.[24] Rossi, Cicci and Cochran Jr.[25] published a paper in 2004 that discussed an analytical study of the dynamics of a TSS to determine the conditions for periodic motions about the equilibrium state of the system. It was determined that when only the gravitational and oblateness forces were placed on the system that the periodic motion of the TSS depended on the physical characteristics of the tether; however, if the aerodynamic drag was placed on the system, the drag must be bounded in order to create a periodic motion.[25] A paper was published by Lovell, Cho, Cochran Jr., and Cicci[19] in 2003, that examined the factors that caused the bodies of a TSS to behave differently and how each of the factors creates a

discrepancy in the determination of a satellite re-entry. The authors determined that the tether force and the librational motion of the system were key factors that caused a tethered satellite to appear to be on a re – entry course.[19] In 2002, Cicci, Cochran Jr, Qualls, and Lovell[9] published a paper that provided a methodology to perform an identification, orbit determination, and orbit prediction of a TSS. For the identification of a TSS preliminary orbit determination methods were used and ridge – type estimation methods were used for the orbit determination of the TSS. The authors used a TSS dynamic model for the long term orbit prediction of the TSS.[9] Another paper would be published by Cicci, Qualls, and Lovell in 2001.[8] This paper discussed the use of ridge – type estimation methods to identify a TSS when a "small arc" of observational data was available.[8] The final paper to be discussed by this group of authors was published in 1998 by Cho, Cochran, Jr., and Cicci.[6] In this paper a perturbed two – body model was used for the TSS during orbit determination. The orbit determination was done using only the observations from one of the satellites in the system. The characteristics of the perturbed motion on the TSS was studied using this data.[6]

Another key author in TSS studies is A. K. Misra. Misra[21] published a paper in 2008 titled "Dynamics and Control of Tethered Satellite Systems." In this paper Misra studies the nonlinear roll and pitch motions on a TSS. Misra found that the aerodynamic drag produced librational motion on the TSS and that electrodynamic forces would affect the pitch and roll of the TSS; therefore, the drag and electrodyanmic forces would change the stability of the TSS.[21] Modi, Gilardi, and Misra[22] published a paper in 1998 that studied the attitude control of a TSS. The authors used an Nth order lagrangian formulation to study the attitude control of space platform based TSS and used a Liapunov method for the control of the system. The Liapunov control was found to be effective in stabilizing the TSS.[22]

Curtis Hilton Stanley wrote his Master's thesis at the University of Colorado at Colorado Springs about apparent impacting trajectories, identification, and orbit determination of TSS in 2010. Stanley defines an apparent trajectory as being the "trajectory that an end mass would follow if not tethered." If the apparent trajectory would intersect the Earth, then it becomes an apparent impact trajectory. He looked at circular and elliptical orbits with and without librational motion to determine the apparent impacting trajectory and used batch filters to determine the trajectory of the satellite and identify the sub-satellite as being a part of a TSS. Stanley's research focused on determining the minimum tether length needed to create an apparent impacting trajectory and simulating a ballistic missile trajectory along with the apparent impacting trajectory to form a comparison between the two. Once the comparison was determined he could use that knowledge to have a program identify an object as being a ballistic missile or a satellite attached to a TSS. Stanley never looked into an actual impacting trajectory and the range that the end mass could obtain once released from a TSS.[28]

In 1994 Naigang, Dun, Yuhua, and Naiming[23] discussed the calculation of the orbital elements for the sub-satellite after it is released from the TSS. The purpose behind this discussion is the momentum transfer between the two satellites that could place a payload in a higher orbit about the Earth. The orbital elements are calculated from position and velocity vectors, which are determined using the pitch angle, roll angle, magnitude of the position, the true anomaly, and their derivatives. The authors then compare the orbital elements before release to those after the release of the satellite. They found that the change in the right ascension and the inclination angle of the sub-satellite after release is small because of the small roll rate present in their examples. The authors also note that the biggest change is found in the semi-major axis.[23]

Nammi Jo Choe and Thomas Alan Lovell did research into the orbit determination and detection of TSS and state estimation of TSS, respectively. Choe looked at a two satellite TSS and a three satellite TSS in 2003. She also developed a basic model for the TSS by assuming a massless tether and representing the end satellites as point masses. An algorithm was developed by Choe to detect the TSS systems. Once the TSS was detected, Choe used an estimation process to determine the orbit of the system over the orbital period of the systems. The process developed by Choe allowed for the detection, state estimation, and calculation of tether parameters for a two and three body TSS.[7] Lovell used a "batch-type differential corrections filtering scheme" or a gradient based algorithm and a genetic algorithm to determine the state estimation of a TSS. He then compared the two techniques in order to determine which one had better accuracy, speed, and robustness of the two algorithms. His research showed that the genetic algorithm could give an accurate solution over short periods of data. Since long term filters such as the gradient based method depend on the initial approximation, Lovell suggested that a hybrid approach be used. This hybrid approach would use the genetic algorithm to determine the initial approximation and the gradient based method would be used to solve for the estimation of the state.[18]

Research addressing TSS dynamics includes the study of perturbed motion, constrained dynamics, attitude and control, librational motion, and stability of the TSS. Sungki Cho[5] analyzed the perturbed motion of TSS and used filters to identify the perturbed motion of the satellite system in 1999. The perturbed motion of one detected satellite could be used to identify the satellite as part of a TSS. Cho used a least squares batch filter in order to identify the satellite as a member of a TSS and to determine the motion of the system.[5] In 2001 Peter Beda used Lagrange's equations to define the equations of motion for the TSS. He then put a constraint on

the system to make sure that the tether length remained constant. The equations of motion and the control constraint were then used in a numerical simulation to determine the attitude of a TSS.[2] Aaron Schutte and Brian Dooley[26] developed a control law for the constrained motion of a TSS. This control law or constraint equations could then be used to simplify the modeling and simulation of a TSS.[26]

An extended rigid body model of a TSS was used by Insu Chang, Sang-Young Park, and Kyu-Hong Choi[4] in 2010 to study the attitude and control of a TSS. In order to simulate this, the authors used a state-dependent Riccati equation to model the nonlinear attitude control of a TSS. A numerical integration was used to determine the stability of the system using the Riccati equation. The TSS was found to be asymptotically stable when using the Riccati equation to model the nonlinearities in the system.[4] Joshua Ellis and Christopher Hall[11] also studied the stability of a TSS by looking at the system's out of plane librations. Equations of motion were developed by Ellis and Hall to model the in-plane and out-of-plane librations of the TSS. The eigenvalues for the librational motions were then used to determine the stable and unstable areas of motion for a TSS.[11]

In 2008 Kosei Ishimura and Ken Higuchi[15] wrote a paper that described the coupling between the pitch, axial vibration, and orbital motion of TSS. The authors looked at the effects of these motions on the eigenvalues and eigenvectors. Ishimura and Higuchi also looked into the influence of the mass ratio and natural frequency on the characteristics of the system, specifically the eigenvalues. The natural frequency was found to have the greatest influence on the coupling between the pitch, axial vibration, and orbital motion while the mass ratio was found to influence the pitch motion and found to affect the value for the eigenvalues and eigenvectors.[15] Also in 2008, Hao Wen, Dongping P. Jin, and Haiyan Y. Hu[29] discussed the relative advances in the

dynamics and control of TSS and provided a comprehensive look at all the advances in TSS dynamics and control. Some of the topics discussed are controls for tether deployment and retrieval of the sub-satellite, further studies into producing artificial gravity with a tethered system, re-entry and rendezvous missions assisted by a tether, and stability of a TSS. Some of the studies discussed by Wen, Jin, and Hu focused on a two satellite tethered system, while others looked at three or more satellites tethered together.[29]

The majority of the research conducted concerning TSS focused on constraints and attitude and control and dynamics of tethered systems. Only a few studies have discussed impact trajectories. Stanley's[28] focus was on the apparent impacting trajectory of a sub-satellite without being cut from the TSS. He compared this apparent impacting trajectory with a typical ballistic missile trajectory. This information was then used to identify a tethered satellite, when only one end of the tethered satellite was detected. After the sub-satellite was identified as part of a TSS, Stanley focused on the orbit determination of a TSS. Naigang, Dun, Yuhua, and Naiming[23] focused on the changes in the orbital elements after the sub-satellite was released from a TSS with librational motion. All the information found in the research stated above was used to help formulate the best model and equations of motion for this study.

1.4 Problem Description

The purpose of this study is to determine the possible ballistic capabilities of a satellite launched from a space based platform. For the purposes of this study a TSS was chosen for the launching platform because it can be used to release the satellite with different release configurations. The sub-satellite of the TSS will be released from the system after a velocity change is placed on the sub-satellite. There are two methods to create such a velocity change on the sub-satellite: an impulsive velocity change maneuver and an increase in the angular velocity

of the system. The impulsive velocity change is achieved when the sub-satellite produces a thrust in a certain direction. The resulting velocity change from the thrust maneuver will affect the velocity of the sub-satellite and may result in an impact trajectory after the sub-satellite is released from the TSS. For the increase in the angular velocity of the system, the sub-satellite and the main satellite will produce a thrust that would cause the TSS to rotate faster. This increase in the rotation of the system will affect the velocity of both satellites and may cause the sub-satellite to impact the Earth after it is released from the system. If an impact does occur, the range covered by the sub-satellite's impacting trajectory and the time it takes for the sub-satellite to impact the Earth after launch will be calculated. Range is used to describe the ground range covered by the sub-satellite after it is released from the TSS. The range and time to impact are the ballistic capabilities that will be analyzed in this study.

Changes in the parameters of the space based platform, or the TSS, are also analyzed to determine how they might affect the capabilities of the sub-satellite after release. The parameters that are investigated are the altitude of the main satellite and the tether length because both of these parameters will affect the launching position of the sub-satellite relative to the Earth. For each combination of parameters an impulsive velocity change maneuver is placed on the sub-satellite and it is released from the system. If the sub-satellite impacts the Earth, the range and time to impact of the impacting trajectory are calculated in order to determine the impact of the changing on the ballistic capabilities of the sub-satellite.

This research takes a threat analysis point of view for a satellite launched from a space based platform. Using the TSS as the platform, the sub-satellite will be placed in different release configurations with various altitudes, tether lengths, and velocity changes placed on the sub-satellite before it is released. For each velocity change evaluated, a corresponding angular

velocity of the TSS is calculated which would produce such a velocity change. The ballistic capabilities for different cases are then compared in order to determine a range of ballistic capabilities for each configuration.

Chapter 2: Relevant Theory Used in TSS Analysis

There are many ways to model a TSS with different coordinate systems and assumptions. Basic effects caused by the tether on the end bodies will be discussed before developing a detailed model for the TSS. After the detailed model is defined, the equations of motion and perturbation effects will be introduced. Since rotational motion is included in the model, attitude control parameters will be used to assist with the transformations between the body coordinate system and the inertial coordinate system. Orbital elements will be described since the elements will be used to determine if the trajectory of the sub-satellite after release will impact the Earth. Finally, discussions of rigid body dynamics, the integration method used to model the TSS, and orbital mechanics will be presented. In the discussion that follows, it will be assumed that the center of mass of the TSS will move in a circular orbit.

2.1 Tethered Satellite System Dynamics

The tether in the system exerts a force on both the main satellite and the sub-satellite. This force leads to a change in the velocities of both of the satellites. Depending on the position of the mass, the tether will either increase or decrease the velocity of each satellite to a point where it is greater than or less than the satellite's untethered circular velocity. For this discussion the set-up for the TSS is shown in Figure 2.1. The main satellite generally has a mass equal to or larger than the sub-satellite. Hoots, Roehrich, and Szebehely[13] discussed the effects of the tether on the masses and developed equations for the velocity of both masses and the center of mass in their study. The first step was to determine the location of the center of mass.

Once the position of the center of mass was determined, the equation for circular velocity was then used to find the circular velocity for the center of mass.[13]

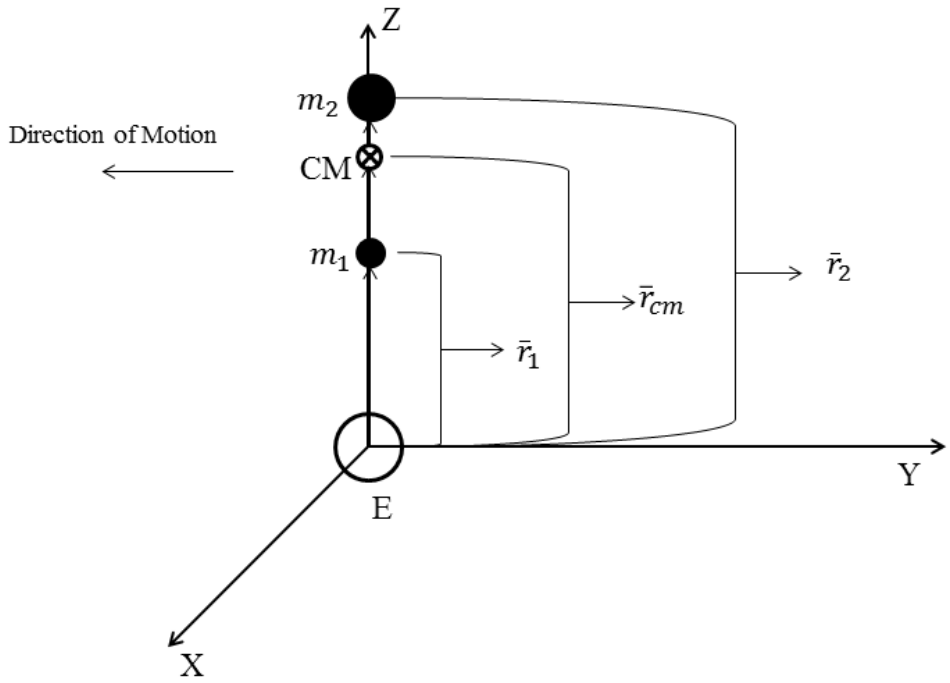

Figure 2.1: Tethered Satellite System Model

For a circular orbit, the position vector of the center of mass relative to the center of the Earth and the circular velocity of the center of mass are calculated using equation (1) and equation (2), respectively. [13]

$$\bar{r}_{cm} = \frac{\bar{r}_1 m_1 + \bar{r}_2 m_2}{m_1 + m_2} \tag{1}$$

$$V_{cmc} = \sqrt{\frac{\mu}{r_{cm}}} \tag{2}$$

The variables m_1 and m_2 are the mass of the sub-satellite and the main satellite, respectively. The magnitude of the position vectors of the sub-satellite and the main satellite are $r_1$and r_2, μ is the gravitational parameter, and the magnitude of the position vector of the center of mass is r_{cm}.

In order to find the velocities of the end masses the mean motion of the center of mass must first be calculated. Equation (3) defines the mean motion as a function of the gravitational constant and the position of the center of mass.[13]

$$n_{cm} = \sqrt{\frac{\mu}{r_{cm}^3}} \tag{3}$$

Once the mean motion is calculated, the velocities of the end masses can be found as a function of the mean motion and the position of each mass. Equation (4) and Equation (5) define the equations used to obtain the velocity of the main satellite and the sub-satellite, respectively.[13]

$$V_2 = n_{cm} r_2 \tag{4}$$

$$V_1 = n_{cm} r_1 \tag{5}$$

Equation (3) can then be substituted into equations (4) and (5) to give equations (6) and (7) for the velocities of the main satellite and the sub-satellite, repectively.[13]

$$V_2 = \frac{r_2}{r_{cm}} \sqrt{\frac{\mu}{r_{cm}}} \tag{6}$$

$$V_1 = \frac{r_1}{r_{cm}} \sqrt{\frac{\mu}{r_{cm}}} \tag{7}$$

When the satellites are not connected by a tether, both the main satellite and sub-satellite have a circular velocity that is defined similar to the circular velocity of the center of mass given

by equation (2). The actual velocities of the satellites when connected with the tether and the unconnected circular velocity of the satellites can then be compared. For the situation shown in Figure 2.1, Hoots, Roehrich, and Szebehely[13] determined that the actual velocity of the main satellite when tethered is larger than the circular velocity of the main satellite when it is not tethered. The sub-satellite's actual velocity when tethered was found to be smaller than the circular velocity the sub-satellite has when not tethered. This means that when the two masses are put together in a TSS formation the main satellite's mass will speed up, while the mass of the sub-satellite will be slowed down relative to their untethered circular velocities.[13]

In order to model a TSS a set of coordinate systems needs to be defined before the equations of motion can be determined. An inertial coordinate system will be used to describe the motion of the system, and will be selected to be the geocentric equatorial coordinate system. The geocentric - equatorial coordinate, Earth – centered Inertial, or ECI system is depicted in Figure 2.2.

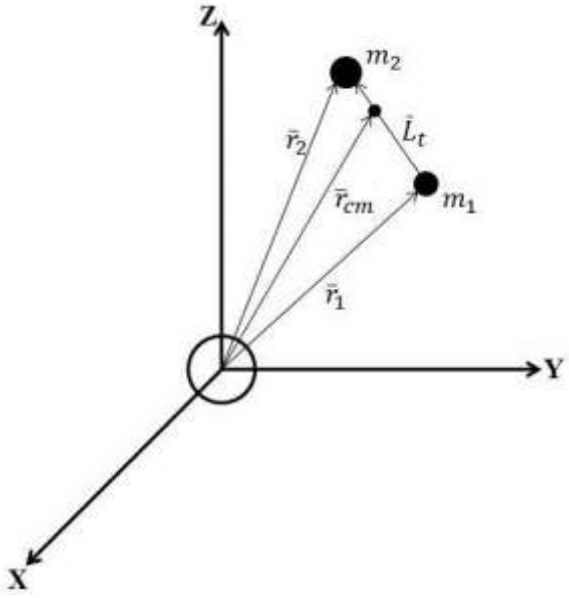

Figure 2.2: Geocentric Equatorial Coordinate System

The origin of the geocentric equatorial system is fixed at the center of the Earth. The positive X-direction points in the vernal equinox direction. The positive Z axis goes through the North Pole and the positive Y axis is ninety degrees from the positive X and Z axes, such that the XY plane lies in the Earth's equatorial plane. $\bar{I}$, $\bar{J}$, and $\bar{K}$ are the unit vectors for the X, Y, and Z axes, respectively.[1] The TSS is also depicted in Figure 2.2. The end masses are considered to be point masses and the tether is assumed to be a massless, rigid tether. The position vector for the main satellite and the sub-satellite are $\bar{r}_2$ and $\bar{r}_1$, respectively, while the position vector, $\bar{r}_{cm}$, represents the position of the center of mass of the TSS. The fourth vector, $\bar{L}_t$, in Figure 2.2 is the tether length vector or the position of m_1 relative to m_2.

Since the end masses are naturally rotating about the center of mass in a counter - clockwise rotation about the positive X – axis due to the gravity gradient affect, a body coordinate system will be needed in order to determine the position of the end masses relative to the center of mass of the system. This position will then be transformed into the inertial coordinate system. Figure 2.3 shows the body coordinate system for the TSS. The fixed coordinate system now has an origin located at the center of mass of the TSS. The X_2, Y_2, and Z_2 coordinate system is the body coordinate system after a rotation about the X axis. The TSS rotates about the center of mass; therefore, the body coordinate system will rotate about the X axis. This means that the X_2 axis will line up with the X axis and an angle will be created between the Y and Y_2 axes and the Z and Z_2 axes. The unit vectors for the body fixed coordinate system are $\bar{I}_2$, $\bar{J}_2$, and $\bar{K}_2$, which correspond to the X_2, Y_2, and Z_2 axes, respectively. The rotation angle, φ, represents the angle between the fixed coordinate system and the body coordinate system caused by the angular velocity. The two vectors in Figure 2.3 represent the distances

from the center of mass to the end bodies. The position vector of m_2 relative to the center of mass of the system is $\bar{L}_{t2}$. The vector, $\bar{L}_{t1}$, is the position vector of m_1 relative to the center of mass. Both vectors are expressed in body components. The rotation angle can be used to express the vectors in the geocentric equatorial system by creating a direction cosine matrix and using attitude dynamics. This methodology will be discussed after the introduction of the equations of motion.

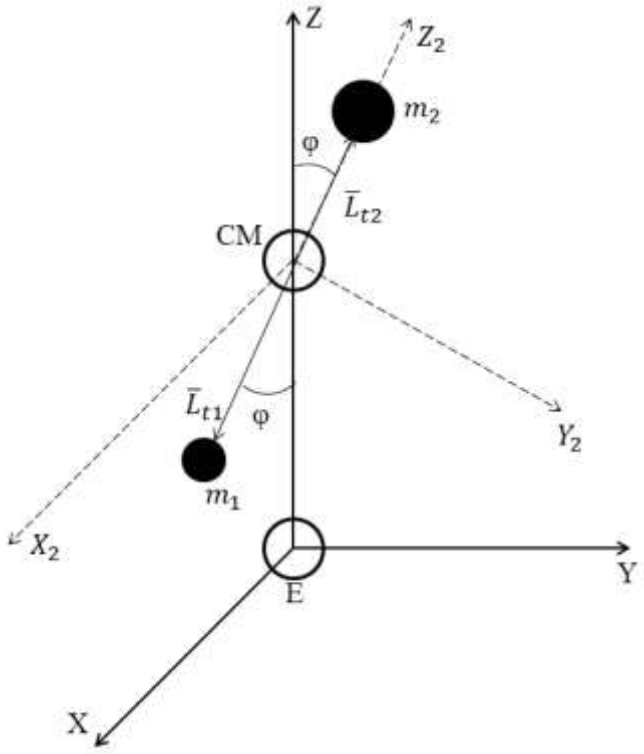

Figure 2.3: Body Fixed Coordinate System for a Negative φ

2.1.1 Equations of Motion

As stated earlier the end satellites will be modeled as two point masses and the tether will be modeled as a massless, rigid tether. It was also mentioned earlier that due to the tether force only the center of mass of the system can be modeled using Keplarian motion. Therefore, the

TSS will be considered as a rigid body in this study. In this section the equations of motion for the center of mass of the system will be determined using two-body forces. The position and velocity of the two end masses will be determined using rigid body dynamics.

The equations of motion of a spacecraft relative to the Earth are well-known and can be written as

$$-\frac{\mu}{r_{cm}^3}\bar{r}_{cm} = \ddot{\bar{r}}_{cm} \tag{8}$$

where

$$\mu = G(M_e + M) \tag{9}$$

Equation (8) is also known as the Keplarian acceleration of the system. Since equation (8) is a vector, it has $\bar{I}$, $\bar{J}$, and $\bar{K}$ components. This means that there are a total of three scalar equations that can be used to describe the motion of the system. These final equations of motion are expressed in equations (10) through (12).

$$-\frac{\mu}{r_{cm}^3}x_{cm} = \ddot{x}_{cm} \tag{10}$$

$$-\frac{\mu}{r_{cm}^3}y_{cm} = \ddot{y}_{cm} \tag{11}$$

$$-\frac{\mu}{r_{cm}^3}z_{cm} = \ddot{z}_{cm} \tag{12}$$

These equations can be used to find the velocity and position components of the center of mass of the TSS using numerical integration; however, the position and velocity of the end masses have yet to be determined. In order to find the position of the end masses, the attitude dynamics of the TSS must be considered.

2.2 Attitude Dynamics Using Euler Parameters

According to Hughes[14], spacecraft attitude dynamics is an applied science that aims to understand and predict spacecraft orientation and how the orientation evolves over time. The part of attitude dynamics that this research utilizes is the determination of equations to describe rotational motion and the differential equations that govern the motion equations. There are many ways to represent the attitude dynamics of a spacecraft. In this text, the Euler parameters are chosen because they have no singularities at any orientation; however, the disadvantage of the Euler parameters is that they lack uniqueness. In other words, a positive Euler parameter can describe the same attitude orientation as a negative Euler parameter. The Euler parameters are then placed into a direction cosine matrix, which describes the rotation of the system and allows for a transformation between two coordinate systems.[14] In this case the direction cosine matrix will allow for the transformation of the body coordinate system into the fixed geocentric equatorial coordinate system.

Euler's theorem states that any rigid body orientation can be achieved by a single rotation about the principal axis, $\bar{a}$, through a principal angle, φ. The principal axis and angle can be determined by examining the eigenvalues and eigenvectors of the direction cosine matrix. The principal axis is a vector made up of three components. If the principal axis and angle are known, the Euler parameters can be found. Equations (13) through (16) define the four Euler parameters in terms of the principal axis and angle.[14]

$$\beta_o = \cos\left(\frac{\varphi}{2}\right) \tag{13}$$

$$\beta_1 = a_1 \sin\left(\frac{\varphi}{2}\right) \tag{14}$$

$$\beta_2 = a_2 \sin\left(\frac{\varphi}{2}\right) \tag{15}$$

$$\beta_3 = a_3 \sin\left(\frac{\varphi}{2}\right) \tag{16}$$

The fourth Euler parameter is labeled using the symbol β_o.[14]

The direction cosine matrix, **C**, is a 3x3 matrix and can be expressed in terms of the four Euler parameters.

$$\boldsymbol{C} = \begin{bmatrix} \beta_o^2 + \beta_1^2 - \beta_2^2 - \beta_3^2 & 2(\beta_1\beta_2 + \beta_o\beta_3) & 2(\beta_1\beta_3 - \beta_o\beta_2) \\ 2(\beta_1\beta_2 - \beta_o\beta_3) & \beta_o^2 - \beta_1^2 + \beta_2^2 - \beta_3^2 & 2(\beta_2\beta_3 + \beta_0\beta_1) \\ 2(\beta_1\beta_3 + \beta_0\beta_2) & 2(\beta_2\beta_3 - \beta_o\beta_1) & \beta_o^2 - \beta_1^2 - \beta_2^2 + \beta_3^2 \end{bmatrix} \tag{17}$$

If the Euler parameters are not known but a direction cosine matrix is known, the Euler parameters can be found using the elements from the direction cosine matrix. This must be done in a series of steps. The first step is to calculate the squared values of each of the Euler parameters.

$$\beta_o^2 = \frac{1}{4}(1 + trace[\boldsymbol{C}]) \tag{18}$$

$$\beta_1^2 = \frac{1}{4}(1 + 2C_{11} - trace[\boldsymbol{C}]) \tag{19}$$

$$\beta_2^2 = \frac{1}{4}(1 + 2C_{22} - trace[\boldsymbol{C}]) \tag{20}$$

$$\beta_3^2 = \frac{1}{4}(1 + 2C_{33} - trace[\boldsymbol{C}]) \tag{21}$$

Where,

$$trace[\boldsymbol{C}] = C_{11} + C_{22} + C_{33} \tag{22}$$

The second step is to determine the largest squared value from equation (18) through (22). Once that is determined, take the square root of the largest value in order to find one of the Euler parameters. Finally, the remaining three Euler parameters can be determined using the three of the following equations.[14]

$$\beta_o\beta_1 = \frac{1}{4}(C_{23} - C_{32}) \tag{23}$$

$$\beta_0\beta_2 = \frac{1}{4}(C_{31} - C_{13}) \tag{24}$$

$$\beta_o\beta_3 = \frac{1}{4}(C_{12} - C_{21}) \tag{25}$$

$$\beta_2\beta_3 = \frac{1}{4}(C_{23} + C_{32}) \tag{26}$$

$$\beta_3\beta_1 = \frac{1}{4}(C_{31} + C_{13}) \tag{27}$$

$$\beta_1\beta_2 = \frac{1}{4}(C_{12} + C_{21}) \tag{28}$$

For example, the value for β_1 was found in step two. In order to find the other three Euler parameters equation (21) can be used to find β_o, equation (28) can be sued to find β_2, and equation (27) can be used to find β_3.[14]

The Euler parameters will change with time and the introduction of an angular velocity. In order to do this kinematics are introduced into the rotational motion equations. The motion of the Euler parameters can be described using the first derivative of the parameters. The first derivative of the Euler parameters is a function of the angular velocity and the original Euler parameters. The first order derivatives are expressed in matrix format in equation (29).[14]

$$\begin{bmatrix} \dot{\beta}_o \\ \dot{\beta}_1 \\ \dot{\beta}_2 \\ \dot{\beta}_3 \end{bmatrix} = \frac{1}{2} \begin{bmatrix} 0 & -\omega_1 & -\omega_2 & -\omega_3 \\ \omega_1 & 0 & \omega_3 & -\omega_2 \\ \omega_2 & -\omega_3 & 0 & \omega_1 \\ \omega_3 & \omega_2 & -\omega_1 & 0 \end{bmatrix} \begin{bmatrix} \beta_o \\ \beta_1 \\ \beta_2 \\ \beta_3 \end{bmatrix} \tag{29}$$

The ω_1, ω_2, and $\omega_3$variables are the X, Y, and Z-components of the angular velocity.[14] Now that the rotational motion equations have been defined, the position and velocity of the end masses in the TSS can be determined using rigid body dynamics.

2.3 Rigid Body Dynamics

Since the TSS will be modeled as a rigid body, the center of mass is the only point on the TSS that can be modeled using Keplarian motion. This means that the position and velocity of the main satellite and the sub-satellite must be calculated using rigid body dynamics. According to Ginsberg[12] the motion of a rigid body is a "superposition of a translation and a pure rotation." For the translational motion all points on the rigid body follow the movement of an arbitrary point on the body.[12] The arbitrary point for the TSS is the center of mass of the system. In Figure 2.3, the X, Y, Z coordinate system is placed at the center of mass of the TSS because when there is no angular velocity on the system the body coordinate system will line up with the geocentric equatorial system.

Another important note is that the position vectors between the center of mass and the two end masses will have constant components relative to the moving reference frame.[12] The moving reference frame in this case is the body fixed coordinate system; however, the final result needs to be expressed in terms of the geocentric equatorial coordinate system. The position of the center of mass is already expressed in terms of the geocentric equatorial coordinate system; therefore, all that is left to do is to convert the position vectors between the center of mass and

the two end masses into geocentric equatorial components. This is done by multiplying the direction cosine matrix by the vector of the distance between the center of mass and the end masses.

$$\bar{L}_{t1)ECI} = [\boldsymbol{C}]\bar{L}_{t1)BC} \tag{30}$$

$$\bar{L}_{t2)ECI} = [\boldsymbol{C}]\bar{L}_{t2)BC} \tag{31}$$

Equations (30) and (31) give the position vector from the center of mass to the sub-satellite and to the main satellite, respectively, in geocentric equatorial coordinates. The next two equations express the position of the sub-satellite and the main satellite in geocentric equatorial coordinates using the relative position equation.[20]

$$\bar{r}_1 = \bar{r}_{cm} + \bar{L}_{t1} \tag{32}$$

$$\bar{r}_2 = \bar{r}_{cm} + \bar{L}_{t2} \tag{33}$$

At this point, the disadvantage to using Euler parameters needs to be considered. Recall that the Euler parameters have a lack of uniqueness and the negative Euler parameters could describe the same position as positive Euler parameters. The sign on the position vectors from the center of mass to the end masses must be checked to make sure that the addition and subtraction of the distances matches up with the model.

Now that the position has been found for the end masses, the velocity of the sub-satellite and the main satellite needs to be found using rigid body dynamics. Ginsberg[12] and Meriam[20] define the velocity as the velocity of an arbitrary point plus the relative velocity between the point where the velocity is to be determined and the arbitrary point.[12,20] The arbitrary point

remains the center of mass of the TSS. Equation (34) and (35) defines the velocity of the sub-satellite and the main satellite, respectively.[12,20]

$$\bar{V}_1 = \bar{V}_{cm} + \bar{V}_{1/cm} \tag{34}$$

$$\bar{V}_2 = \bar{V}_{cm} + \bar{V}_{2/cm} \tag{35}$$

The second term on the right hand side of both equations is the relative velocity between the two end masses and the center of mass. The relative velocity is defined as the angular velocity vector crossed with the position vector between both points.[12,20]

$$\bar{V}_{1/cm} = \bar{\omega} \times \bar{L}_{t1} \tag{36}$$

$$\bar{V}_{2/cm} = \bar{\omega} \times \bar{L}_{t2} \tag{37}$$

The angular velocity is described in geocentric equatorial coordinates and the position vectors that will be used are those defined in equations (30) and (31). Equation (36) can be substituted into equation (34) to get the velocity of the sub-satellite. The velocity of the main satellite can be found by substituting equation (37) into equation (35).

$$\bar{V}_1 = \bar{V}_{cm} + \bar{\omega} \times \bar{L}_{t1} \tag{38}$$

$$\bar{V}_2 = \bar{V}_{cm} + \bar{\omega} \times \bar{L}_{t2} \tag{39}$$

Equations (32), (33), (38), and (39) are the rigid body equations used to find the position and velocity of the end masses of the TSS.

The movement of the center of mass of the TSS and the end masses differ slightly. The center of mass will move in a circular orbit. Rossi[25] states that if the TSS is modeled as a solid body it will rotate with a constant angular velocity in a counter – clockwise direction. If the TSS

moves only in an orbital plane, the system will have a radial configuration or it will form a straight line that is tangent to the circular orbit of the center of mass. The points of the TSS, the center of mass and the two end masses, must be collinear because the system is being treated as a rigid solid body.[25] If there is no librational motion, the center of mass and both the end mass of the TSS will move in concentric circles with the lower mass always being the sub-satellite.[19] Kaplan[16] states that the lower mass of the TSS will always remain in the sub-satellite position because of the gravity gradient on the system. The gravity gradient will create a spin stabilization that will keep the system at a local vertical; therefore, the sub-satellite will always be below the main.[16] The natural motion of the TSS is a rotation of the system in a counter – clockwise direction with the lower satellite always remaining the sub-satellite because of the gravity gradient.

2.4 Orbital Elements of a Trajectory

At the time of the sub-satellite's release, the orbital elements of the sub-satellite's impact trajectory will be calculated. The six orbital elements that describe an orbit are the semi-major axis (a), the eccentricity (e), the inclination (i), the longitude of the ascending node (Ω), the argument of periapsis (ω), and the true anomaly (θ). Figure 2.4 labels some of the orbital elements of an orbit.

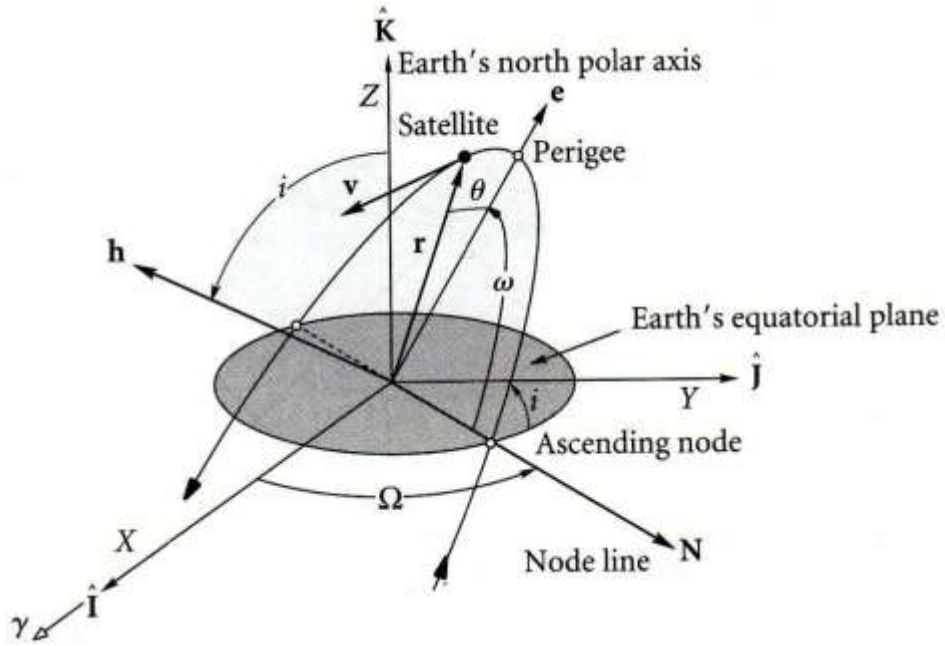

Figure 2.4: Orbital Elements of a Trajectory[10]

The semi-major axis defines the size of the orbit and the eccentricity defines the shape of a conic orbit.[1] The other four orbital elements are the inclination, the longitude of the ascending node, the argument of perigee or periapsis, and the true anomaly. The inclination is the angle between the $\bar{K}$ geocentric equatorial unit vector and the angular momentum vector, $\bar{h}$. The longitude of the ascending node is measured counter clockwise about the Z-axis from the X-axis to the ascending node on the orbit. The argument of periapsis is the angle between the ascending node and the periapsis or perigee point of the orbit. The argument of periapsis is measured in the plane of the satellite's orbit in the direction of travel of the satellite. The true anomaly, ν, is measure from the perigee point to the position vector of the satellite. The true anomaly is measured in the direction of travel of the satellite.[1] Each of these four parameters are shown in the orbit depicted in Figure 2.4.[10]

The orbital elements can be determined when the position and the velocity vector are known for a satellite. The eccentricity can be found by calculating the eccentricity vector.

$$\bar{e} = \left(\frac{V^2}{\mu} - \frac{1}{r} \right) \bar{r} - \frac{1}{\mu} (\bar{r} \cdot \bar{V}) \bar{V} \tag{40}$$

The magnitude of the eccentricity vector can then be found to get the eccentricity. Equation (41) is used to calculate the magnitude of the eccentricity vector.[10]

$$e = \sqrt{e_x^2 + e_y^2 + e_z^2} \tag{41}$$

The second orbital element that can be found is the semi-major axis. In order to find the semi-major axis the angular momentum must be calculated.

$$\bar{h} = \bar{r} \times \bar{V} \tag{42}$$

The magnitude of the angular momentum vector can then be calculated using the same formula that was used to find the eccentricity vector.

$$\frac{h^2}{\mu} = a(1 - e^2) \tag{43}$$

Equation (43) can then be rearranged to find the semi-major axis in terms of the eccentricity, the angular momentum, and the gravitational parameter.[10]

$$a = \frac{\frac{h^2}{\mu}}{1 - e^2} \tag{44}$$

The inclination can then be found by using the vector properties for an angle between two vectors. The two vectors that will be used are the angular momentum vector and the unit vector for the Z axis.[10]

$$\bar{h} \cdot \bar{K} = h|\bar{K}|cosi \tag{45}$$

The magnitude of a unit vector is always one and the angular momentum vector dotted with the unit vector will lead to the Z-component of the angular momentum vector.

$$h_k = hcosi \tag{46}$$

Equation (46) can then be arranged to find the inclination angle.[10]

$$i = \cos^{-1}\left(\frac{h_k}{h}\right) \tag{47}$$

The inclination will always be less than or equal to one hundred and eighty degrees.

The longitude of the ascending node can be found by forming the node vector, $\bar{N}$. The node vector is a constant vector that points in the direction of the ascending node. Equation (48) can be used to find the node vector.[10]

$$\bar{N} = \bar{K} \times \bar{h} = h_i\bar{J} - h_j\bar{I} \tag{48}$$

The node vector consists of the X and Y components of the angular momentum. The magnitude of the node vector can be found in the same way that the magnitude of the eccentricity vector was found. The longitude of the ascending node is the angle between the X unit vector and the node vector.[10]

$$\bar{N} \cdot \bar{I} = N|\bar{I}|cos\Omega \tag{49}$$

$$-h_j = N cos\Omega \tag{50}$$

$$\Omega = \cos^{-1}(\frac{-h_j}{N}) \tag{51}$$

Equation (51) can be used find the longitude of the ascending node; however, the quadrant of the longitude of the ascending node must be determined. In order to find the quadrant for the longitude of the ascending node the Y-component for the node vector must be looked at. The test to determine the quadrant of the longitude of the ascending node is described in equation (52).[10]

$$\begin{aligned} if\ N_j > 0 \ &=> \ \Omega < 180° \\ if\ N_j < 0 \ &=> \ \Omega > 180° \end{aligned} \tag{52}$$

For the case when the Y-component of the node vector is less than zero, the longitude of the ascending node must be recalculated. The new longitude of the ascending node can be found in equation (53).[10]

$$\Omega = 360° - \ \Omega \tag{53}$$

The argument of periapsis is the angle between the node vector and the eccentricity vector. The same process to find the longitude of the ascending node and the inclination are used to find the argument of periapsis.[10]

$$\omega = \cos^{-1}\left(\frac{\bar{N} \cdot \bar{e}}{Ne}\right) \tag{54}$$

The quadrant for the argument of periapsis must also be determined. This time the variable that will be looked at to determine the quadrant is the Z-component of the eccentricity vector. The test is described in Equation (55).[10]

$$\begin{aligned} if\ e_z > 0 &=>\ \omega < 180° \\ if\ e_z < 0 &=>\ \omega > 180° \end{aligned} \tag{55}$$

For the case when the Z-component of the eccentricity vector is negative, the argument of periapsis must be subtracted from three hundred and sixty degrees. This will result in an angle greater than one hundred and eighty degrees.[10]

$$\omega = 360° - \omega \tag{56}$$

The final orbital element to be found is the true anomaly. The true anomaly is the angle between the eccentricity vector and the position vector. This means that the true anomaly can be found using the same method that was used for the previous three orbital elements. Equation (57) gives the true anomaly as a function of the eccentricity vector and position vector, as well as their magnitudes.[10]

$$\theta = \cos^{-1}\left(\frac{\bar{e} \cdot \bar{r}}{er}\right) \tag{57}$$

The quadrant for the true anomaly must be determined as well. The test involves the result from taking the dot product of the position vector with the velocity vector.[10]

$$\begin{aligned} if\ \bar{r} \cdot \bar{V} > 0 &=>\ \theta < 180° \\ if\ \bar{r} \cdot \bar{V} < 0 &=>\ \theta > 180° \end{aligned} \tag{58}$$

If the dot product is found to be negative, the true anomaly must be recalculated in order to be greater than one hundred and eighty degrees. The new true anomaly for a negative dot product is given in equation (59).[10]

$$\theta = 360° - \theta \tag{59}$$

The six orbital elements found in this section can be used to describe the trajectory of the sub-satellite once it is released from the TSS. Some of the elements can be used to determine if the sub-satellite will impact the Earth without having to propagate the trajectory of the sub-satellite forward in time. The elements that are used to determine impact are the semi-major axis and the eccentricity vector. These two orbital elements can be used to calculate the distance at the perigee point of the trajectory. The perigee point on a trajectory is the lowest point of the satellite's orbit.[10]

$$r_p = a(1 - e) \tag{60}$$

If the perigee point is found to be less than the radius of the Earth, then the satellite will impact the Earth. Being able to determine if the sub-satellite will impact before propagating the motion forward in time will save computational time. The goal of this study is to determine the impact capabilities of the impact trajectories after release and how different changes affect the time to impact and range; therefore, if the satellite does not impact the Earth, the propagation of the motion of the satellite does not need to be done.

2.5 Numerical Integration Using a 4th Order Runge Kutta

Numerical integration is used to solve ordinary differential equations. This feature allows a state matrix consisting of position, velocity, and constants to be propagated forward in time. Numerical integration methods use a Taylor series expansion to solve the ordinary differential equations. The Euler method approximates the solution to the ordinary differential equations using the first-order term from the Taylor series. The first and second terms of the Taylor series are used for the improved Euler method. The Runge Kutta method used for this research approximates the higher derivatives using finite-difference expressions. This means

that the higher derivatives do not have to be calculated from the original ordinary differential equation that is given.[17]

The approximation for the Runge Kutta is done by calculating data through a series of time steps from an initial time, t_o, to a final time, t_f. The order of the Runge Kutta method is determined by the number of steps used to estimate the state vector after a time step. For this research a fourth order Runge Kutta is used because it is the most common version of the Runge Kutta method. Equations (61) through (64) list the four steps used for the fourth order Runge Kutta method.[17]

$$k_1 = f[\bar{X}(t_o), t_o] \tag{61}$$

$$k_2 = f\left[\bar{X}(t_o) + \Delta t\frac{k_1}{2}, t_o + \frac{\Delta t}{2}\right] \tag{62}$$

$$k_3 = f\left[\bar{X}(t_o) + \Delta t\frac{k_2}{2}, t_o + \frac{\Delta t}{2}\right] \tag{63}$$

$$k_4 = f[\bar{X}(t_o) + \Delta t k_3, t_o + \Delta t] \tag{64}$$

The function, f, is used to find the first derivative of the state vector using the state vector, $\bar{X}$, at the initial time. After the first step, step two and three are calculated after half of the time step, Δt, has passed. The fourth step is calculated at the initial time plus the time step. After each time step a new state vector is calculated.[17]

$$\bar{X}(t_o + \Delta t) = \bar{X}(t_o) + \frac{\Delta t}{6}(k_1 + 2k_2 + 2k_3 + k_4) \tag{65}$$

The four step process is continued until the final time is reached and a final state vector is calculated. A Runge Kutta method can be implemented in MATLAB using a WHILE loop or a

for loop to get from the initial time to the final time using any time step. Typical values for the final time are the orbital period of the satellite and the time for a single day. The set-up of the state vector and the terms of the first derivative of the state vector are discussed in chapter three.

2.6 Analytical Approach

In order to establish an analytical approach to the TSS problem more orbital mechanics equations must be introduced. The energy of an orbit remains constant and can be calculated by using the semi-major axis or the position and velocity magnitudes of the satellite. Both ways to calculate the energy of an orbit are shown in equation (66).[10]

$$E = \frac{V^2}{2} - \frac{\mu}{a} = \frac{-\mu}{2a} \tag{66}$$

The trajectory equation is used to find the position of a satellite when the semi-major axis, the eccentricity, and the true anomaly of the satellite are known as given in equation (67).

$$r = \frac{a(1 - e^2)}{1 + e\cos\theta} \tag{67}$$

The energy equation and the trajectory equation will be used later in chapter 3 to find an analytical solution to the range and time to impact problem for the sub-satellite.

The next equation set will be used to find the time to impact for the analytical solutions. Kepler's Equation gives the mean anomaly in terms of the eccentric anomaly, E, and the eccentricity.[10]

$$M = E - e\sin E \tag{68}$$

The mean anomaly can be expressed in terms of the mean motion, n, and a difference in time.[10]

$$M = n(t_1 - t_o) \tag{69}$$

The difference in time stands for the time at the eccentric anomaly minus the time at perigee. Equations (68) and (69) can be defined at two different points, a point one and a point two, and combined into the differenced Kepler's equation.[10]

$$n(t_{rel} - t_o - t_{imp} + t_o) = E_{rel} - e\sin E_{rel} - E_{imp} + e\sin E_{imp} \tag{70}$$

$$n(t_{rel} - t_{imp}) = E_{rel} - e\sin E_{rel} - E_{imp} + e\sin E_{imp} \tag{71}$$

Where,

$$n = \sqrt{\frac{\mu}{a^3}} \tag{72}$$

$$E = 2\tan^{-1}\left[\left(\frac{1-e}{1+e}\right)^{1/2}\tan\left(\frac{\theta}{2}\right)\right] \tag{73}$$

The difference in time expressed in equation (71) is the time from release to impact. Point one is the place in the orbit where the sub-satellite is released from the TSS and point two is the place in the impact trajectory of the sub-satellite where the sub-satellite impacts the Earth. Equations (71), (72), and (73) can be used to find the time to impact. Equation (73) is the same for points one and two. The only value that changes is the true anomaly. The first true anomaly corresponds to the true anomaly at release and the second true anomaly corresponds to the true anomaly at impact.

Chapter 3: Model and Problem Formulation

In order to investigate this problem, a simplified model is developed for the TSS and the initial velocity for the center of mass of the TSS is determined. A numerical integration method is used to propagate the motion of the center of mass of the system using Keplerian motion. The position and velocity of the end masses is then determined relative to the center of mass. Once the system successfully travels in its baseline orbit, changes into the system can be introduced. There are three main changes that are applied to the system: a velocity change on the sub-satellite, a change in the altitude of the TSS, a change in tether length of the TSS, and a change in the release point location. The change in velocity is needed in order to cause the sub-satellite to enter an impact trajectory, while the tether length and altitude are changed in order to determine their effect on the range and time to impact. As stated before, the velocity change placed on the sub-satellite will be a result of an impulsive velocity change maneuver or a change to the angular velocity of the system. The tether is cut after the velocity change is implemented and the trajectory of the released mass is calculated to determine if the trajectory of the sub-satellite impacts the Earth after release. If the sub-satellite impacts the Earth, then the time to impact and the range from release to impact are calculated. This information is then used to determine how the changes in the system affect the ballistic capabilities of the sub-satellite after release. An analytical solution is also developed to examine situations where the sub-satellite is directly above, below, to the right, and to the left of the main satellite. At each of these orientations the analytical solution can be used to determine the maximum and minimum ranges and times to impact when given a range of velocity changes. A second set of analytical solutions

are also developed in order to determine an equivalent angular velocity that can be done in place of an impulsive velocity change. The set-up and algorithms for the simulation and analytical solutions are discussed in this chapter.

3.1 Problem Set-up of the TSS

Before numerical integration of the equations of motion can be performed and before an impact of the sub-satellite can be evaluated an initial position and velocity must be determined. The initial set-up of the TSS needs to be performed in such a way that the position and velocity of the center of mass and the end masses can be easily determined. The initial set-up for the TSS is shown in Figure 3.1.

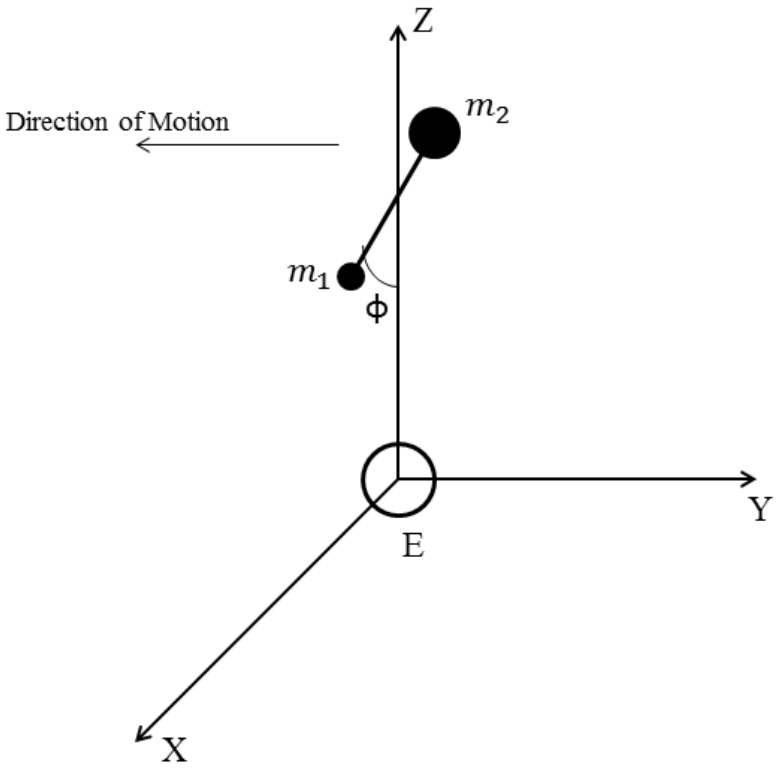

Figure 3.1: Initial Set-up of the TSS for a Negative φ

The center of mass of the TSS is initially placed along the Z axis so that the position of each of the end masses can be determined from the altitude, TSS orientation, and tether length. The direction of travel of the TSS is counter-clockwise about the origin of the geocentric equatorial coordinate system and about the positive X - axis. The orbit for the center of mass is assumed to be circular in shape.

In order to determine the positions of the end masses and the center of mass the altitude, tether length, and the size of the masses must be chosen. It's also important to keep in mind that the tether itself is modeled as a massless, rigid tether. A 10:1 ratio between the main satellite and the sub-satellite was selected; therefore, the mass of the main satellite was assigned a value of 1000 kg and the sub-satellite was assigned a mass of 100 kg. The altitude measures the height of the main satellite above the Earth. The sub-satellite is then "lowered down" from the main satellite until the tether is completely extended. For the baseline case the altitude was 500 km above the Earth's surface with a tether length of 4 km. The angular velocity of the system is set to zero. Changes to the baseline values will be made in order to determine the effects of the altitude and tether length on the range and time to impact for an impact trajectory of the sub-satellite. The masses of the two satellites will always remain constant.

With the baseline values determined, the position of the end masses and the position and velocity of the center of mass can be determined. In order to determine the positions of the TSS, the system is assumed to be completely aligned with the Z axis. In other words the rotation angle is zero. Since the TSS is aligned with the Z axis of the geocentric equatorial system, the positions of the end masses can be determined by adding and subtracting values without having to worry about the other two axes directions. The main satellite position can be calculated by adding the radius of the Earth to the altitude. The tether length can then be subtracted from the

position of the main satellite to get the position of the sub-satellite. The calculations for the position of the main satellite and for the sub-satellite are shown in equations (74) and (75), respectively.

$$r_2 = R_e + H \tag{74}$$

$$r_1 = R_e + H - L_t \tag{75}$$

Both of the positions are initially in the $\bar{K}$ direction. The position and velocity of the center of mass are then calculated using equations (1) and (2). The position for the center of mass is along the $\bar{K}$ direction. The velocity of the center of mass that is calculated is the circular velocity and is tangent to the circular orbit. Since the TSS moves in a counter-clockwise direction, the initial velocity of the center of mass is in the negative $\bar{J}$ direction.

With the position of the center of mass determined, the length between the center of mass and the two end masses can be calculated. For this initial case the direction of the lengths between the center of mass and the two end masses is in the $\bar{K}$ direction.

$$L_{t1} = r_{cm} - r_1 \tag{76}$$

$$L_{t2} = r_2 - r_{cm} \tag{77}$$

The next step after determining the distances between the end masses and the center of mass is to find the four Euler parameters with the rotation angle in place. In order to find the four Euler parameters a direction cosine matrix must be generated. The direction cosine matrix for this instant in time and with a rotation angle can be calculated using the rotation transformation about an X axis.[12]

$$C = \begin{bmatrix} 1 & 0 & 0 \\ 0 & \cos\varphi & \sin\varphi \\ 0 & -\sin\varphi & \cos\varphi \end{bmatrix} \quad (78)^{9}$$

The process described in chapter 2 to find the Euler parameters from a given direction cosine matrix using equations (18) through (28) are used to find the Euler parameters for the initial set-up of the TSS. As the direction cosine matrix changes the direction of the distance between the end masses and the center of mass will change; however, the magnitude of the distances will remain constant. In order to determine the new directions the direction cosine matrix must be pre-multiplied by the magnitude of the two lengths. This process is shown in equations (30) and (31). The vector components are then added or subtracted from the position of the center of mass to determine the new position of the end masses. This process is shown in equations (32) and (33).

Before the numerical integration is started the velocity for the main satellite and sub-satellite must be calculated. Equations (38) and (39) are used to find the velocity vector for the sub-satellite and the main satellite, respectively. The determination of the velocity vector and the determination of the position vector for the end masses will be done at each time step until the sub-satellite is released. This is done in order to keep track of the position and velocity vector for the sub-satellite at release. Once the position and the velocity vectors have been calculated the numerical integration can be started.

In order to do a numerical integration, the initial and final time and an initial state vector are needed. The initial time for the system is set to zero and a final time is set to one day. Giving a day for the motion of the TSS, the release of the sub-satellite, and the motion of the sub-satellite allows for the determination of the time to impact and the range of an impact

trajectory. The time step used for the numerical integration is five seconds; however, the time step is decreased later when the tether length is increased. Before the release of the sub-satellite, the state vector will contain 15 terms. The terms include the position and velocity components of the center of mass, the true anomaly, the four Euler parameters, the angular velocity, and the rotation angle.

$$\bar{X} = \begin{bmatrix} \bar{r}_{cm} \\ \bar{V}_{cm} \\ \theta \\ \beta_o \\ \beta_1 \\ \beta_2 \\ \beta_3 \\ \bar{\omega} \\ \varphi \end{bmatrix} \tag{79}$$

The function in the numerical integration calculates the first derivative of the state vector. The derivative of the state vector is calculated in four steps as described in equations (61) through (64). In order to get the derivative of the state vector the derivatives of the individual elements must be taken. The first derivative of the state vector contains the velocity of the center of mass, the acceleration of the center of mass, the first derivative of the true anomaly, the first derivative of the four Euler parameters, the angular acceleration, and the derivative of the rotation angle. Equation (80) gives the first derivative of the state vector.

$$\dot{\bar{X}} = \begin{bmatrix} \bar{V}_{cm} \\ \bar{a}_{cm} \\ \dot{\theta} \\ \dot{\beta}_o \\ \dot{\beta}_1 \\ \dot{\beta}_2 \\ \dot{\beta}_3 \\ \bar{\alpha} \\ \dot{\varphi} \end{bmatrix} \tag{80}$$

The velocity of the center of mass is taken from the original state vector. The first derivative of the velocity of the center of mass is equal to the acceleration of the center of mass. Since the acceleration of the center of mass was not in the original state vector, the acceleration must be calculated using equations (10) through (12). The derivative of the true anomaly must now be calculated.

Lovell's procedure[18] is used to determine the first derivative of the true anomaly using the position and velocity of the center of mass. The first step is to calculate the magnitude of the angular momentum in geocentric coordinates and polar coordinates. Equation (81) gives the magnitude of the angular momentum for geocentric coordinates.[18]

$$h = |\bar{r} \times \bar{V}| = \sqrt{(r_y V_z - r_z V_y)^2 + (r_z V_x - r_x V_z)^2 + (r_x V_y - r_y V_x)^2} \tag{81}$$

Lovell then finds the magnitude of the angular momentum in terms of the body fixed coordinate system expressed in polar coordinates. Equation (82) gives the magnitude for the angular momentum using the body fixed coordinates assigned earlier in chapter two.[18]

$$h = |\bar{r} \times \bar{V}| = \left| r\bar{X}_2 \times (\dot{r}\bar{X}_2 + r\dot{\theta}\bar{Y}_2) \right| = r^2\dot{\theta} \tag{82}$$

The angular momentum of an orbit remains constant and the magnitude will always be the same value no matter what coordinate system is used to express the components. The next step is to set equation (81) and (82) equal to each other and solve for the first derivative of the true anomaly. The solution is given below.

$$\dot{\theta} = \frac{\sqrt{(r_y V_z - r_z V_y)^2 + (r_z V_x - r_x V_z)^2 + (r_x V_y - r_y V_x)^2}}{r^2} \tag{83}$$

The X, Y, and Z components from the position vector and the velocity vector can be taken from any position or velocity vector. For this case the components will come from the position and velocity vector of the center of mass, so that the true anomaly of the system can be tracked.

The first derivatives of the Euler parameters, the angular acceleration, and the first derivative of the rotation angle now have to be determined. The derivatives of the four Euler parameters are calculated using equation (29). The angular acceleration and angular velocity for all cases is kept at zero. The derivative of the rotation angle is equal to the angular velocity. The equivalent angular velocity needed to replace the impulsive velocity change for impact is in the negative or positive X_2 – direction of the body coordinate system, which is parallel to the X – direction of the ECI coordinate system. Since the study is focused on the in-plane motion of the sub-satellite, rotation of the TSS about the Y_2 and Z_2 axes is zero. This means that the Y_2 and Z_2 components of the equivalent angular velocity will be zero.

This process is continued within a loop until the point that the sub-satellite is released. Prior to release an impulsive velocity change is done by the sub-satellite. After the velocity change, the sub-satellite is released from the system at the desired configuration and the release point position and velocity of the sub-satellite are calculated as described below.

$$\bar{V}_{1rel} = \bar{V}_1 - \Delta\bar{V} \tag{84}$$

The term on the left hand side of equation (84) stands for the velocity of the sub-satellite at release. An equivalent angular velocity that could cause impact can then be calculated by setting equation (84) equal to equation (38).

$$\bar{V}_{1rel} = \bar{V}_{cm} + \bar{\omega} \times \bar{L}_{t1} \tag{85}$$

The angular velocity in the X - direction can then be solved for using equation (85). There are two ways to calculate the angular velocity in the X - Direction. If the velocity of the sub-satellite changes in the Y-direction, equation (86) is used; and equation (87) is used to find the angular velocity when the velocity changes in the Z-direction.

$$\omega_1 = \frac{V_{1rely} - V_{cmy}}{-(r_{1z} - r_{cmz})} \tag{86}$$

$$\omega_1 = \frac{V_{1relz} - V_{cmz}}{r_{1y} - r_{cmy}} \tag{87}$$

Equations (86) and (87) can then be solved for the velocity change of the sub-satellite. The velocity change is expressed in vector form in equation (88).

$$\Delta\bar{V} = \bar{\omega} \times \bar{L}_{t1} \tag{88}$$

From equation (88), it can be seen that the velocity change of the sub-satellite is related to the angular velocity of the system. This is why an impulsive velocity change or a change in the angular velocity can lead to the same ballistic capabilities of the sub-satellite.

Before a new numerical integration is done for the sub-satellite only, the orbital elements of the sub-satellite's impact trajectory are calculated in order to determine if the sub-satellite will impact the earth. Since the position and velocity vectors of the sub-satellite have been calculated the orbital elements can be calculated using the process discussed in section 2.4. Equation (60) is then used to calculate the perigee position of the sub-satellite along its impact trajectory. If the perigee position of the sub-satellite is greater than the radius of the Earth, the sub-satellite will not impact the earth and the program breaks out of the loop to begin a new test from the beginning. This is done in order to save computational time. When the perigee position is found

to be less than the radius of the Earth, a new state vector is created in order to model the motion of the sub-satellite after release from the system.

The state vector for the sub-satellite after release is smaller than the state vector needed for the TSS. The Euler parameters are no longer needed to model the sub-satellite, since the sub-satellite is considered to be a point mass. There is also no rotation angle for the sub-satellite because all vectors can now be expressed in terms of the geocentric coordinates only. The new state vector that will be used in a 4th order Runge Kutta is expressed in equation (89).

$$\bar{X} = \begin{bmatrix} \bar{r}_1 \\ \bar{V}_1 \end{bmatrix} \tag{89}$$

The first derivative of the state vector is then calculated for the numerical integration.

$$\dot{\bar{X}} = \begin{bmatrix} \bar{V}_1 \\ \bar{a}_1 \end{bmatrix} \tag{90}$$

The velocity vector is taken from the original state vector. The acceleration of the sub-satellite can be calculated using the same equations as before by replacing the position and acceleration center of mass values with the position and acceleration of the sub-satellite.

$$-\frac{\mu}{r_1^3} x_1 = \ddot{x}_1 \tag{91}$$

$$-\frac{\mu}{r_1^3} y_1 = \ddot{y}_1 \tag{92}$$

$$-\frac{\mu}{r_1^3} z_1 = \ddot{z}_1 \tag{93}$$

The state vector for the sub-satellite is then propagated forward in time using the numerical integration. This is done until impact occurs or a full day goes by. After a full day

goes by, the simulation stops because a day to reach an impact point is too long of a travel time for a threat. When the magnitude of the position vector is equal to or less than the radius of the Earth, impact of the sub-satellite will occur. When this happens, the program breaks out of the loop and completes the numerical integration.

Before the range and time to impact can be calculated, the true anomaly at impact and the true anomaly at release must be calculated using the eccentricity and the semi-major axis from the impact trajectory. The first step is to take the trajectory equation in equation (67) and solve for the true anomaly.

$$\theta_{rel} = \cos^{-1}\left(\frac{a(1-e^2)-r_1}{r_1 e}\right) \tag{94}$$

The magnitude for the position of the sub-satellite in equation (94) is dependent upon the true anomaly that is trying to be found. If equation (94) is used to find the true anomaly at impact than the position of the sub-satellite is equal to the radius of the Earth.

$$\theta_{imp} = \cos^{-1}\left(\frac{a(1-e^2)-R_e}{R_e e}\right) \tag{95}$$

Equation (95) may give a true anomaly at impact that is less than the true anomaly at release. Since impact occurs after the true anomaly at release, the true anomaly at impact must be greater than the true anomaly at release. This change can be done by following the test in equation (96).

$$\begin{gathered} if\ \theta_{imp} < \theta_{rel} \\ \theta_{imp} = 2\pi - \theta_{imp} \end{gathered} \tag{96}$$

With the true anomaly at impact in the correct quadrant, the range and time to impact can be calculated using the following equations.

$$R = R_e\left(|\theta_{imp} - \theta_{rel}|\right) \tag{97}$$

$$t_{impact} = t_f - t_{rel} \tag{98}$$

The angle for the arc length in equation (97) is the absolute value of the true anomaly at impact minus the true anomaly at release. The time to impact subtracts the time at release from the final time when impact occurs. The impact of the sub-satellite can take longer than a day depending on the type of changes that are placed on the system. Usually an impact that takes longer than a day means that the impact trajectory of the sub-satellite is hyperbolic. If the impact takes longer than a day, the program continues to run until the end of the day but will not calculate the range or time to impact because the sub-satellite has not impacted yet. For the range and time to impact to be calculated the total time for the numerical integration to run must be increased. With this test complete the process can be continued with new altitude and tether length values. The changes placed on the system to create an impact trajectory will be discussed in the next section.

3.2 Changes Applied to the System to Create Impact of Sub-Satellite

For this research two configurations are chosen for the sub-satellite upon release during the numerical simulation. These configurations were chosen to model possible real world scenarios for releasing the sub-satellite from the TSS. The first configuration of the sub-satellite at release will have the sub-satellite located below the main satellite with a rotation angle of -0.5 radians. The second configuration will place the sub-satellite above the main satellite using a rotation angle of about -3.6416 radians. The rotation angle is depicted in figure 3.1 and measures the position of the sub-satellite from the vertical Z – axis. The rotation angle also

keeps the sub-satellite in a leading position. More points can be chosen and the program can be easily changed to reflect the new configuration or configurations of the sub-satellite at release.

Simply releasing the sub-satellite from the TSS by cutting the tether does not always create an impact trajectory. In order to create impact trajectories an impulsive velocity change of the sub-satellite or a change in the angular velocity of the system must be introduced prior to the time of release. The change in velocity of the sub-satellite is increased or decreased in the Z direction or the Y direction. All changes in velocity are tested within the program because a velocity change in the positive Y direction may cause the impact of the sub-satellite to occur at a small velocity change, while a large change in velocity in the negative Z direction may be needed in order to cause an impact. In order to get the change in the sub-satellite velocity to occur, a thrust force is generated by the sub-satellite. The thrust force is not modeled in the program because the research is not concerned with how the velocity change occurs, but on what is the minimum velocity change needed to cause impact and how the velocity change will affect the range and time to impact for the sub-satellite system. It is also important to note that a change in velocity still may not cause the sub-satellite to impact. The test for impact is done because of the fact that an impact still may not occur even with a large velocity change. If a change in velocity is not done on the sub-satellite, a change in the angular velocity can be placed on the system prior to the time of release in order to create an impact. This angular velocity is produced by the main satellite and sub-satellite generating a thrust that would cause the TSS to rotate about the center of mass. Once again, the thrust changes are not modeled.

The velocity of the sub-satellite can also be changed by introducing a velocity change in the X direction; however, this case is not investigated because the motion of the TSS is restricted to the Y-Z plane. Introducing a change in the X direction will cause out of plane librational

motion that will need to be accounted for. While the out of plane librational motion can be introduced into the program, it will severely complicate the program and the set-up or model of the TSS. One of the goals of this research is to investigate the impact of the changes in altitude, tether length, and angular velocity using a simplified model for the TSS. For this reason velocity changes in the X direction on the sub-satellite are not considered in this research.

3.3 Variations to the Problem Set-up

The changes in the velocity of the sub-satellite discussed in the previous section will help to lead to an impact and will affect the range and time to impact for the sub-satellite. The main properties of the TSS that will be changed are the altitude and the tether length of the system. When a change in the velocity of the sub-satellite leads to an impact, changes in the altitude and tether length will be analyzed in order to determine if these changes lead to an increase or a decrease in the range and time to impact.

The altitude that is being changed is the altitude for the main satellite. In this case the tether length of the TSS is kept constant at four kilometers. The range of the altitude goes from five hundred kilometers to fifteen hundred kilometers. The minimum value of five hundred kilometers was chosen because the drag force due to the Earth's atmosphere does not have to be taken into account at this point. As the altitude of a satellite decreases and gets closer to the Earth, the atmospheric drag must be taken into account. The altitude is increased in increments of fifty kilometers. At each altitude the program is run as discussed in section 3.1 in order to determine the range and time to impact for the sub-satellite after release. The increase in altitude should lead to an increase in the range and time to impact because the sub-satellite is located at a higher position at release.

The range of values used for the tether length is one kilometer to one hundred kilometers. Three kilometers are used as the increment change from one kilometer to one hundred kilometers. For this case the altitude is held constant at a value of five hundred kilometers. The tether length can either increase or decrease the range and time to impact of the sub-satellite depending on the location of the sub-satellite relative to the main satellite at the point of release. For example, if the sub-satellite is located above the main satellite, an increase in the tether length should lead to an increase in the range and time to impact. On the other hand, if the sub-satellite is located below the main satellite, an increase in the tether length should decrease the range and time to impact of the sub-satellite.

3.4 Analytical Solutions

This section discusses the formulation of equations and algorithms for the analytical solution to the impact problem of a sub-satellite after it is released from a TSS. The first analytical solution that is determined can be used to find the range and time to impact given initial conditions for the TSS. The second analytical solution solves the problem backwards. In other words, given the range, true anomaly at impact, and some other initial conditions find the change in the angular velocity of the TSS or the impulsive velocity change needed in order to achieve the desired range at impact. The reason behind the analytical approach is to force the sub-satellite to be directly below, above, to the right, or to the left of the main satellite. The set up for the four cases are depicted in figure 3.2, which is located before the next section.

The position of the center of mass, the main satellite, and the sub-satellite must be determined for each case. Each position component can be described in terms of the radius of the Earth, the altitude of the main satellite, and the tether length. The position of the main satellite will always be in the positive Z – direction and equal to the radius of the Earth plus the

altitude. Table 3.1 gives the position of the sub-satellite for each of the four cases. Case A, B, C, and D correspond to when the sub-satellite is located above, below, to the right, and to the left of the main satellite, respectively. In table 3.1 the components of the sub-satellite position are given for each case. The X-component of the sub-satellite position vector is always equal to zero because the orbital motion is kept in the Y-Z plane.

Table 3.1 Sub-satellite Position Components for Cases A - D

Case	X-Component (km)	Y-Component (km)	Z-Component (km)
A	0	0	$R_e + H + L_t$
B	0	0	$R_e + H - L_t$
C	0	L_t	$R_e + H$
D	0	$- L_t$	$R_e + H$

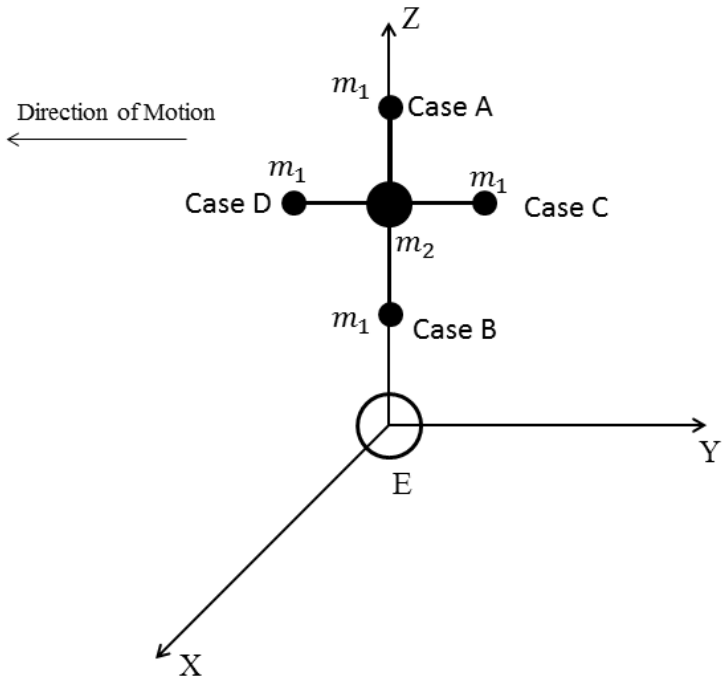

Figure 3.2 Analytical Cases

3.4.1 Equations to Find the Range and Time to Impact

For this set of analytical equations the goal is to find expressions for the range and time to impact. It is assumed that the altitude of the main satellite, the length of the tether, the angular velocity of the TSS, and the impulsive velocity change of the sub-satellite are known. The angular velocity can have three components in the X_2, Y_2, and Z_2 – directions; however, the Y_2 and Z_2 – components of the angular velocity are equal to zero because the trajectory of the TSS remains in the Y-Z plane. For all cases an impulsive velocity change is placed on the sub-satellite; therefore, the angular velocity in the X_2 or X direction will also be zero . Since the only known values are the altitude, tether length, angular velocity, and the velocity change of the sub-satellite, the range and time to impact must be functions of these four known values for the given mass ratio.

In order to find the range the true anomaly at impact and the true anomaly at release, equation (97) must be expressed in terms of the four known variables. Since the radius of the Earth is a constant and the magnitude of the position vector is a function of the altitude, the tether length, and the radius of the Earth, the semi-major axis and the eccentricity of the impacting trajectory must now be expressed in terms of the four known values. The energy equation, or equation (66), can be used to find the semi-major axis.

$$a = \frac{-\mu}{V_{1rel}^2 - \frac{2\mu}{r_1}} \tag{99}$$

Equation (43) can then be used to solve for the eccentricity.

$$e = \sqrt{1 - \frac{h^2}{\mu a}} \tag{100}$$

Equation (99) can then be substituted into equation (100).

$$e = \sqrt{1 + \frac{h^2(V_{1rel}^2 - 2\mu)}{\mu^2 r_1}} \tag{101}$$

Equation (102) expresses the angular momentum of the sub-satellite's impact trajectory.

$$h = \bar{r} \times \bar{V} = |\bar{r}||\bar{V}| \cos\gamma \tag{102}$$

The point of release for the sub-satellite is located at the point near the apogee of the impact trajectory, where the flight path angle is zero. The angular momentum can now be expressed in terms of the magnitudes of the position and velocity vectors of the sub-satellite after release.

$$h = r_1 V_{1rel} \tag{103}$$

The velocity of the sub-satellite can be written as

$$\bar{V}_1 = \bar{V}_{cm} + \bar{\omega} \times (\bar{r}_1 - \bar{r}_{cm}) \tag{104}$$

The velocity of the center of mass can be found by using equation (2). The angular velocity only has a single vector component.

$$\bar{\omega} = \omega\,(\bar{I}) \tag{105}$$

The velocity vector for the sub-satellite can be written as

$$\bar{V}_1 = \left[V_{cmy} - \omega_x(r_{1z} - r_{cmz})\right](\bar{J}) + [(V_{cmz}) + \omega_x\left(r_{1y} - r_{cmy}\right)](\bar{K}) \tag{106}$$

The final step is to calculate the magnitude of the sub-satellite velocity at release. A change in velocity can then be added to the velocity of the sub-satellite to get the velocity at release, as

shown in equation (84). The magnitude of the sub-satellite velocity can then be found by taking the square root of the components squared.

Now that all the terms have been found for the true anomaly the range equation can be defined. The true anomaly at release is assumed to be one hundred and eighty degrees. Equations (99), (101), and (102) are substituted into equation (95) to get the true anomaly at the impact point. The true anomaly at the impact point is then substituted into equation (97). The range formula given in equation (107) is now a function of the altitude, tether length, angular velocity, and velocity change of the sub-satellite.

$$R = R_e\left(\left|\cos^{-1}\left(\frac{b(1-c^2)-R_e}{R_e c}\right)-\pi\right|\right) \tag{107}$$

Where,

$$b = \frac{-\mu}{V_{1rel}^2 - \frac{2\mu}{r_1}} \tag{108}$$

$$c = \sqrt{1-\frac{(r_1 V_{1rel})^2}{\mu b}} \tag{109}$$

In order to get the time to impact for the impact trajectory, the time at release and the time at impact must be calculated. The time at release can then be found by taking half of the orbital period, given by

$$t_{rel} = \frac{1}{2}T = \pi\sqrt{\frac{a^3}{\mu}} \tag{110}$$

Since the true anomaly at impact is known, it can be substituted into equation (73) to get the eccentric anomaly at impact. The time at impact can then be found by using equations (68) and (69), giving

$$t_{imp} - t_o = \frac{E_{imp} - e \sin E_{imp}}{\sqrt{\frac{\mu}{a^3}}} \tag{111}$$

The initial time in equation (111) is equal to zero because it is the time at perigee.

$$t_{imp} = \frac{E_{imp} - e \sin E_{imp}}{\sqrt{\frac{\mu}{a^3}}} \tag{112}$$

This same method can be used to find the time at release if the true anomaly at release is not equal to one hundred and eighty degrees. The true anomaly at release would be used in equation (73) to find the eccentric anomaly at release.

The time to impact can now be found by subtracting the time at impact from the time at release, as

$$t_{impact} = t_{imp} - t_{rel} \tag{113}$$

Another method can be used to find the position of the sub-satellite if the center of mass position and velocity vector, and the rotational angle are known in addition to the other values. The position vector between the center of mass and the sub-satellite is defined in equation (114).

$$\bar{L}_{t1} = L_{t1} \sin\varphi \ (\bar{J}) + L_{t1} \cos\varphi \ (\bar{K}) \tag{114}$$

Substituting into equation (32) gives

$$\bar{r}_1 = \left(r_{cmy} + L_{t1}\sin\varphi\right)(\bar{J}) + (r_{cmz} + L_{t1}\cos\varphi)(\bar{K}) \tag{115}$$

which has a magnitude of

$$r_1 = \sqrt{(r_{cmy} + L_{t1}\sin\varphi)^2 + (r_{cmz} + L_{t1}\cos\varphi)^2} \tag{116}$$

For the case when the angular momentum of the sub-satellite is

$$\bar{h} = \left(r_{1y}\bar{J} + r_{1z}\bar{K}\right) \times \left(V_{1rely}\bar{J} + V_{1relz}\bar{K}\right) \tag{117}$$

Equation (117) can then be simplified to

$$\bar{h} = \left(r_{1y}V_{1relz} - r_{1z}V_{1rely}\right)\bar{I} \tag{118}$$

Having the magnitude of

$$h = \sqrt{(r_{1y}V_{1relz} - r_{1z}V_{1rely})^2} = r_{1y}V_{1relz} - r_{1z}V_{1rely} \tag{119}$$

Equation (116) and (119) can then be used in the second method to find the range and time to impact, when the center of mass position and velocity vector, and the rotational angle are known.

3.4.2 Algorithm to Find the Range and Time to Impact

Since all the equations are defined for the analytical solution to find the range and time to impact, an algorithm can be developed for use in a computer program, such as MATLAB, or for use in a hand calculation of the results. Remember that the known values for this algorithm are the altitude of the main satellite, the tether length, the angular velocity, and the impulsive velocity change of the sub-satellite. The algorithm is listed in step format beginning on the next page.

Step 1: Calculate the position of the sub-satellite at release, position of the main satellite, and the position of the center of mass. The position of the sub-satellite is calculated using table 3.1 and the position of the center of mass is calculated using

$$\bar{r}_{cm} = \frac{\bar{r}_1 m_1 + \bar{r}_2 m_2}{m_1 + m_2} \tag{1}$$

Step 2: Calculate the velocity of the center of mass using

$$V_{cmc} = \sqrt{\frac{\mu}{r_{cm}}} \tag{2}$$

Step 3: Calculate the velocity of the sub-satellite at release using

$$\bar{V}_1 = \left[V_{cmy} - \omega_x (r_{1z} - r_{cmz})\right](\bar{J}) + \left[(V_{cmz}) + \omega_x \left(r_{1y} - r_{cmy}\right)\right](\bar{K}) \tag{106}$$

$$\bar{V}_{1rel} = \bar{V}_1 - \Delta\bar{V} \tag{84}$$

Step 4: Calculate the semi-major axis using

$$a = \frac{-\mu}{V_{1rel}^2 - \frac{2\mu}{r_1}} \tag{99}$$

Step 5: Calculate the angular momentum using

$$h = r_1 V_{1rel} \tag{103}$$

Step 6: Calculate the eccentricity using

$$e = \sqrt{1 - \frac{h^2}{\mu a}} \tag{100}$$

Step 7: Calculate the perigee position using

$$r_p = a(1 - e) \tag{60}$$

and test for impact using equation (119).

$$\begin{gathered} if\ r_p > R_e => no\ impact,\ \ stop \\ if\ r_p \leq R_e => impact \end{gathered} \tag{120}$$

Step 8: Calculate true anomaly at impact using

$$\theta_{imp} = \cos^{-1}\left(\frac{a(1 - e^2) - R_e}{R_e e}\right) \tag{95}$$

And assign the true anomaly at release value using equation (121).

$$\theta_{rel} = 180° = \pi \tag{121}$$

The true anomaly at impact must then be placed in the correct quadrant using

$$\begin{gathered} if\ \theta_{imp} < \theta_{rel} \\ \theta_{imp} = 2\pi - \theta_{imp} \end{gathered} \tag{96}$$

Step 9: Calculate the range using

$$R = R_e\left(|\theta_{imp} - \theta_{rel}|\right) \tag{97}$$

Note: Step eight and nine can be combined into one step by using

$$R = R_e\left(\left|\cos^{-1}\left(\frac{b(1 - c^2) - R_e}{R_e c}\right) - \pi\right|\right) \tag{107}$$

Where,

$$b = \frac{-\mu}{V_{1rel}^2 - \frac{2\mu}{r_1}} \tag{108}$$

$$c = \sqrt{1 - \frac{(r_1 V_{1rel})^2}{\mu b}} \tag{109}$$

Step 10: Calculate the time at release using

$$t_{rel} = \frac{1}{2}T = \pi\sqrt{\frac{a^3}{\mu}} \tag{110}$$

Step 11: Calculating the eccentric anomaly at impact using

$$E = 2\tan^{-1}\left[\left(\frac{1-e}{1+e}\right)^{1/2}\tan\left(\frac{\theta}{2}\right)\right] \tag{73}$$

Step 12: Calculating the time at impact using

$$t_{imp} = \frac{E_{imp} - e\sin E_{imp}}{\sqrt{\frac{\mu}{a^3}}} \tag{112}$$

If the true anomaly at release is much less than or much greater than one hundred and eight degrees use equation (122) to find the time at impact.

$$t_{imp} = T + t_{imp} \tag{122}$$

Step 13: Calculate the time to impact. If the true anomaly at impact was found to already be greater than the true anomaly at release use

$$t_{impact} = t_{imp} - t_{rel} \tag{113}$$

If the true anomaly at impact was changed in step 8, use equation (123) to calculate the time to impact. This eliminates the issue caused by a negative eccentric anomaly.

$$t_{impact} = -t_{imp} - t_{rel} \tag{123}$$

If the true anomaly at release is much less than or much greater than one hundred and eight degrees use equations (122) and (113) to find the time to impact.

If the center of mass position and velocity vectors and the rotational angle are known in addition to the other values, some steps in the algorithm will change. The changes to the algorithm are listed below.

Step 1: Calculate the length between the center of mass and the sub-satellite using

$$L_{t1} = r_{cm} - r_1 \tag{76}$$

Then calculate the position of the sub-satellite at release using

$$\bar{r}_1 = \left(r_{cmy} + L_{t1} \sin\varphi\right)(\bar{J}) + (r_{cmz} + L_{t1} \cos\varphi)(\bar{K}) \tag{115}$$

Step two can then be omitted.

Step 5: Calculate the angular momentum using equation (119).

$$h = \sqrt{(r_{1y}V_{1relz} - r_{1z}V_{1rely})^2} = r_{1y}V_{1relz} - r_{1z}V_{1rely} \tag{119}$$

Step 8: Calculate the true anomaly at release using

$$\theta_{rel} = \cos^{-1}\left(\frac{a(1-e^2) - r_1}{r_1 e}\right) \tag{94}$$

The final steps remain the same for this set of given values.

3.4.3 Equations to Find the Velocity Change and Angular Velocity

In this section equations are developed to find the impulsive velocity change of the sub-satellite and the equivalent angular velocity of the TSS needed to cause an impact if an impulsive velocity change is not to be placed on the system given a set of known values. Five known values are needed for each solution. Four of the known values remain the same for each solution. These are the range, the true anomaly at impact, the altitude, and the tether length. The fifth known value depends upon what is being solved for. If the velocity change of the sub-satellite is to be determined, the angular velocity of the TSS must be known. When the change in the angular velocity of the TSS is being solved for, the velocity change of the sub-satellite caused by the angular velocity must be known. Since the known values have changed the equations found in section 3.4.1 need to be rearranged to find the velocity change and the change angular velocity.

With this analytical solution the assumption that the point of release is located at the apogee of the impact trajectory no longer holds. This means that the true anomaly at release must be determined. This is done by first getting rid of the absolute value in equation (97) by multiply the left hand side by a negative one and then solving for the true anomaly at the release point for the sub-satellite.

$$\theta_{imp} - \theta_{rel} = -\frac{R}{R_e} \tag{124}$$

$$\theta_{rel} = \frac{R}{R_e} + \theta_{imp} \tag{125}$$

The next step is to use the true anomaly at impact to find the semi-major axis of the impacting trajectory in terms of the eccentricity of the impacting trajectory. This is done by solving for the semi-major axis in equation (99).

$$a = \frac{R_e + eR_e \cos\theta_{imp}}{1 - e^2} \tag{126}$$

Equation (126) is then substituted into equation (94).

$$\theta_{rel} = \cos^{-1}\left(\frac{R_e\left(1 + e\cos\theta_{imp}\right) - r_1}{er_1}\right) \tag{127}$$

Equation (127) is then used to solve for the eccentricity of the impact trajectory.

$$e = \frac{r_1 - R_e}{R_e\cos\theta_{imp} - r_1\cos\theta_{rel}} \tag{128}$$

Two different equations must be developed for finding the impulsive velocity change of the sub-satellite and for finding the change in angular velocity of the TSS. In order to find the velocity change of the sub-satellite when given an angular velocity, equation (38) must be substituted into equation (84).

$$\bar{V}_{1rel} = \bar{V}_1 - \Delta\bar{V} = \bar{V}_{cm} + \bar{\omega} \times \bar{L}_{t1} + \Delta\bar{V} \tag{129}$$

Since the angular velocity of the TSS is assumed to be zero when an impulsive velocity change is applied, the cross product in equation (129) is dropped and the velocity change can be solved for by using equations (130) and (131).

$$\Delta V_y = V_{1rely} - V_{cmy} \tag{130}$$

$$\Delta V_z = V_{1relz} - V_{cmz} \tag{131}$$

The equivalent angular velocity for a velocity change of the sub-satellite can be found using equations (86) and (87) depending upon the direction of the velocity change.

3.4.4 Algorithm to Find the Velocity Change and Angular Velocity

The algorithm to find the impulsive velocity change of the sub-satellite and the algorithm to find the change in the angular velocity of the TSS to cause an impact of the sub-satellite given a set of known parameters vary slightly. The first algorithm that will be looked at is the algorithm to solve for the impulsive velocity change of the sub-satellite.

Step 1 – 6: Same as the steps discussed in section 3.4.2.

Step 7: Calculate the velocity change using equation (130) or equation (131).

$$\Delta V_y = V_{1rely} - V_{cmy} \tag{130}$$

$$\Delta V_z = V_{1relz} - V_{cmz} \tag{131}$$

If the velocity change calculated is reasonable, then the algorithm can be stopped. If the velocity change is not reasonable, the altitude or tether length must be increases for decreased to reach a reasonable value.

The second algorithm that will be looked at is the algorithm to solve for the equivalent angular velocity change of the sub-satellite.

Step 1 – 6: Same as the steps discussed in section 3.4.2.

Step 7: Calculate the equivalent angular velocity using equation (86) or equation (87).

$$\omega_1 = \frac{V_{1rely} - V_{cmy}}{-(r_{1z} - r_{cmz})} \tag{86}$$

$$\omega_1 = \frac{V_{1relz} - V_{cmz}}{r_{1y} - r_{cmy}} \tag{87}$$

If the angular velocity change calculated is reasonable, then the algorithm can be stopped. If the angular velocity change is not reasonable, the altitude or tether length must be increases for decreased to reach a reasonable value. The effects of the change in altitude and tether length on the angular velocity and on the velocity change of the sub-satellite are shown in chapter four.

Chapter 4: Results for Analytical Solutions

The cases that will be considered for this chapter are cases A through D, which were described in chapter three, section four. Case A and B are when the sub-satellite is located directly above and directly below the main satellite, while Case C and D are when the sub-satellite is located immediately to the right, in the direction opposite the velocity vector, and immediately to the left, in the same direction as the velocity vector, of the main satellite. The first section of this chapter will discuss the ground range and the time to impact found by using the algorithm discussed in chapter three, section 3.2. The second section discusses the results when the algorithm discussed in chapter three, section 3.4 is used to find the impulsive velocity change and the change in the angular velocity of the TSS.

4.1 Analytical Results for the Range and Time to Impact

For this case the altitude, tether length and the impulsive velocity change are known and are used to calculate the ground range and time to impact. For the results presented here, the altitude and tether length are kept constant, while the impulsive velocity change is increased from zero kilometers per second to six kilometers per second. Three different set-ups for the altitude and the tether length are evaluated. The three set-ups are a five hundred kilometer altitude and a four kilometer tether length, an eight hundred kilometer altitude and a four kilometer tether length, and a five hundred kilometer tether length and a forty kilometer tether. These three set-ups are used in order to investigate the results obtained by increasing the altitude and increasing the tether length.

4.1.1 Case A Results

The position of the TSS at the point of release was shown in figure 3.2. In this situation the velocity of the sub-satellite is directed solely in the negative Y – direction and it is assumed any impulsive velocity change that takes place must be done in the positive Y – direction to create impact. The trends for the ground range and the time to impact as the magnitude of the impulsive velocity change increases hold for all three set-ups.

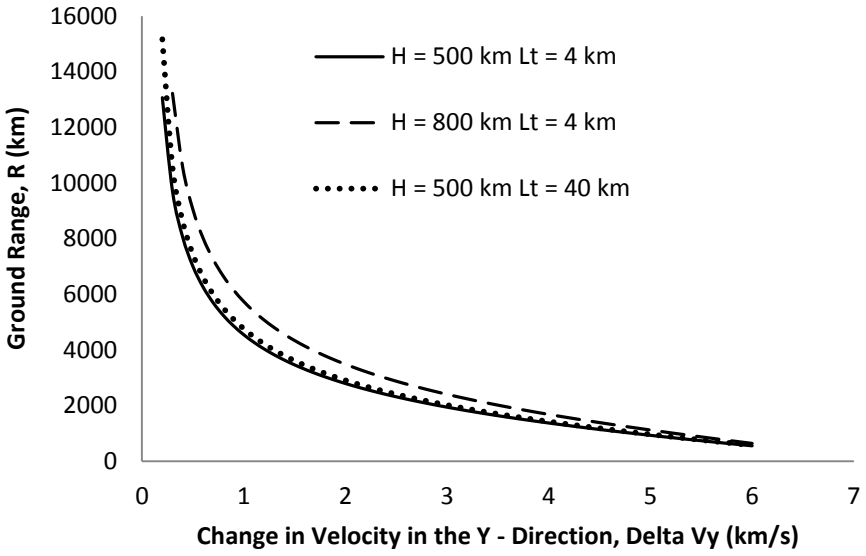

Figure 4.1: Ground Range vs. $+\Delta V_{1y}$ for Case A

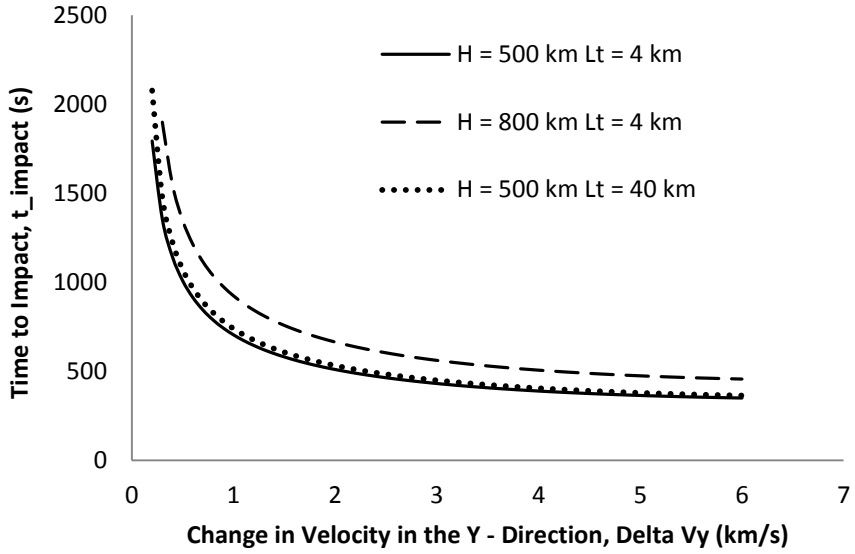

Figure 4.2: Time to Impact vs. $+\Delta V_{1y}$ Increases for Case A

A minimum impulsive velocity change in the positive Y – direction is required in order to create an impact trajectory for each of the three set-ups. The minimum impulsive velocity needed to create an impact point changes when the altitude is increased to eight hundred kilometers; however, a change in the tether length does not result in a change to the minimum impulsive velocity change needed for an impact trajectory. The minimum impulsive velocity change values needed for the three set-ups are listed in table 4.1.

Table 4.1: Minimum Impulsive Velocity Change Needed for Case A

Altitude (km)	**Tether Length (km)**	**Minimum Velocity Change needed in + Y - direction (km/s)**
500	4	0.2
800	4	0.3
500	40	0.2

The maximum ground range and time to impact occur at the minimum impulsive velocity change, while the minimum ground range and time to impact occur at the maximum impulsive

velocity change. Depending upon the altitude and the tether length the value for the ground range and time to impact could increase or decrease. For these three cases an increase in the tether length to a value of forty kilometers, results in the largest increase in the ground range and the time to impact. The increase in the altitude to eight hundred kilometers results in a small decrease in the ground range and time to impact. These effects are shown in figures 4.1 and 4.2. The next two tables list the actual maximum and minimum values for the ground range and time to impact for each of the set-ups. The maximum values occur at the minimum impulsive velocity change placed on the sub-satellite for the three cases listed.

Table 4.2 Maximum Ground Range and Time to Impact for Case A

Altitude (km)	**Tether Length (km)**	**Ground Range (km)**	**Time to Impact (s)**
500	4	13065.3	1793.5
800	4	13220.3	1899.3
500	40	15165.6	2077.0

The maximum value for the ground range and the time to impact occur when the tether length increases to forty kilometers and the velocity change is 0.2 kilometers per second in the positive Y – direction. The increase in altitude leads to an increase in the ground range and the time to impact, but an increased velocity change is needed in order to create an impact point at the higher altitude. This results in the smaller increase to the ground range and time to impact.

Table 4.3: Minimum Ground Range and Time to Impact for Case A

Altitude (km)	**Tether Length (km)**	**Ground Range (km)**	**Time to Impact (s)**
500	4	549.9	349.8
800	4	636.5	456.4
500	40	570.1	363.8

The minimum values for the ground range and time to impact occur when the maximum impulsive velocity change is placed on the sub-satellite. For Cases A through D this maximum velocity change is six kilometers per second in the positive Y – direction. As the velocity change increases the ground range and the time to impact are decreased. The true minimum value comes from the first set-up, where the altitude is five hundred kilometers and the tether length is four kilometers. This time the increase in altitude results in a higher minimum value for the ground range and time to impact. The third set-up serves as a midpoint for the minimum values that can be obtained.

4.1.2 Case B Results

For case B, the sub-satellite is located below the main satellite. The center of mass, main satellite, and sub-satellite have a velocity solely in the negative Y – direction. In order to cause the sub-satellite to enter an impact trajectory, the impulsive velocity change of the sub-satellite must be in the positive Y – direction. The ground range and time to impact decrease as the impulsive velocity change in the positive Y – direction is increase. The decrease in the ground range and the time to impact as the impulsive velocity change increases are shown in figures 4.3 and 4.4 on the next page.

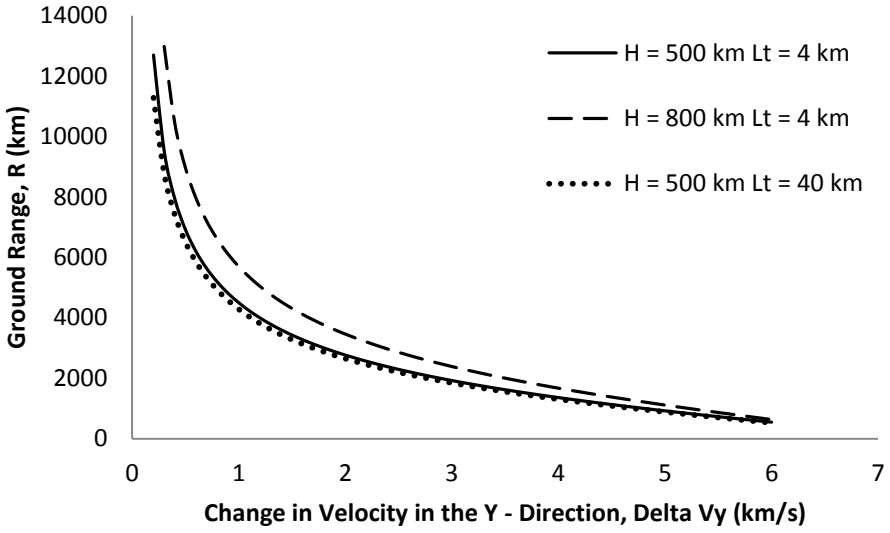

Figure 4.3: Ground Range vs. $+\Delta V_{1y}$ for Case B

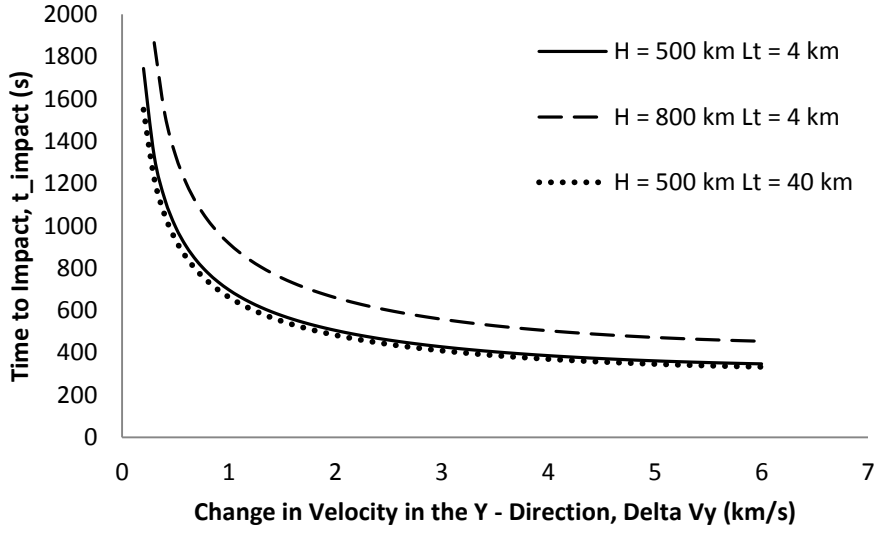

Figure 4.4: Time to Impact vs. $+\Delta V_{1y}$ for Case B

The minimum impulsive velocity change in the positive Y – direction needed for the sub-satellite to have an impact trajectory for each of the three set-ups is listed in table 4.4.

Table 4.4: Minimum Impulsive Velocity Change Needed for Case B

Altitude (km)	Tether Length (km)	Minimum Velocity Change needed in + Y - direction (km/s)
500	4	0.2
800	4	0.3
500	40	0.2

The maximum and minimum ground range and time to impact occur at the minimum impulsive velocity change and the maximum impulsive velocity change of six kilometers per second, respectively. An increase in the altitude leads to a larger increase in the ground range and time to impact, than an increase in the tether length.

Table 4.5: Maximum Ground Range and Time to Impact for Case B

Altitude (km)	Tether Length (km)	Ground Range (km)	Time to Impact (s)
500	4	12696.5	1743.2
800	4	12980.0	1865.2
500	40	11279.4	1548.9

The maximum ground range and time to impact occur when the altitude is increased because as the altitude increases the sub-satellite moves further away from the surface of the Earth. The lowest maximum value occurs when the tether length is increased, because the sub-satellite gets closer to the surface of the Earth as the tether increases. If the altitude is increased further, the ground range and time to impact should also increase; however, if the tether length increases instead, the ground range and time to impact will decrease.

Table 4.6: Minimum Ground Range and Time to Impact for Case B

Altitude (km)	Tether Length (km)	Ground Range (km)	Time to Impact (s)
500	4	545.3	346.7
800	4	633.1	453.7
500	40	524.3	332.4

The minimum values for the ground range and the time to impact are affected by the increase in the altitude and tether length in the same way that the maximum values are affected. The largest ground range and time to impact happens when the altitude increases, while the true minimum occurs when the tether length is increased. The ground range and time to impact calculated for case B in all set-ups is less than the ground range and time to impact calculated in case A.

4.1.3 Case C Results

The sub-satellite is located immediately to the right of the main satellite. In this position the sub-satellite's velocity is only in the negative Y – direction; therefore, an impulsive velocity change in the positive Y – direction is needed in order to create an impact for the sub-satellite. As the impulsive velocity change in the positive Y – direction is increased, the ground range and the time to impact decrease. The trends mentioned above can be seen in figures 4.5 and 4.6 on the next page.

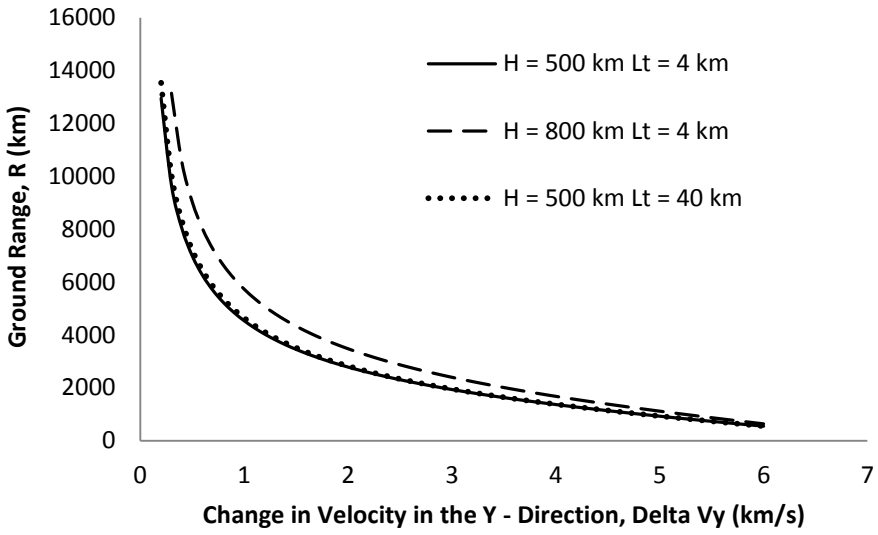

Figure 4.5: Ground Range vs. $+\Delta V_{1y}$ for Case C

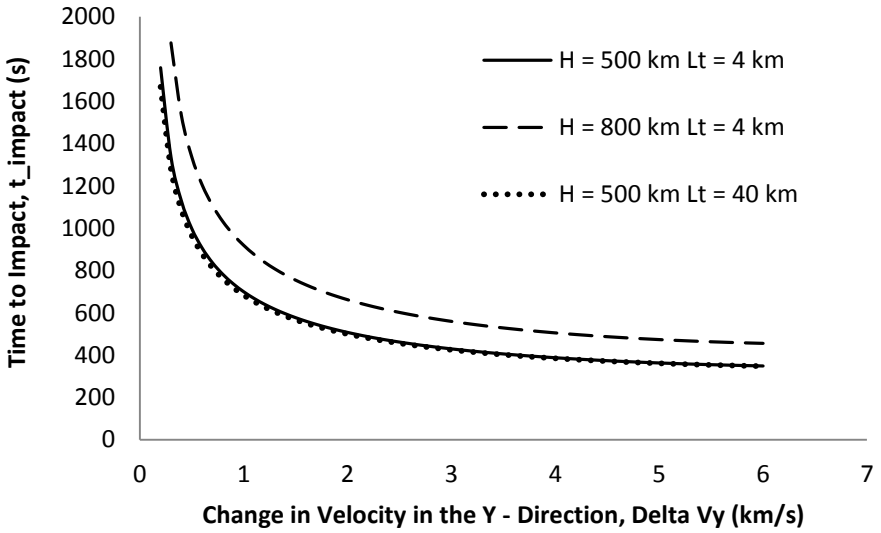

Figure 4.6: Time to Impact vs. $+\Delta V_{1y}$ for Case C

The minimum impulsive velocity change needed to create the first impact trajectory for each set-up is listed on the next page in table 4.7.

Table 4.7: Minimum Impulsive Velocity Change Needed for Case C

Altitude (km)	Tether Length (km)	Minimum Velocity Change needed in + Y - direction (km/s)
500	4	0.2
800	4	0.3
500	40	0.2

The maximum ground range and time to impact will occur at the minimum impulsive velocity changes listed in table 4.7 for each set-up. When the impulsive velocity change reaches the maximum value of six kilometers per second, the ground range and time to impact will be at their minimum values. The maximum and minimum values are listed for the ground range and time to impact below in table 4.8 and table 4.9.

Table 4.8: Maximum Ground Range and Time to Impact for Case C

Altitude (km)	Tether Length (km)	Ground Range (km)	Time to Impact (s)
500	4	12945.5	1758.1
800	4	13140.0	1875.6
500	40	13535.9	1667.9

Table 4.9: Minimum Ground Range and Time to Impact for Case C

Altitude (km)	Tether Length (km)	Ground Range (km)	Time to Impact (s)
500	4	547.8	348.2
800	4	635.0	455.0
500	40	549.4	347.2

The largest maximum value that is obtained for case C occurs when the tether is increased, because an increase in the tether length places the sub-satellite further away from the impact

point. The largest minimum value for case C occurs when the altitude is increased because the altitude places the sub-satellite in a higher orbit.

4.1.4 Case D Results

The position of the sub-satellite for case D is directly to the left main satellite. In this set-up the velocity of the main satellite, the center of mass, and the sub-satellite is only in the negative Y – direction; therefore, the impulsive velocity change needs to be in the positive Y – direction in order to cause the sub-satellite to enter an impact trajectory. The ground range and time to impact for all three set-ups decreases as the impulsive velocity change in the positive Y – direction increases. The change in ground range is shown below, while the change in the time to impact is shown in figure 4.8 on the next page.

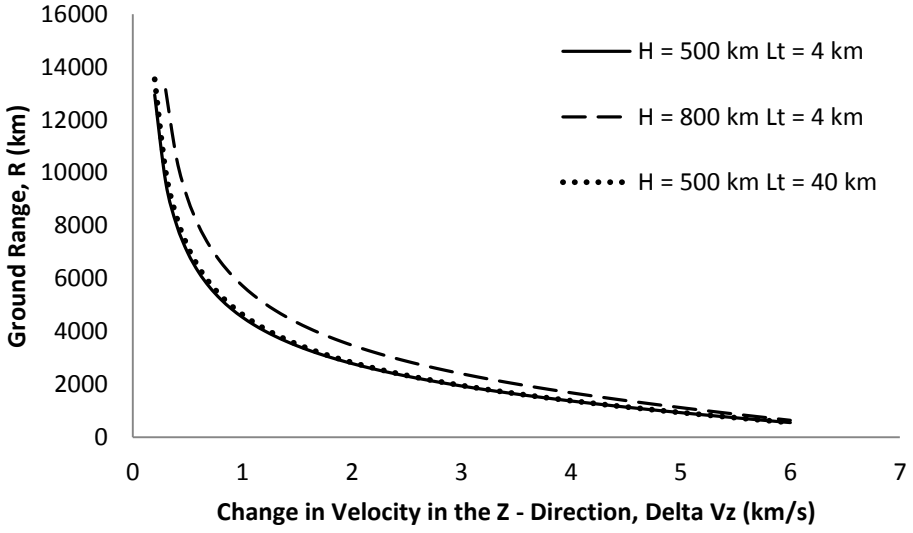

Figure 4.7: Ground Range vs. $+\Delta V_{1y}$ for Case D

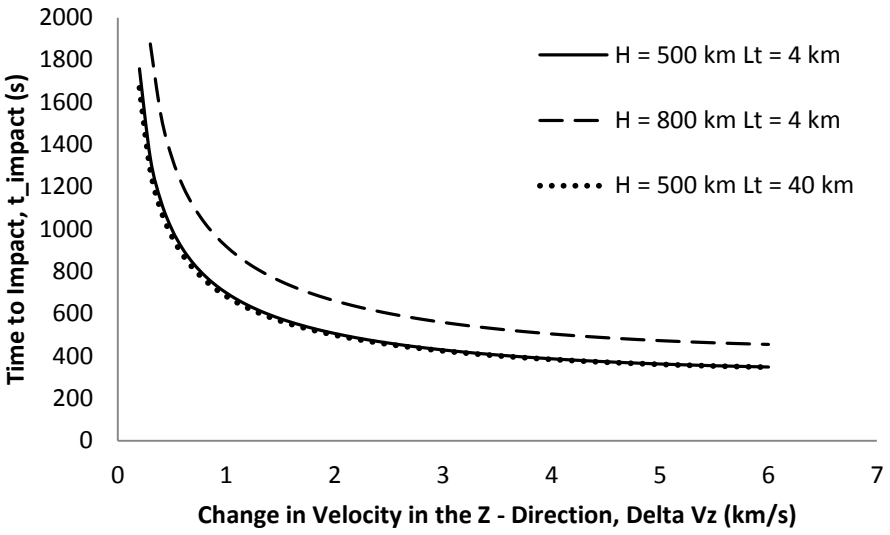

Figure 4.8: Time to Impact vs. $+\Delta V_{1y}$ for Case D

The minimum impulsive velocity change needed to send the sub-satellite on an impact trajectory follows the same trends that are in the previous cases.

Table 4.10 Minimum Impulsive Velocity Change Needed for Case D

Altitude (km)	**Tether Length (km)**	**Minimum Velocity Change needed in + Y - direction (km/s)**
500	4	0.2
800	4	0.3
500	40	0.2

The maximum and minimum values for the ground range and the time to impact are listed in tables 4.11 and 4.12, respectively. The maximum ground range and time to impact occur when the minimum impulsive velocity changes listed in table 4.10 are placed on the sub-satellite. The minimum ground range and time to impact occur when the impulsive velocity change is equal to six kilometers per second.

Table 4.11: Maximum Ground Range and Time to Impact for Case D

Altitude (km)	Tether Length (km)	Ground Range (km)	Time to Impact (s)
500	4	12945.5	1758.1
800	4	13140.2	1875.6
500	40	13535.1	1667.9

Table 4.12: Minimum Ground Range and Time to Impact for Case D

Altitude (km)	Tether Length (km)	Ground Range (km)	Time to Impact (s)
500	4	547.8	348.2
800	4	635.0	455.0
500	40	549.4	347.2

The values for the maximum and minimum ground range and time to impact are the same as the values in case C. The only difference is the position vector of the sub-satellite in both cases; therefore, the trajectories are only shifted over because of the sub-satellite's orientation with the main satellite.

4.2 Analytical Results for the Impulsive Velocity Change and the Angular Velocity

In this section it is assumed that the altitude, tether length, ground range, and true anomaly at impact are known. The algorithm discussed in chapter three, section 3.4 is used to get the results in this section. Two scenarios are looked at to use the analytical results to find the impulsive velocity change and change in angular velocity of the TSS at different altitudes and tether lengths. The first scenario sets the ground range at fifteen hundred kilometers with a true anomaly at impact of two hundred and forty degrees or 4.1888 radians. The second scenario sets the ground range at three thousand kilometers with a true anomaly at impact of two hundred and forty degrees. As each scenario is looked at, case A and B are placed on the same plot because

in both situations the velocity of the sub-satellite and the impulsive velocity change are along the Y – axis, while case C and D are placed on the same plot. For all cases the velocity of the sub-satellite is in the negative Y – direction and the impulsive velocity change is in the positive Y – direction.

4.2.1 Ground Range of 1500 km and $\theta_{imp} = 240°$

The impulsive velocity change and the equivalent change in angular velocity of the TSS were first found for case A and case B. The altitude starts at five hundred kilometers and is then increased to fifteen hundred kilometers in increments of one hundred kilometers. As the altitude increases the impulsive velocity change and the change in angular velocity of the TSS needed to reach a ground range of fifteen hundred kilometers decreases in magnitude. The impulsive velocity change for case A and B are slightly different as the altitude increases and are in the same direction. For case A the change in angular velocity must be in the negative X – direction to cause a clockwise rotation of the TSS to create the same velocity change. The change in angular velocity must be in the positive direction for case B to cause a counter-clockwise rotation. The plots of the impulsive velocity change and the change in angular velocity as a function of changing altitude are shown on the next page and are followed by a table that gives specific values for the velocity change and the angular velocity at three different altitudes.

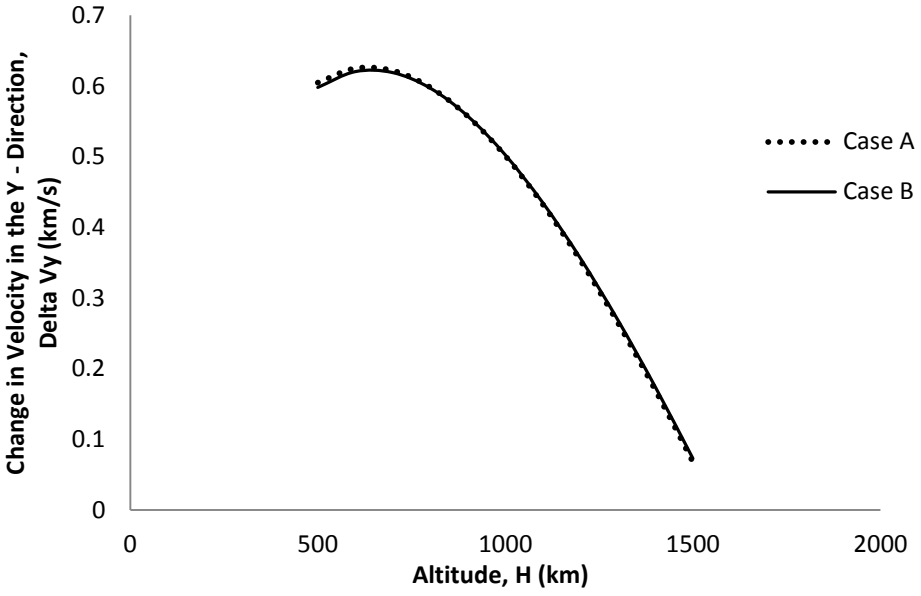

Figure 4.9 Velocity Change vs. Altitude for Case A and B; R = 1500 km and θ_{imp} = 240°

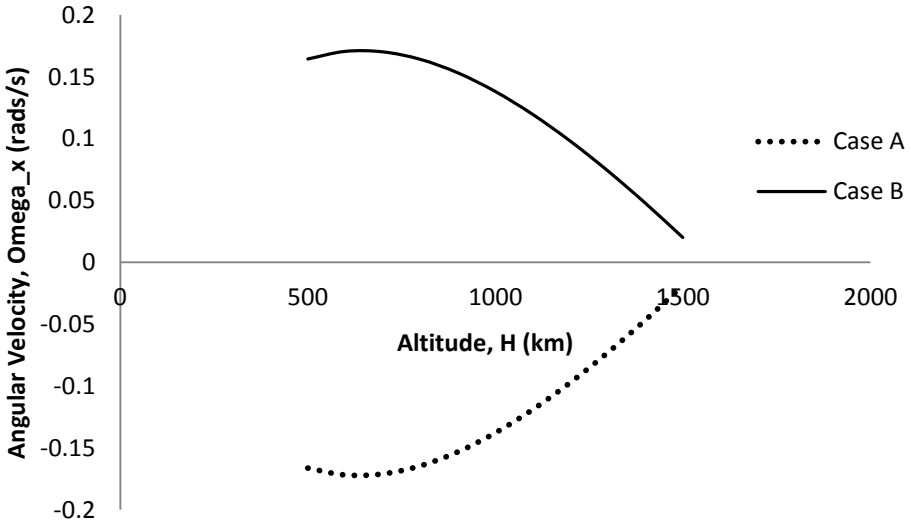

Figure 4.10 Angular Velocity vs. Altitude for Case A and B; R = 1500 km and θ_{imp} = 240°

Table 4.13 Impulsive Velocity Change and Angular Velocity at Three Altitudes for Case A and B When R = 1500 km and $\theta_{imp} = 240°$

	Case A		Case B	
Altitude (km)	**Velocity Change (km/s)**	**Angular Velocity (rads/s)**	**Velocity Change (km/s)**	**Angular Velocity (rads/s)**
500	0.6048	-0.1663	0.5981	0.1645
1000	0.5012	-0.1378	0.5025	0.1382
1500	0.0681	-0.0187	0.0731	0.0201

From table 4.13 it can be seen that the values for the impulsive velocity change and the magnitude of the change in angular velocity differ slightly, because of the placement of the sub-satellite with respect to the main satellite. For both cases as the altitude increases the required impulsive velocity change and change in angular velocity of the system is decreased.

The next change that is placed on case A and B is an increase in the tether length. The tether length starts at four kilometers and is increased to one hundred and fourteen kilometers in increments of ten kilometers. As the tether length increases the impulsive velocity change of the sub-satellite is decreased for case B, while the impulsive velocity change increases for case A. The magnitude of the equivalent angular velocity needed to reach the same ground range and true anomaly at impact decreases as the tether length increases. These trends are shown in figures 4.11 and 4.12. The plots are then followed by a table that lists specific impulsive velocity changes and angular velocities that are needed to achieve the desired ground range and impact point.

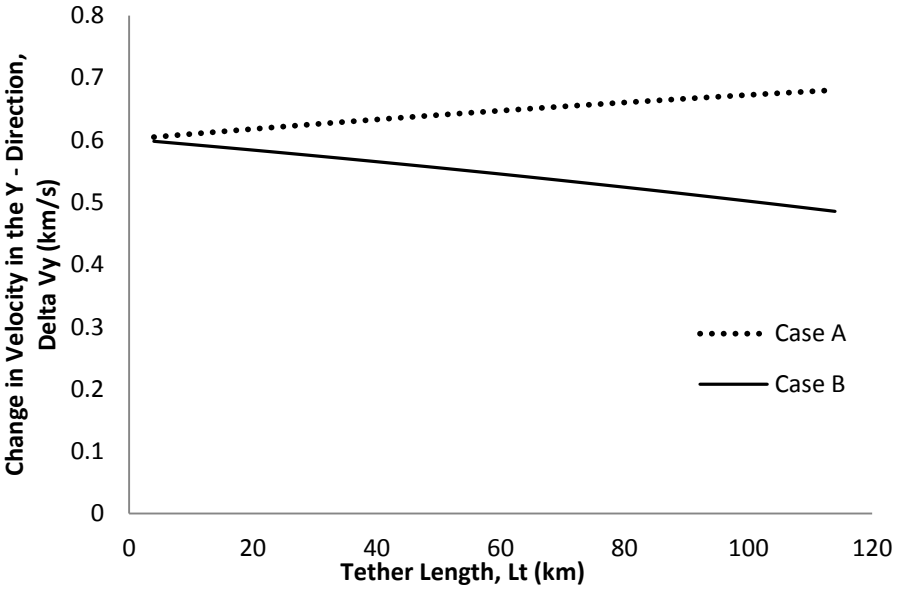

Figure 4.11 Velocity Change vs. Tether Length for Case A and B; R = 1500 km and θ_{imp} = 270°

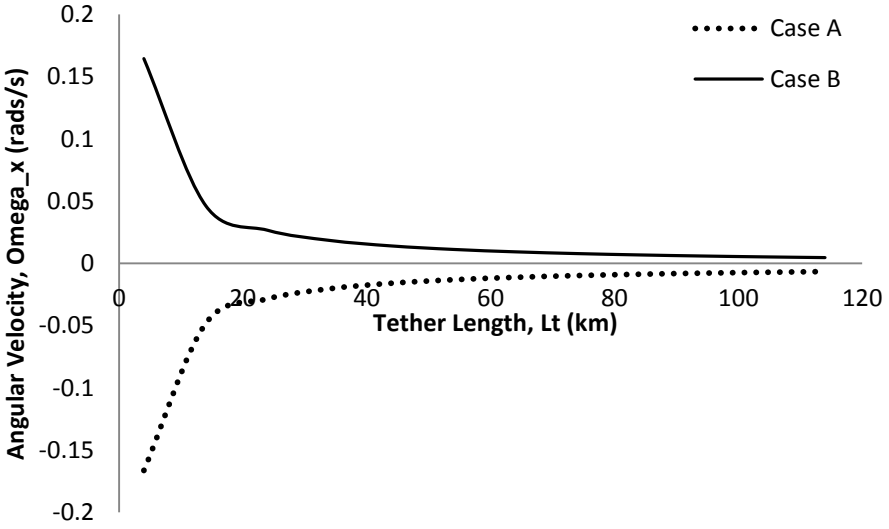

Figure 4.12 Angular Velocity vs. Tether Length for Case A and B; R = 1500 km and θ_{imp} = 240°

Table 4.14: Impulsive Velocity Change and Angular velocity at Three Tether Lengths for Case A and B When R = 1500 km and θ_{imp} = 240°

	Case A		Case B	
Tether Length (km)	**Velocity Change (km/s)**	**Angular Velocity (rads/s)**	**Velocity Change (km/s)**	**Angular Velocity (rads/s)**
4	0.6048	-0.1663	0.5981	0.1645
54	0.6431	-0.0131	0.5515	0.0112
114	0.6804	-0.0066	0.4856	0.0047

The impulsive velocity changes increase for case A as the tether length increases because the sub-satellite is located above the main satellite. The impulsive velocity change decreases for case B because the sub-satellite is located below the main satellite. The change in angular velocity of the TSS needed to create the same ground range and impact point in case A and B decrease because the increase in tether length is a larger value than the velocity change.

Now the effect of increasing altitude and tether length will be investigated for cases C and D. The change in angular velocity of the TSS for both cases was found to be zero because an impulsive change in velocity in the positive Y – direction on the sub-satellite will not lead to a rotation of the TSS. A change in velocity in the positive or negative Z – direction will lead to a rotation. For a ground range of fifteen hundred kilometers and a true anomaly of two hundred and forty degrees, the increase in altitude will results in a decrease of the magnitude of the velocity change.

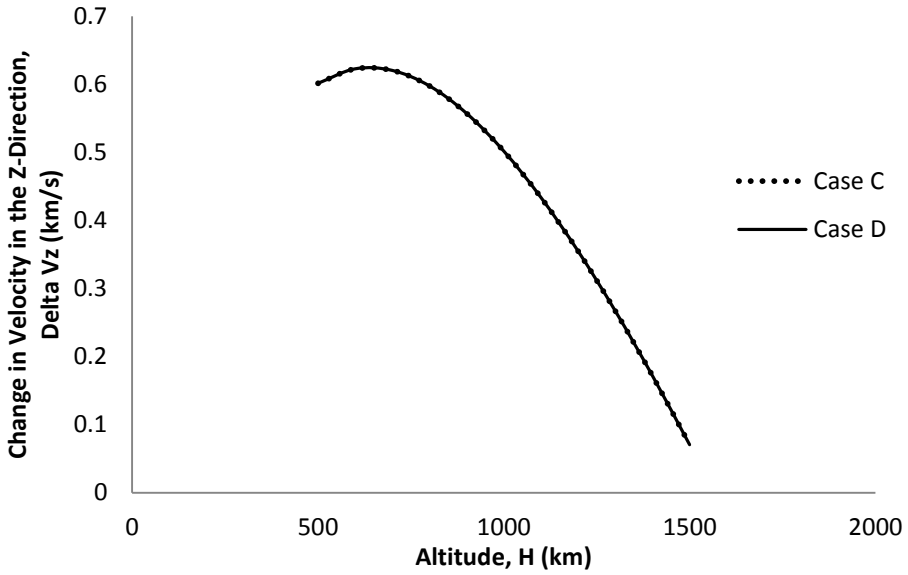

Figure 4.13 Velocity Change vs. Altitude for Case C and D; R = 1500 km and θ_{imp} = 240°

Table 4.15: Impulsive Velocity Change and Angular Velocity at Three Altitudes for Case C and D When R = 1500 km and θ_{imp} = 270°

	Case C		Case D	
Altitude (km)	**Velocity Change (km/s)**	**Angular Velocity (rads/s)**	**Velocity Change (km/s)**	**Angular Velocity (rads/s)**
500	0.6015	N/A	0.6015	N/A
1000	0.5019	N/A	0.5019	N/A
1500	0.0706	N/A	0.0706	N/A

At each altitude the magnitude of the impulsive velocity change is the same for each case. This similarity occurs because the sub-satellite in case C and D has the same altitude as the main satellite.

The increasing tether length for case C and D leads to an increase in the magnitude of the impulsive velocity change. The change in angular velocity is still equal to zero because of the reasons explained for the changing altitude. Three values for impulsive velocity change and

change in angular velocity are shown in table 4.16 for both cases at an altitude of five hundred kilometers, one thousand kilometers, and fifteen hundred kilometers.

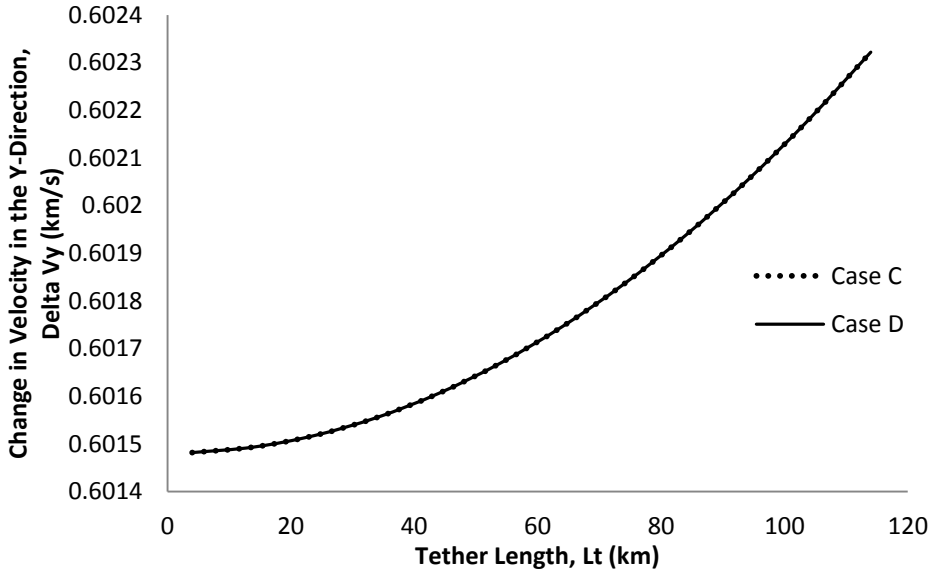

Figure 4.14 Velocity Change vs. Tether Length for Case C and D; R = 1500 km and θ_{imp} = 240°

Table 4.16: Impulsive Velocity Change and Angular Velocity at Three Tether Lengths for Case C and D When R = 1500 km and θ_{imp} = 240°

	Case C		Case D	
Tether Length (km)	**Velocity Change (km/s)**	**Angular Velocity (rads/s)**	**Velocity Change (km/s)**	**Angular Velocity (rads/s)**
4	0.6015	N/A	0.6015	N/A
54	0.6017	N/A	0.6017	N/A
114	0.6023	N/A	0.6023	N/A

4.2.2 Ground Range of 3000 km and $\boldsymbol{\theta_{imp} = 240°}$

The same increase in altitude and tether length are placed on the four cases; however, the desired ground range has been doubled in order to see if there are any changes to the impulsive velocity change and change in angular velocity trends by increasing the altitude and tether

length. As in the previous section, the first two cases that will be looked at are case A and B and the first change that will be investigated is the increase in the altitude of the main satellite. The increase in altitude leads to an increase in the magnitude of the impulsive velocity change and change in angular velocity for both cases. The impulsive velocity change and change in angular velocity of the TSS as a function of altitude are shown in figures 4.15 and 4.16.

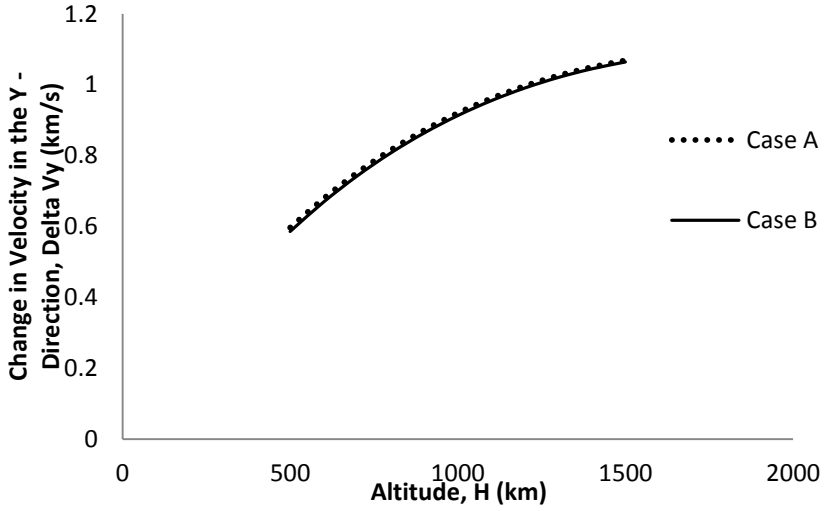

Figure 4.15 Velocity Change vs. Altitude for Case A and B; R = 3000 km and θ_{imp} = 240°

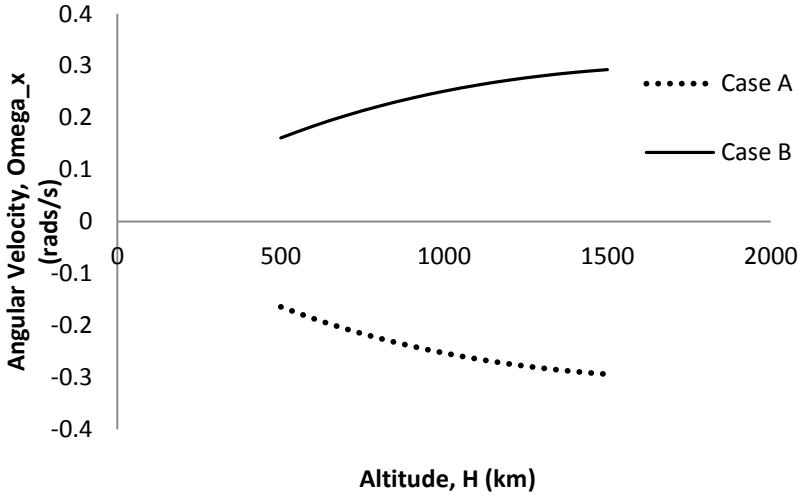

Figure 4.16 Angular Velocity vs. Altitude for Case A and B; R = 3000 km and θ_{imp} = 240°

Table 4.17: Impulsive Velocity Change and Angular Velocity at Three Altitudes for Case A and B When R = 3000 km and θ_{imp} = 240°

	Case A		Case B	
Altitude (km)	**Velocity Change (km/s)**	**Angular Velocity (rads/s)**	**Velocity Change (km/s)**	**Angular Velocity (rads/s)**
500	0.5968	-0.1641	0.5857	0.1611
1000	0.9200	-0.2530	0.9128	0.2510
1500	1.0687	-0.2939	1.0641	0.2926

With this ground range the increase in altitude leads to an increase in the impulsive velocity change because a greater velocity change is needed in order to create an impact at a higher altitude and to achieve a greater ground range. As the velocity change increases, the change in angular velocity increases as well because a larger equivalent angular velocity is needed to create the same impact point. The angular velocity for case A is negative because the angular velocity of the system needs to be in the negative X – direction in order to create a clockwise rotation. The angular velocity is positive in order to create a counter-clockwise rotation for case B.

The increase in tether length will also affect the impulsive velocity change and the change in angular velocity for case A and B. The impulsive velocity change placed on the sub-satellite at release decreases with the increasing tether length for case B; however, the impulsive velocity change increases with increase tether length in case A. The increase in tether length also causes the change in angular velocity of the TSS to decrease in magnitude. This decrease in angular velocity is a result of the increase in the distance between the center of mass and the sub-satellite. As the distance increases the amount of rotation or angular velocity that is required to place the TSS in the proper orientation to cause the sub-satellite to enter an impact trajectory decreases. The impulsive velocity change and change in angular velocity as a function of increasing tether length are shown in figures 4.17 and 4.18.

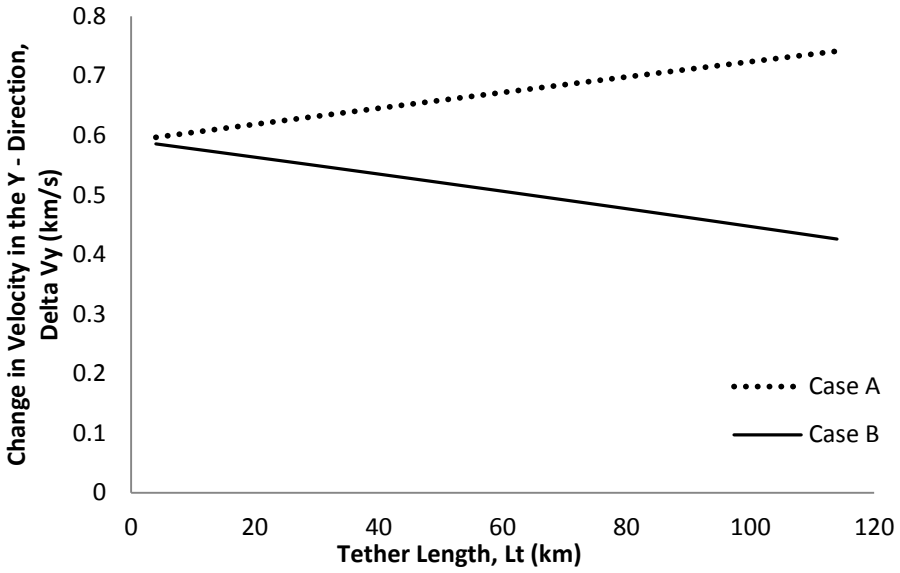

Figure 4.17 Velocity Change vs. Tether Length Case A and B; R = 3000 km and θ_{imp} = 240°

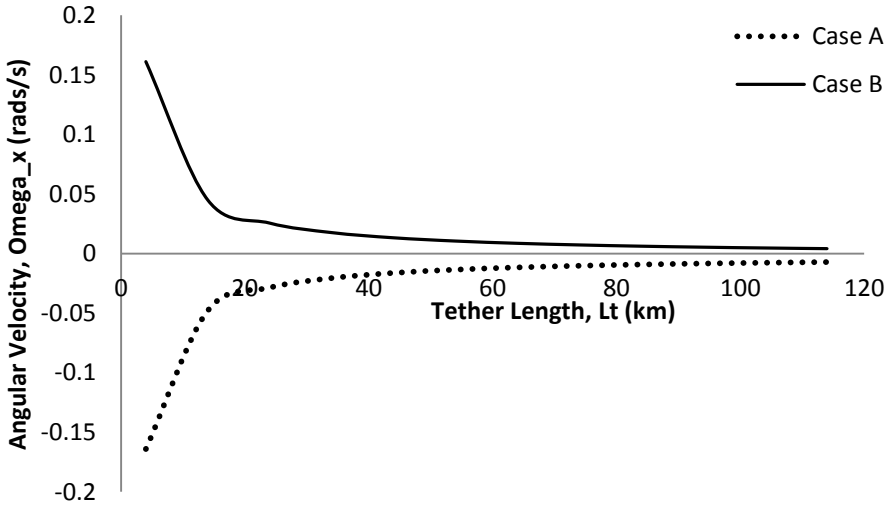

Figure 4.18 Angular Velocity vs. Tether Length for Case A and B; R = 3000 km and θ_{imp} = 240°

Table 4.18: Impulsive Velocity Change and Angular Velocity at Three Tether Lengths for Case A and B When R = 3000 km and θ_{imp} = 240°

	Case A		Case B	
Tether Length (km)	**Velocity Change (km/s)**	**Angular Velocity (rads/s)**	**Velocity Change (km/s)**	**Angular Velocity (rads/s)**
4	0.5968	-0.1641	0.5857	0.1611
54	0.6642	-0.0135	0.5149	0.0105
114	0.7414	-0.0072	0.4260	0.0041

The impulsive velocity change for case A increases with increasing tether length because the sub-satellite is placed in a higher orbit away from the Earth. The impulsive velocity change for case B decreases with increasing tether length because the sub-satellite is lowered into an orbit closer to the Earth. The change in angular velocity of the TSS needed for impact decreases with increasing tether length. The magnitudes of the angular velocities differ between the two cases because of the different impulsive velocity changes. The angular velocity in case A is in the negative X – direction because a clockwise rotation is needed for impact.

The increase in altitude and increase in tether length will now be applied to case C and D. From the previous case in section 4.2.1, it is expected that the results for case C and D for each change should be equal in magnitude and direction. The first parameter that will be increased on case C and D is the altitude. As the altitude increases the impulsive velocity change required for the sub-satellite to reach a ground range of three thousand kilometers at a true anomaly at impact of two hundred and forty degrees increase as well. The change in angular velocity remains at zero because the impulsive velocity change direction in the positive Y – direction does not create a rotation on the system. Figure 4.19 shows the impulsive velocity change as a function of the

increase in altitude, and is followed by a table that list specific impulsive velocity change and change in angular velocity values for three altitudes.

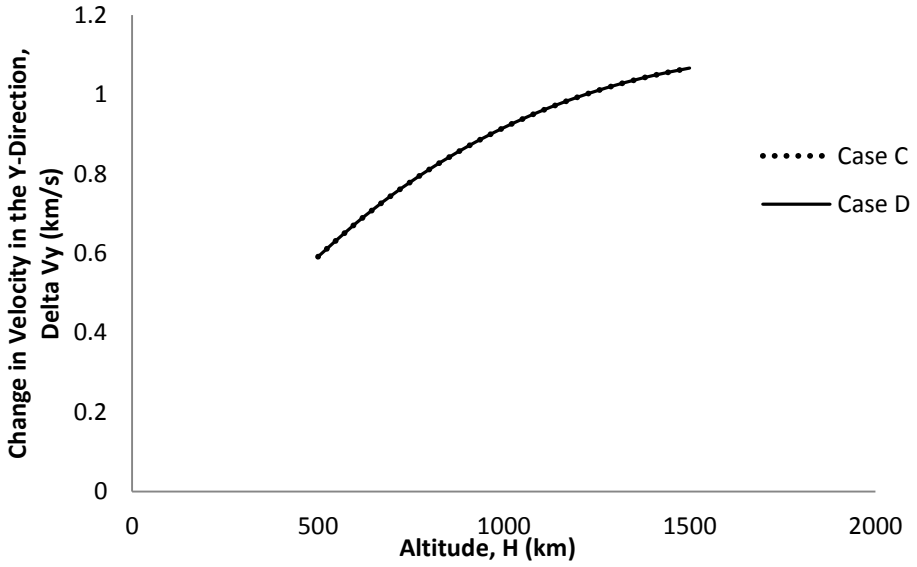

Figure 4.19 Velocity Change vs. Altitude for Case C and D; R = 3000 km and θ_{imp} = 240°

Table 4.19: Impulsive Velocity Change and Angular Velocity at Three Altitudes for Case C and D When R = 3000 km and θ_{imp} = 240°

	Case C		Case D	
Altitude (km)	**Velocity Change (km/s)**	**Angular Velocity (rads/s)**	**Velocity Change (km/s)**	**Angular Velocity (rads/s)**
500	0.5912	N/A	0.5912	N/A
1000	0.9164	N/A	0.9164	N/A
1500	1.0664	N/A	1.0664	N/A

As expected the magnitudes and directions of the impulsive velocity change are equal between the two cases. This is a result of the placement of the sub-satellite in the same orbit height as the main satellite at release. The larger ground range causes the impulsive velocity change to increase in order to reach the desired impact.

The last change that will be looked at is the increase in the tether length for case C and D. As the tether length increases the impulsive velocity change increases. The change in angular velocity of the TSS is once again zero because of the direction of the velocity change. The increase in the impulsive velocity change as a function of the tether length is shown below. Table 4.20 lists the values for the impulsive velocity change and the change in angular velocity at a tether length of four kilometers, fifty-four kilometers, and one hundred and fourteen kilometers. The table can be found on the next page.

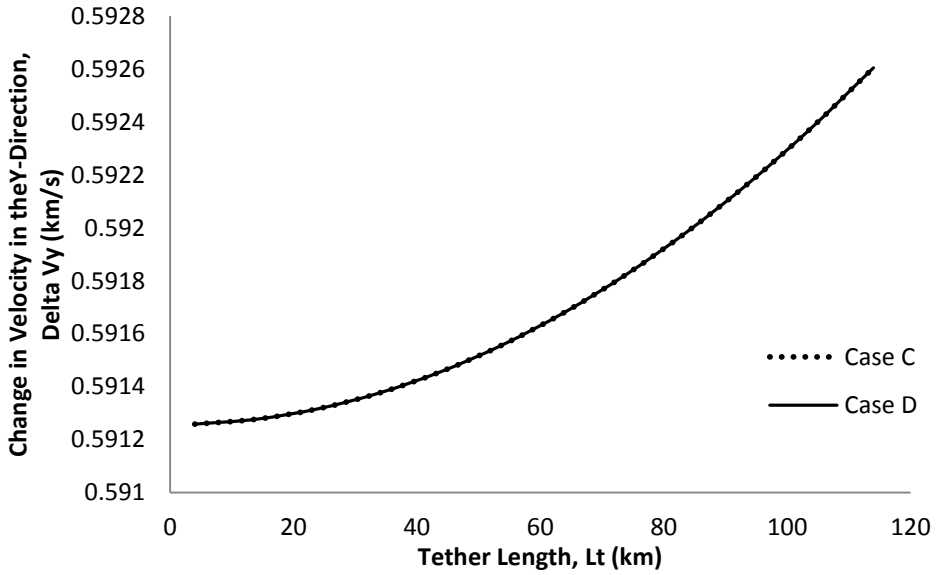

Figure 4.20 Velocity Change vs. Tether Length for Case C and D; R = 3000 km and θ_{imp} = 240°

Table 4.20: Impulsive Velocity Change and Angular Velocity at Three Tether Lengths for case C and D When R = 3000 km and θ_{imp} = 240°

	Case C		Case D	
Tether Length (km)	**Velocity Change (km/s)**	**Angular Velocity (rads/s)**	**Velocity Change (km/s)**	**Angular Velocity (rads/s)**
4	0.5912	N/A	0.5912	N/A
54	0.5916	N/A	0.5916	N/A
114	0.5926	N/A	0.5926	N/A

The impulsive velocity change for both case C and D have the same magnitudes and directions because the sub-satellite for both cases is located at the same orbit height as the main satellite.

Chapter 5: Results for Numerical Integration Simulation

The process discussed in section 3.1 is now implemented with the changes discussed in sections two and three in chapter three. Three different impulsive velocity changes were chosen for the two different release configurations. For each configuration and impulsive velocity change the effect of changes in altitude and tether length were investigated. The first configuration corresponds to when the sub-satellite is below the main satellite. The second configuration corresponds to when the sub-satellite is above the main satellite. For each change in altitude and tether length three values are chosen to discuss in detail after the general trend is introduced. For the change in altitude the tether length is kept constant at four kilometers. The altitude is kept at five hundred kilometers when the tether length is changed. A range of impulsive velocity changes are then looked at to determine the minimum impulsive velocity change needed to impact and the change in angular velocity of the TSS needed to impact. For the range of impulsive velocity changes the altitude is kept at five hundred kilometers and the tether length is kept at four kilometers. For all cases and release points the rotation angle is -0.5 radians because it is a good mid-range oscillation that will keep the sub-satellite leading the system. Some sample results for the numerical integration simulation can be found in Appendix A.

5.1 Results for First Configuration or Case 1

Three values were chosen for the impulsive velocity change of the sub-satellite as shown in table 5.1. An impulsive velocity change in the negative Y-direction was not chosen because the velocity change would only increase the sub-satellite velocity and an impact trajectory would not be created.

Table 5.1: Impulsive Velocity Changes for Case 1

	Velocity Change (km/s)
ΔV_{1y}	1.0
ΔV_{1y}	N/A
ΔV_{1z}	1.0
ΔV_{1z}	-3.0

5.1.1 Impulsive Velocity Change of 1.0 km/s in the Positive Y-Direction

The first change that will be looked at is the change in altitude. Remember that the altitude defines the height above the Earth for the main satellite and the sub-satellite is a distance away from the main satellite equal to the tether length.

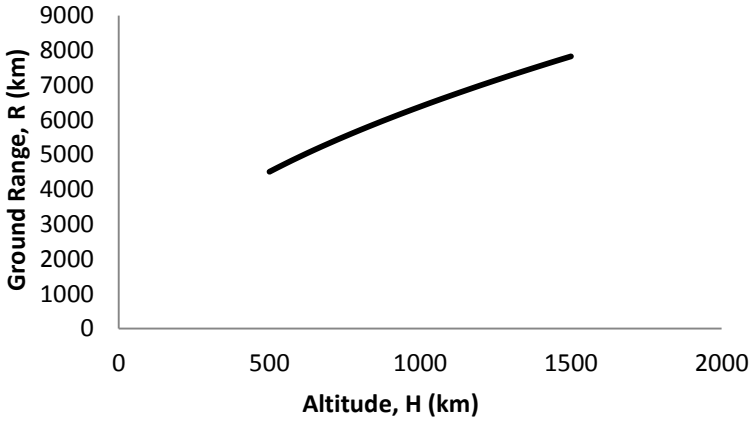

Figure 5.1 Ground Range vs. Altitude for ΔV_{1y} = 1.0 km/s in Case 1

For the first configuration an increase in the altitude of the main satellite leads to an increase in the range. This makes sense because as the altitude is increased the sub-satellite is in a higher orbit and it travels for a longer time before impact is reached. The time increase can be seen in Figure 5.2. As the orbit of the sub-satellite gets higher the ground range covered by the sub-satellite in its impact trajectory will increase as well.

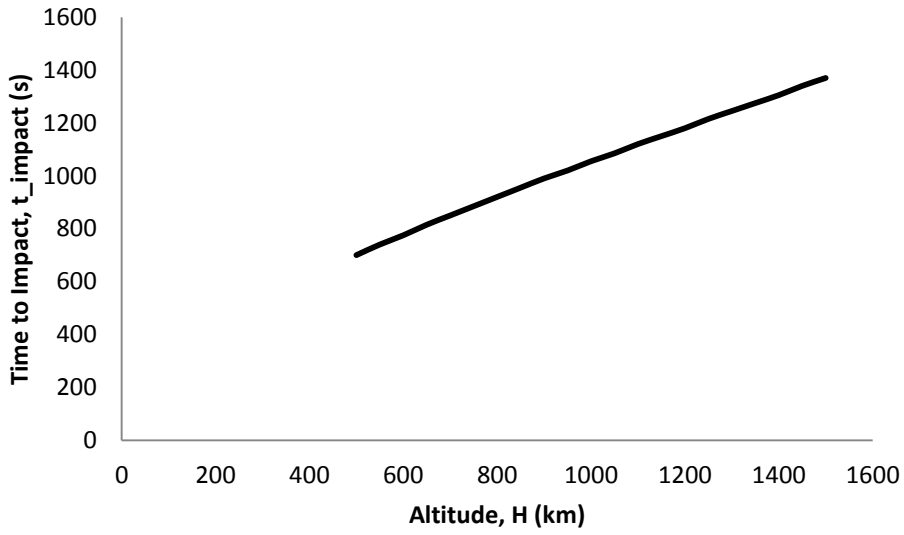

Figure 5.2 Time to Impact vs. Altitude for ΔV_{1y} = 1.0 km/s in Case 1

An altitude of five hundred kilometers, one thousand kilometers, and one thousand five hundred kilometers are looked at in more detail. Table 5.2 lists the ground range covered by the sub-satellite after release and the time to impact.

Table 5.2 Range and Impact Time for $\Delta V_{1y} = 1.0$ km/s at three Altitudes for Configuration 1

Altitude (km)	Ground Range (km)	Time to Impact (s)
500	4505.7	700
1000	6377.7	1055
1500	7822.9	1370

The lowest ground range and time to impact happen at an altitude of five hundred kilometers, while the maximum for each happens at an altitude of one thousand five hundred kilometers. To achieve maximum ground range covered by the sub-satellite with a constant tether length and impulsive velocity change the altitude should be increased. If a minimum ground range is needed the altitude should be decreased. The next three figures show the trajectory for the sub-satellite after release at the three altitude values and illustrate how the range and time to impact increase as the altitude increases.

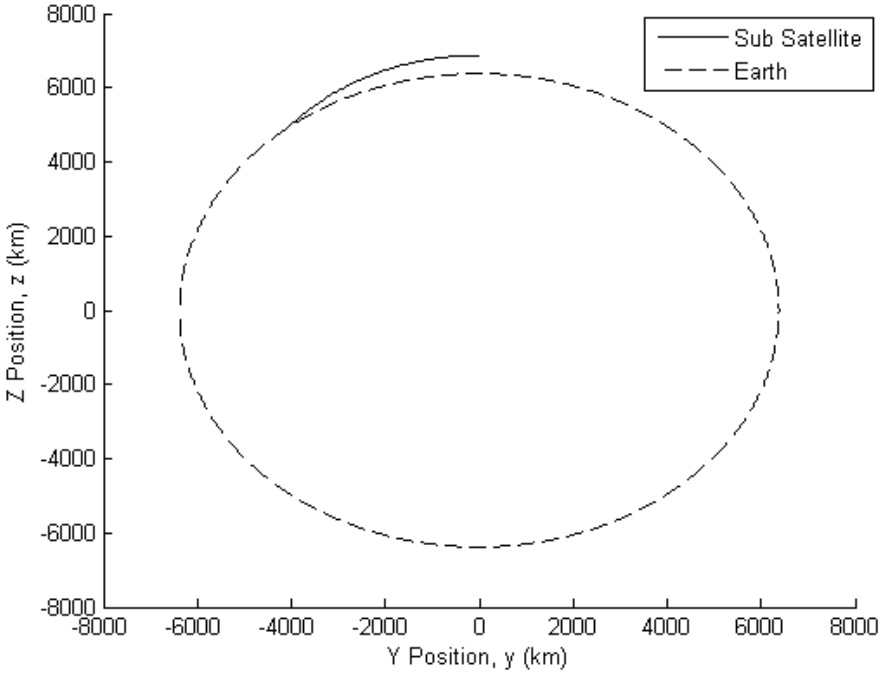

Figure 5.3 Trajectory at 500 km Altitude for ΔV_{1y} = 1.0 km/s in Case 1

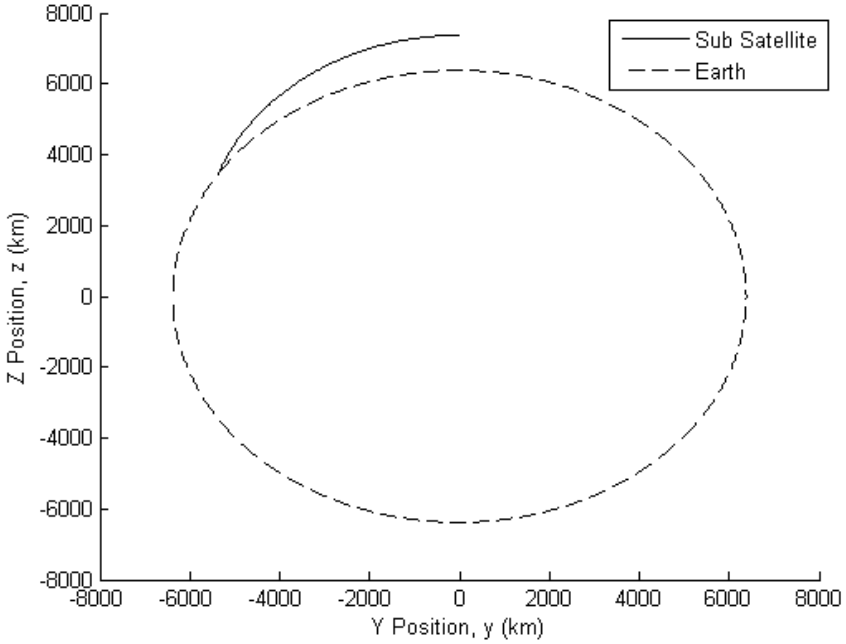

Figure 5.4 Trajectory at 1000 km Altitude for ΔV_{1y} = 1.0 km/s in Case 1

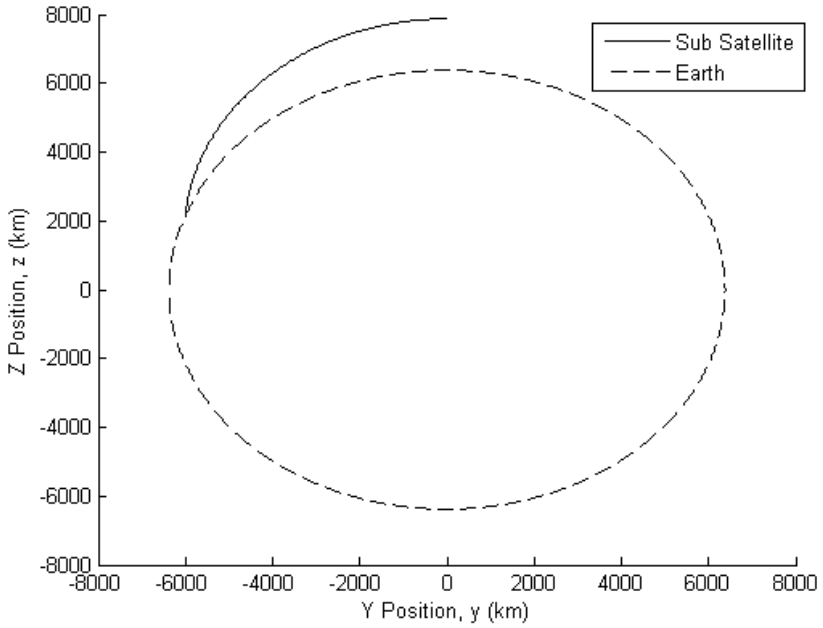

Figure 5.5 Trajectory at 1500 km Altitude for ΔV_{1y} = 1.0 km/s in Case 1

Increasing the tether length also affects the time to impact and the ground range covered by the sub-satellite after release. As the tether length increases the ground range and the time to impact decrease as well. This is due to the fact that the sub-satellite is located below the main satellite.

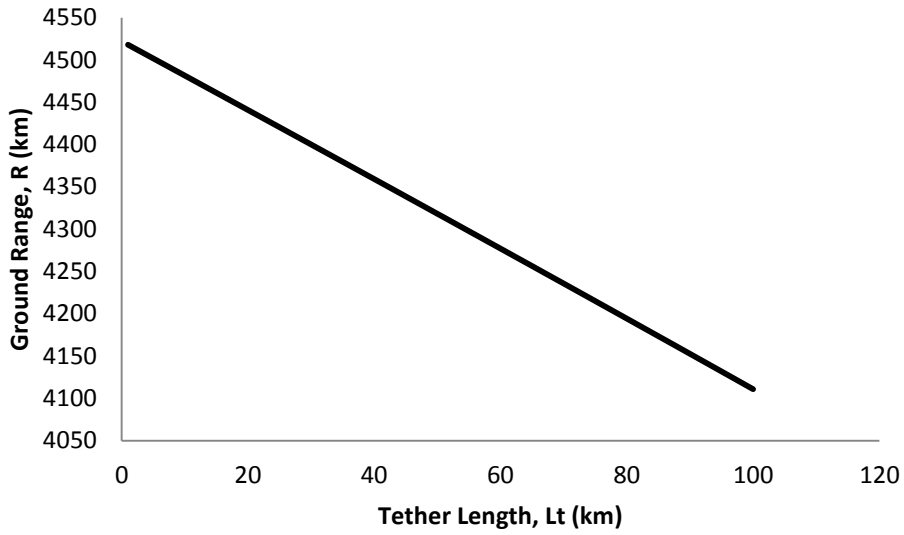

Figure 5.6 Ground Range vs. Tether Length for ΔV_{1y} = 1.0 km/s in Case 1

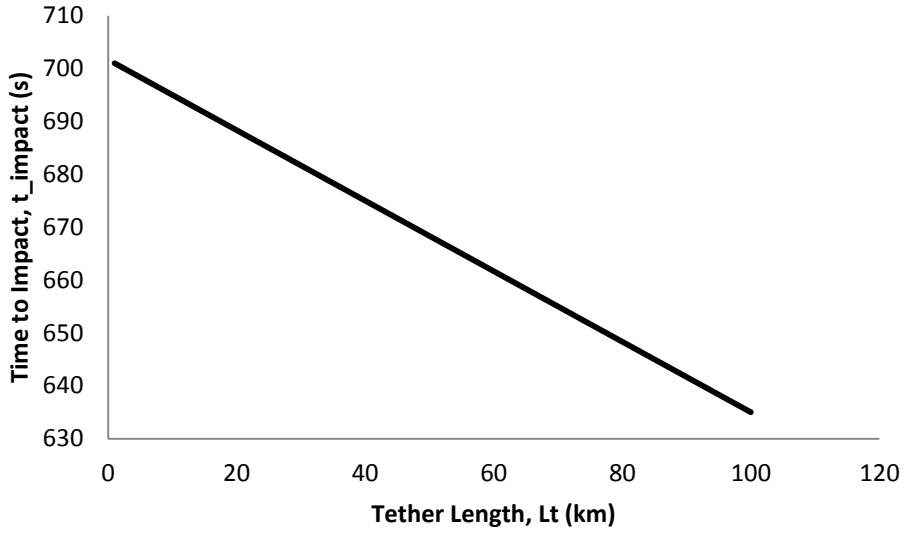

Figure 5.7 Time to Impact vs. Tether Length for ΔV_{1y} = 1.0 km/s in Case 1

A tether length of four kilometers, fifty-five kilometers, and one hundred kilometers are examined in more detail. The ground range and time to impact for these three cases can be found in table 5.3.

Table 5.3: Range and Impact Time for $\Delta V_{1y} = 1.0$ km/s at Three Tether Lengths for Case 1

Tether Length (km)	**Ground Range (km)**	**Time to Impact (s)**
4	4505.7	699
55	4297.5	665
100	4110.8	635

The maximum range and time to impact occur when the tether length is shorter. If a shorter ground range or time to impact is desired, an increase in tether length can achieve the desired results instead of decreasing the altitude. Figure 5.3 shows the impact trajectory of the sub-satellite at an altitude of five hundred kilometers and a tether length of four kilometers. The next two figures show the impact trajectories of the sub-satellite for the other two tether lengths. The changes in the impact trajectory of the sub-satellite after release are small. The sub-satellite travels along a similar impact trajectory path for each tether length; however, as the tether increases the point of impact moves closer to the point of release. This movement of the impact point results in a decrease of the ground range and time to impact of the sub-satellite.

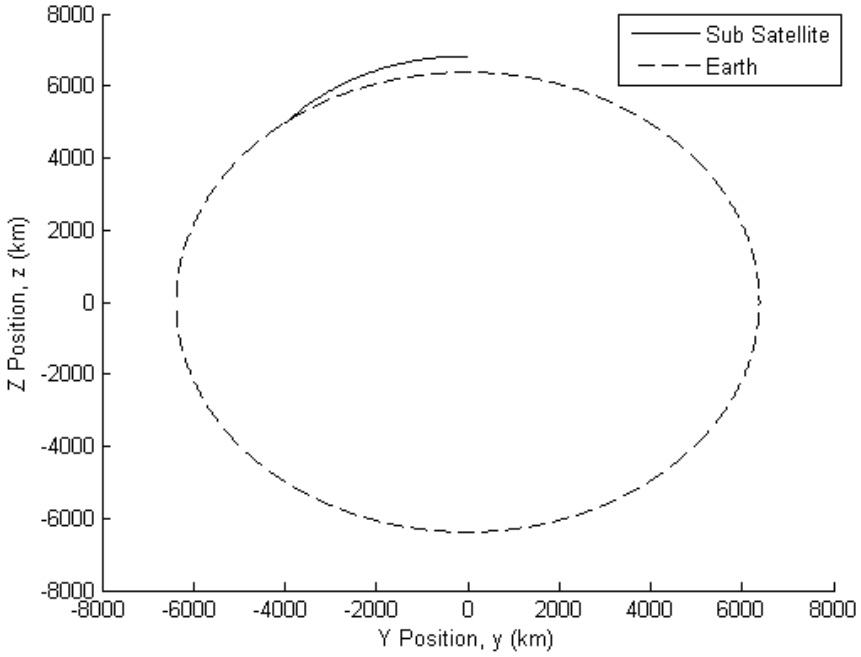

Figure 5.8 Trajectory at 55 km Tether Length for ΔV_{1y} = 1.0 km/s for Case 1

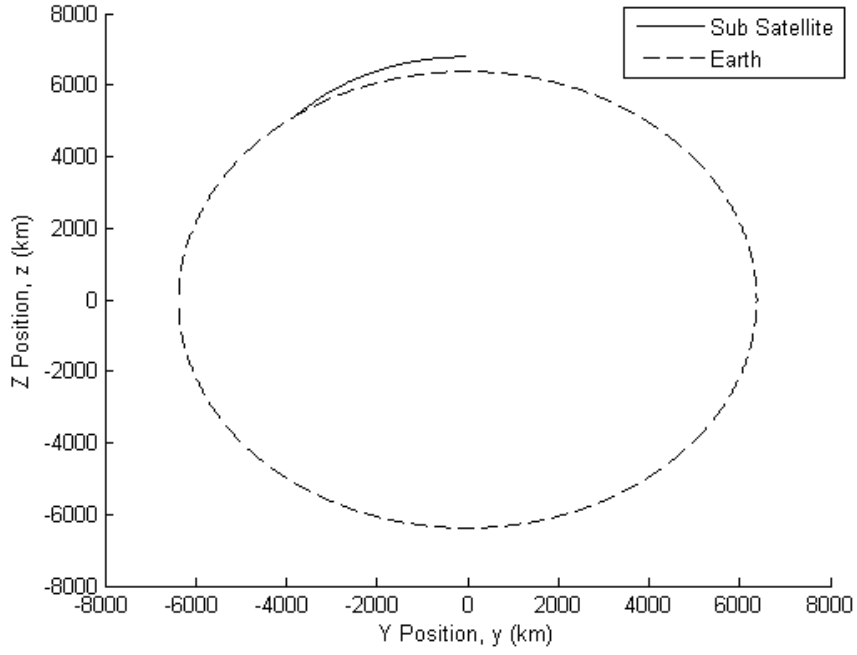

Figure 5.9 Trajectory at 100 km Tether Length for ΔV_{1y} = 1.0 km/s for Case 1

Finally, the impulsive velocity change of the sub-satellite is increased while the altitude and tether length are kept constant at five hundred kilometers and four kilometers, respectively. The effect of the impulsive velocity change increase on the ground range and time to impact can be determined by inspecting figures 5.10 and 5.11.

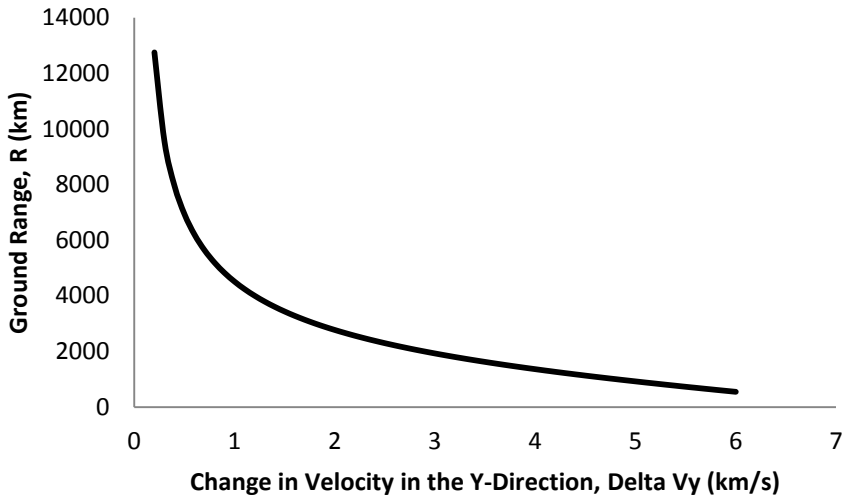

Figure 5.10 Ground Range vs. $+\Delta V_{1y}$ for Case 1

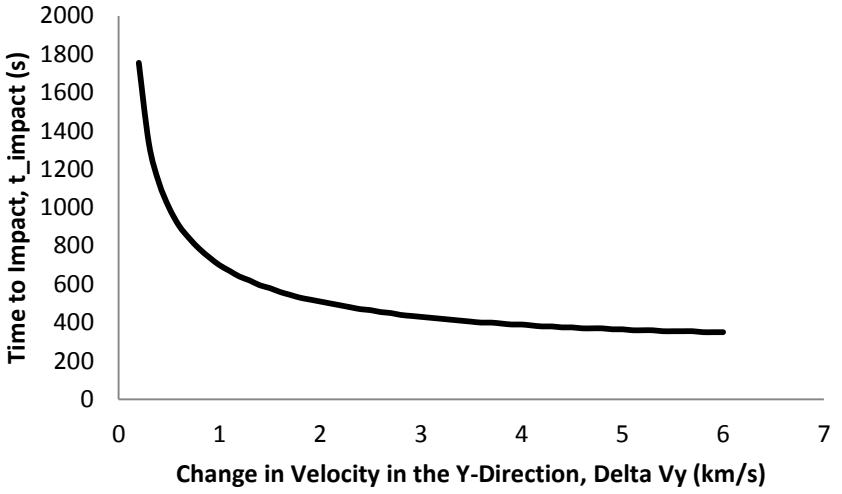

Figure 5.11 Time to Impact vs. $+\Delta V_{1y}$ for Case 1

As the impulsive velocity change is increased the ground range and the time to impact decreases because the larger the impulsive velocity change is the smaller the impact orbit will be. In other words the point of impact will move closer to the release point. The minimum impulsive velocity change needed to cause an impact was 0.2 km/s in the positive Y-direction. The maximum and minimum values for the ground range and time to impact are shown in table 5.4.

Table 5.4 Maximum and Minimum Values as $+\Delta V_{1y}$ Increases for Case 1

Velocity Change (km/s)	**Ground Range (km)**	**Time to Impact (s)**
0.2	12746.8	1755
3	1924.3	430
6	545.6	350

While an impulsive velocity change of six kilometers achieves the shortest ground range and time to impact, the fuel needed to achieve this impulsive velocity change and impact values will be greater than the fuel needed to achieve impact at the lowest impulsive velocity change. It is important to remember that there are trade-offs when selecting an impulsive velocity change.

5.1.2 Impulsive Velocity Change of 1.0 km/s in the Positive Z – Direction

For this impulsive velocity change, an increase in the altitude will also lead to an increase in the ground range covered by the sub-satellite at release and the time to impact. This matches with the results found in the previous section. The increase of the ground range and time to impact can be seen in figures 5.12 and 5.13. The maximum and minimum values for the ground range and time to impact are listed in table 5.5.

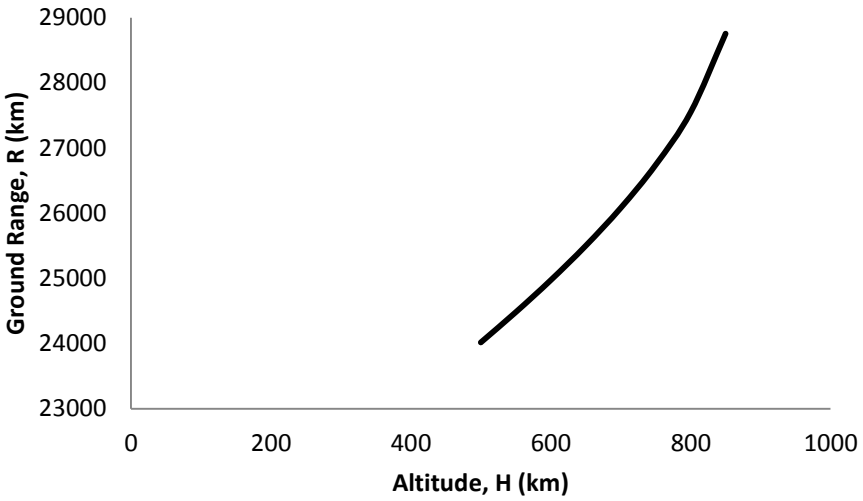

Figure 5.12 Ground Range vs. Altitude for ΔV_{1z} = 1.0 km/s in Case 1

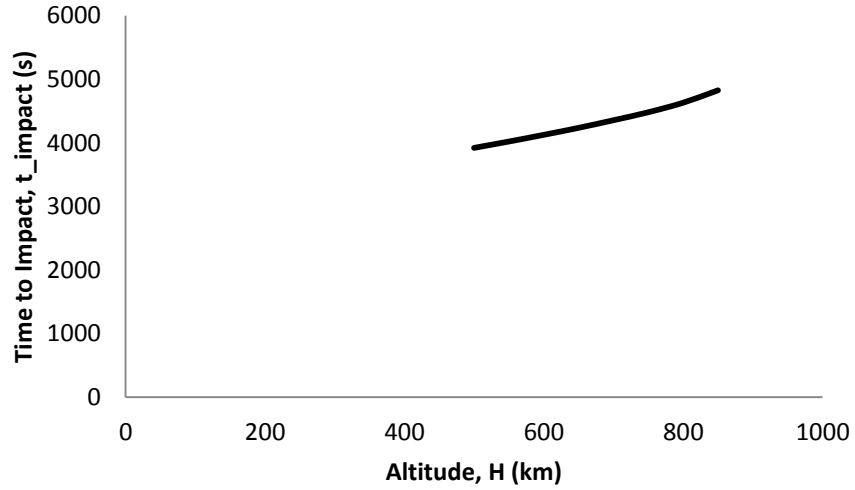

Figure 5.13 Time to impact vs. Altitude for ΔV_{1z} = 1.0 km/s in Case 1

The impulsive velocity change placed on the sub-satellite does not result in an impact at higher altitudes; however, if the impulsive velocity change for the sub-satellite is increased an impact can occur. For this velocity change an altitude of five hundred kilometers, six hundred and fifty kilometers, and eight hundred and fifty kilometers will be looked at in more detail.

Table 5.5 Range and Impact Time for $\Delta V_{1z} = 1.0$ km/s at Three Altitudes for Case 1

Altitude (km)	Ground Range (km)	Time to Impact (s)
500	24015.7	3920
650	25498.6	4235
850	28753.9	4825

The ground range and time to impact are larger than the values in the previous section in table 4.2 because the sub-satellite is lofted up higher in its impact trajectory. Another way to phrase it is that the angle of the sub-satellite's impact trajectory at release is greater than the angle for the impact trajectory at release when the velocity change in the positive Y – Direction was done. As the altitude is increased the impact trajectory of the sub-satellite becomes longer and the point of impact moves further around the Earth. The impact trajectories for the sub-satellite at an altitude of five hundred kilometers, six hundred and fifty kilometers, and eight hundred and fifty kilometers can be seen in figures 5.14, 5.15, and 5.16.

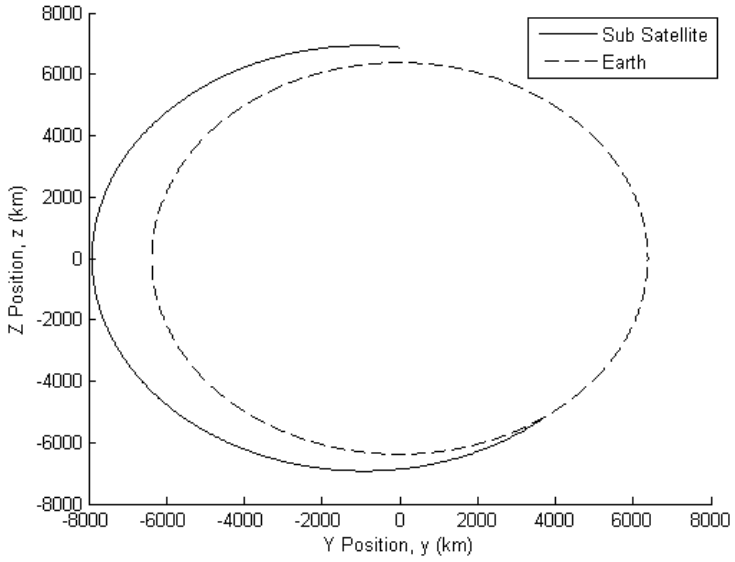

Figure 5.14 Trajectory at 500 km Altitude for $\Delta V_{1z} = 1.0$ km/s in Case 1

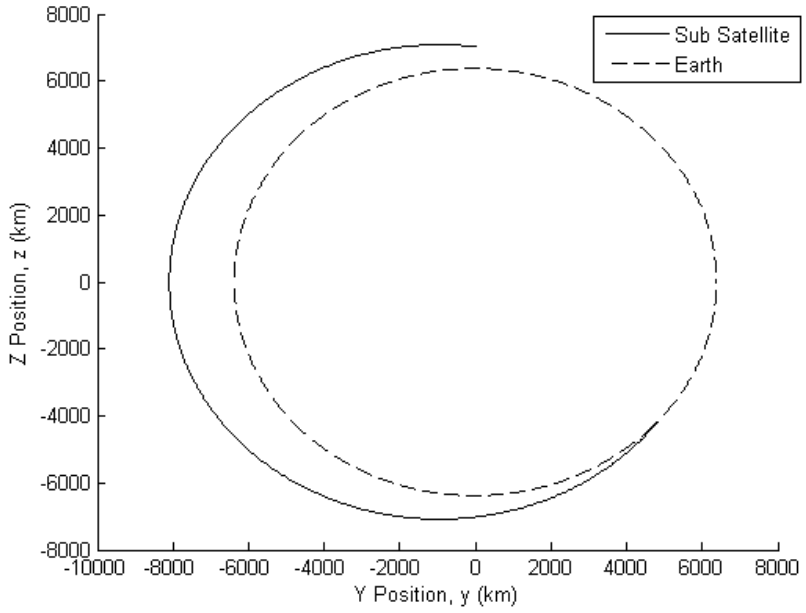

Figure 5.15 Trajectory at 650 km Altitude for ΔV_{1z} = 1.0 km/s in Case 1

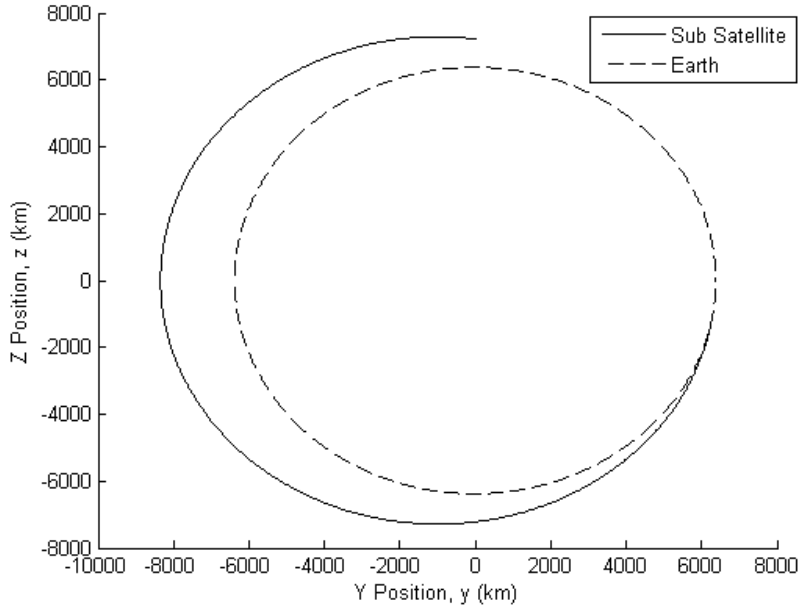

5.16 Trajectory at 850 km Altitude for ΔV_{1z} = 1.0 km/s in Case 1

An increasing tether length for an impulsive velocity change in the positive Z – direction has the same impact on the ground range and time to impact as it did when the impulsive

velocity change was in the positive Y – direction. Both values decrease as the tether length increases; therefore, the maximum ground range and time to impact will occur at the smallest tether length and the minimum ground and time to impact will occur at the largest tether length value. The decrease in ground range and time to impact can be seen in figures 5.17 and 5.18. A list of ground ranges and times to impact are given in table 5.6.

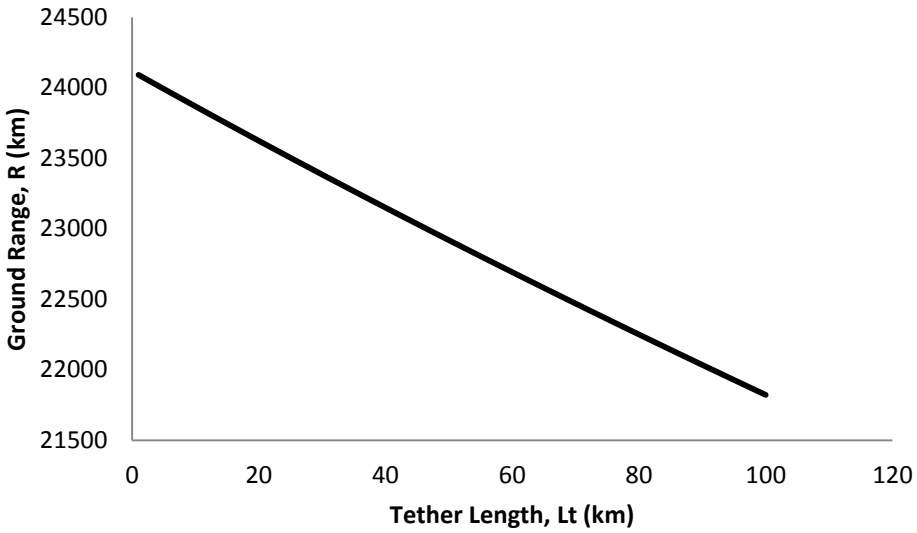

Figure 5.17 Ground Range vs. Tether Length for ΔV_{1z} = 1.0 km/s in Case 1

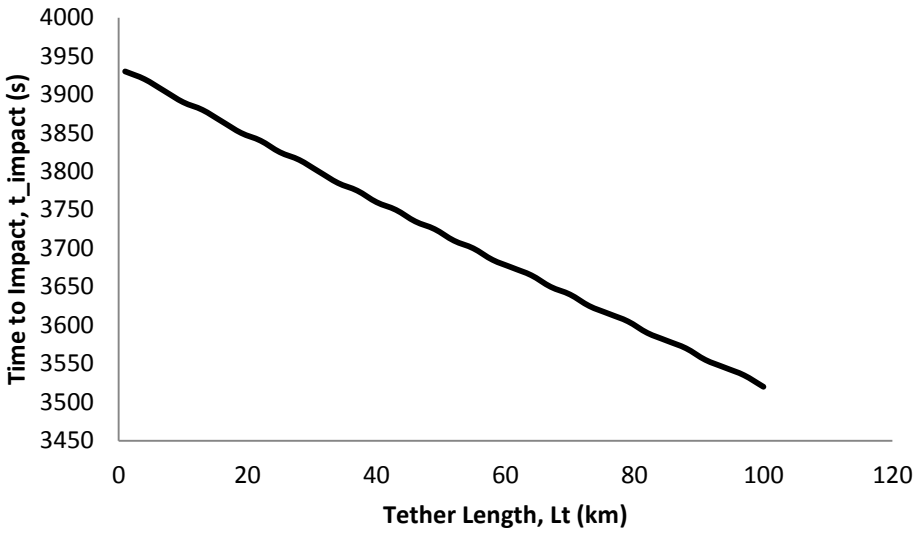

Figure 5.18 Time to Impact vs. Tether Length for ΔV_{1z} = 1.0 km/s in Case 1

Table 5.6 Range and Impact Time for $\Delta V_{1z} = 1.0$ km/s at Three Tether Lengths for Case 1

Tether Length (km)	Ground Range (km)	Time to Impact (s)
4	24015.7	3920
55	22804.3	3700
100	21821.4	3520

The ground range and time to impact for an impulsive velocity change in the positive Z – direction is greater than the ground range and time to impact for an impulsive velocity change in the positive Y – direction for an increasing tether length because of the lofted trajectory. Figure 5.14 shows the impact trajectory for an altitude of 500 km and a tether length of 4 km. The other two impact trajectories are shown in figures 5.19 and 5.20.

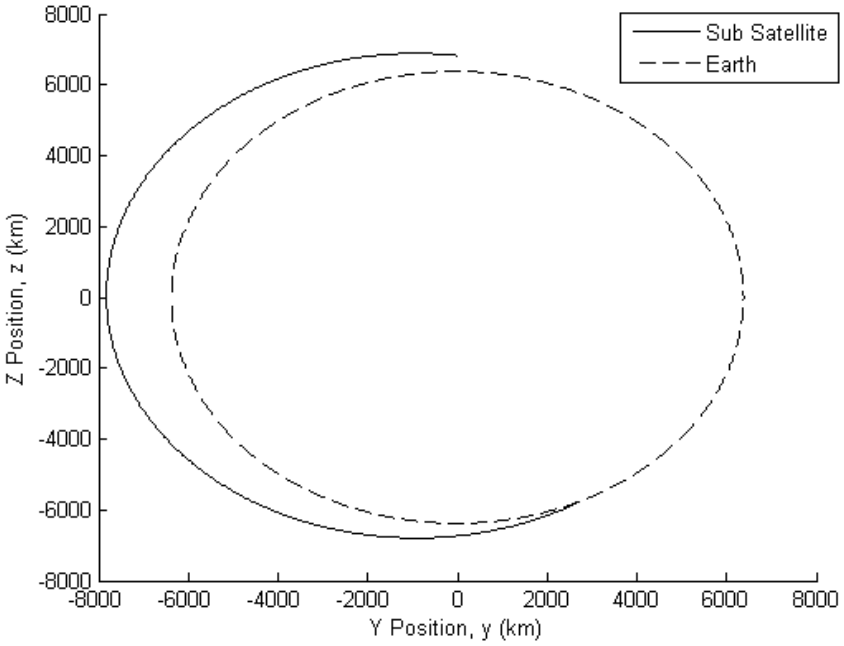

Figure 5.19 Trajectory at 55 km Tether Length for ΔV_{1z} = 1.0 km/s in Case 1

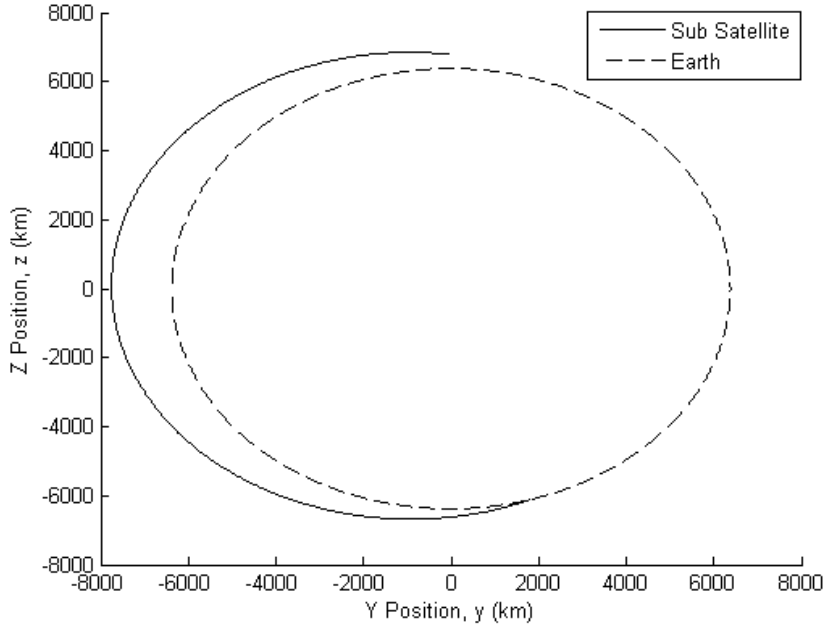

Figure 5.20 Trajectory at 100 km Tether Length for ΔV_{1z} = 1.0 km/s in Case 1

Figures 5.21 to 5.22 show the decrease of the ground range and the increase of the time to impact as the impulsive velocity change is increased.

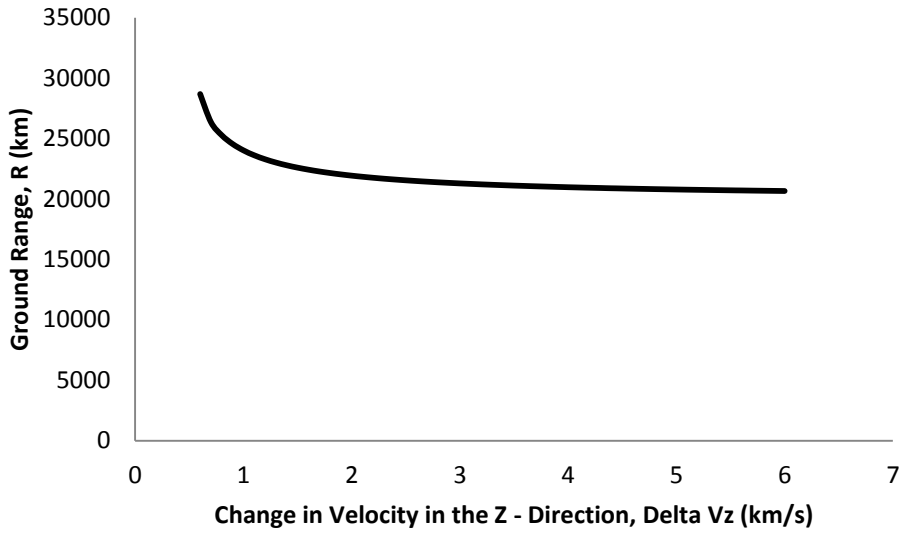

Figure 5.21 Ground Range vs. $+\Delta V_{1z}$ for Case 1

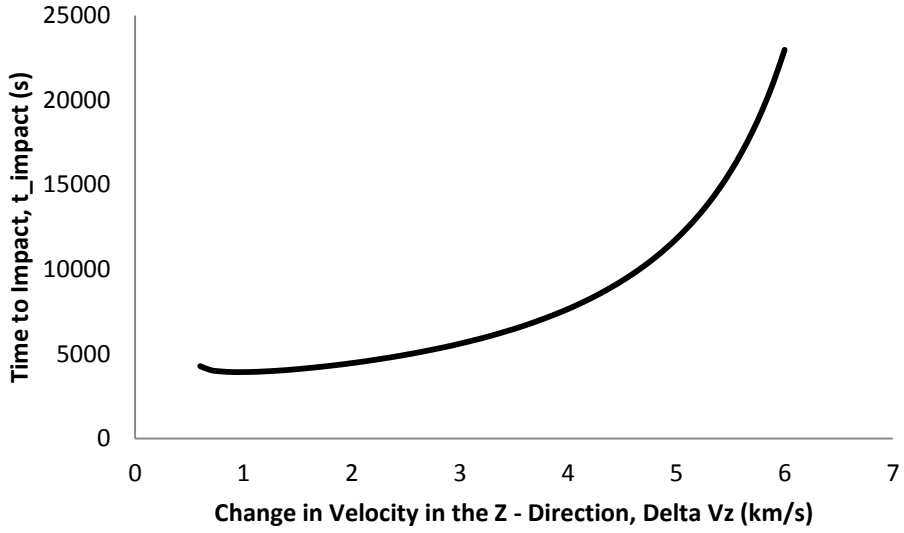

Figure 5.22 Time to Impact vs. $+\Delta V_{1z}$ for Case 1

The increase of the impulsive velocity change in the positive Z – direction also leads to a decrease in the ground range of the sub-satellite; however, the time to impact starts to increase after a three kilometer per second impulsive velocity change. This happens because the sub-satellite is getting lofted higher but is impacting at a closer point to the release point. Figure 5.23

shows the impact trajectory for an impulsive velocity change of three kilometers per second. The sub-satellite is lofted higher after it is released from the TSS with an impulsive velocity change of three kilometers per second in the positive Z – direction than it is when the impulsive velocity change is one kilometer per second.

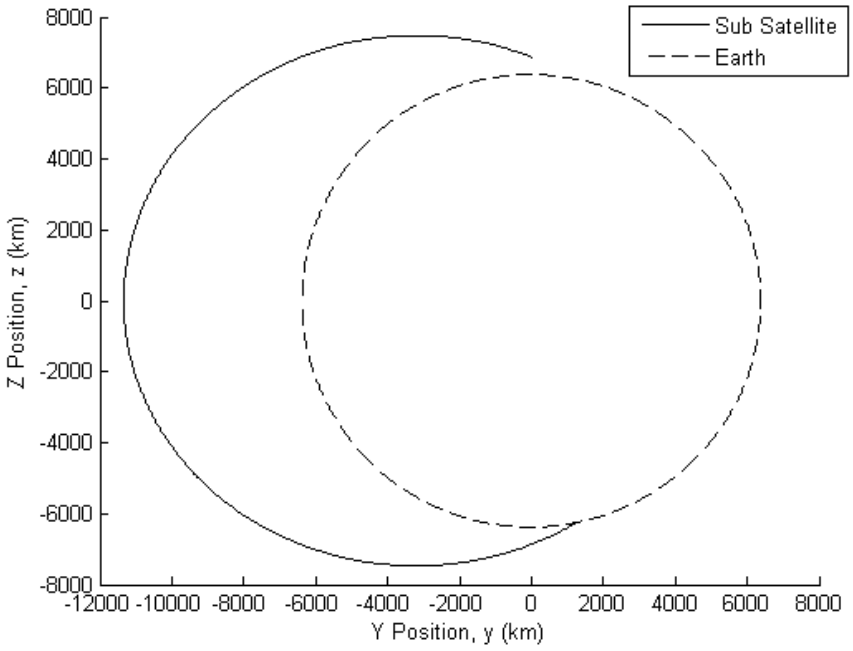

Figure 5.23 Lofted Trajectory at ΔV_{1z} = 3.0 km/s for Case 1

The minimum impulsive velocity change needed to cause impact was 0.6 km/s in the positive Y-direction. The maximum and minimum values for the ground range and time to impact are shown in table 5.7 on the next page.

Table 5.7 Maximum and Minimum Values as $+\Delta V_z$ Increases for Case 1

Velocity Change (km/s)	**Ground Range (km)**	**Time to Impact (s)**
0.6	28675.1	4270
3	21282.8	5600
6	20654.0	22965

For an impulsive velocity change in the positive Z – direction a smaller ground range can be achieved by increasing the impulsive velocity change; however, the time to impact will increase as the impulsive velocity change becomes greater than three kilometers per second.

5.1.3 Impulsive Velocity Change of 3.0 km/s in the Negative Z – Direction

The third impulsive velocity change investigated in this section is higher than the previous two sections because a larger impulsive velocity change in the negative Z – Direction was needed in order to create impacts at higher altitudes. During this altitude range the ground range covered by the sub-satellite during its impact trajectory and the time to impact increases because of reasons explained in the previous two sections. Figures 5.24 and 5.25 show the increasing trend of the ground range and time to impact as the altitude of the sub-satellite increases. The values for the ground range and time to impact for three altitudes are given in table 5.8.

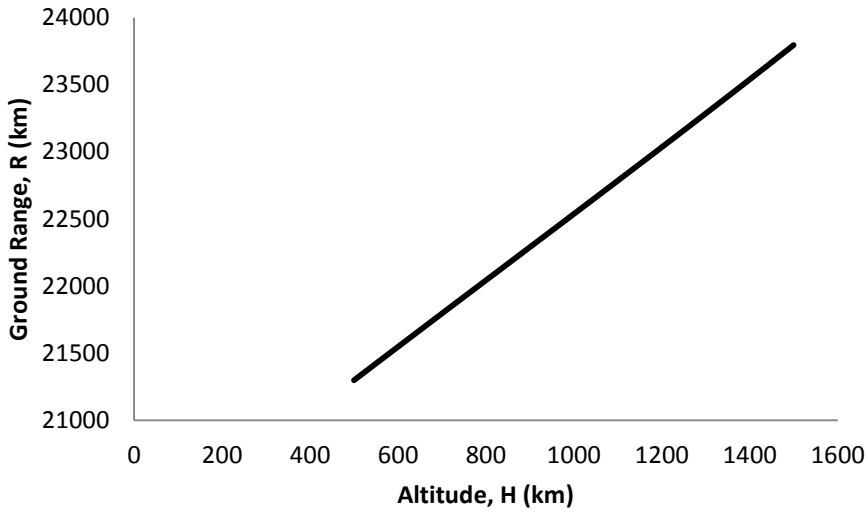

Figure 5.24 Ground Range vs. Altitude for ΔV_{1z} = -3.0 km/s in Case 1

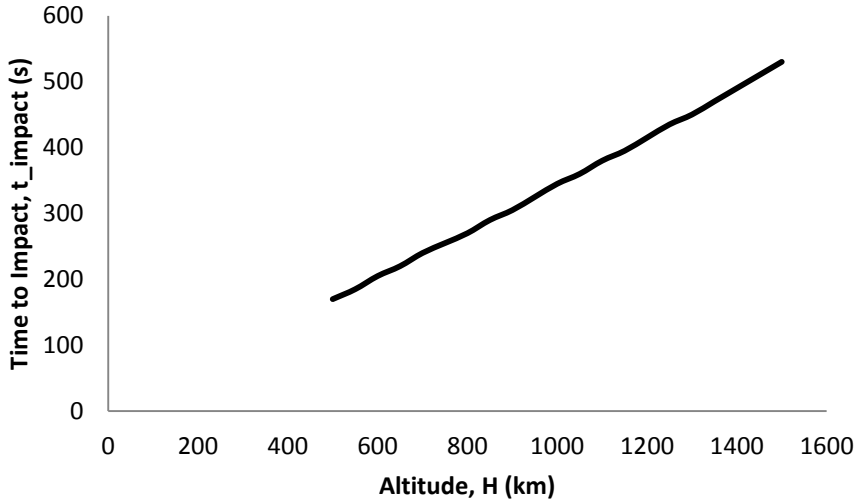

Figure 5.25 Time to Impact vs. Altitude for ΔV_{1z} = -3.0 km/s in Case 1

Table 5.8 Range and Impact Time for $\Delta V_{1z} = -3.0$ km/s at Three Altitudes for Case 1

Altitude (km)	Ground Range (km)	Time to Impact (s)
500	21297.8	170
1000	22536.7	345
1500	23795.4	530

The ground range and time to impact are lower than the ground range and time to impact that were calculated in the previous section. The time to impact is significantly smaller because of the steep descent of the impact trajectory caused by the large impulsive velocity change in the negative Z - direction. The large impulsive change in velocity in the negative Z – direction, causes the sub-satellite to enter a very small orbit that will send the sub-satellite into the Earth quicker than the other impulsive velocity changes. The impact trajectories can be seen in the next three figures.

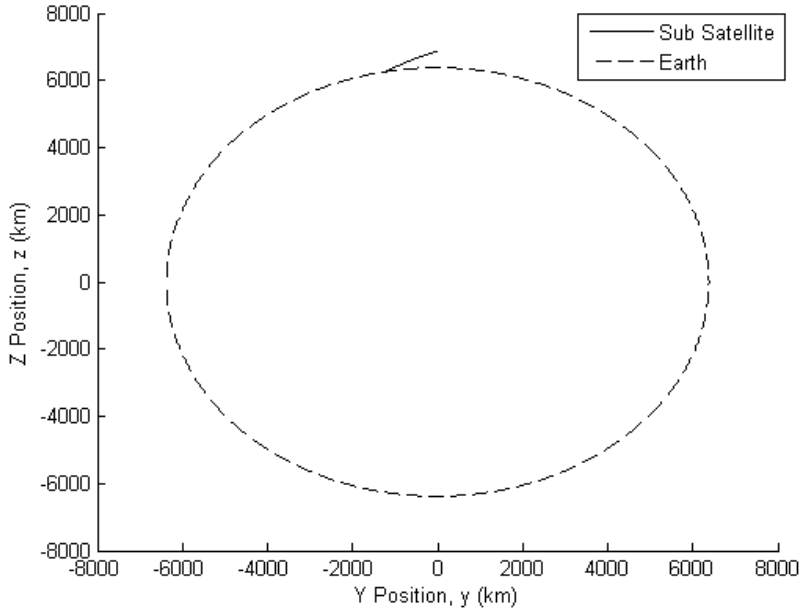

Figure 5.26 Trajectory at 500 km Altitude for ΔV_{1z} = -3.0 km/s in Case 1

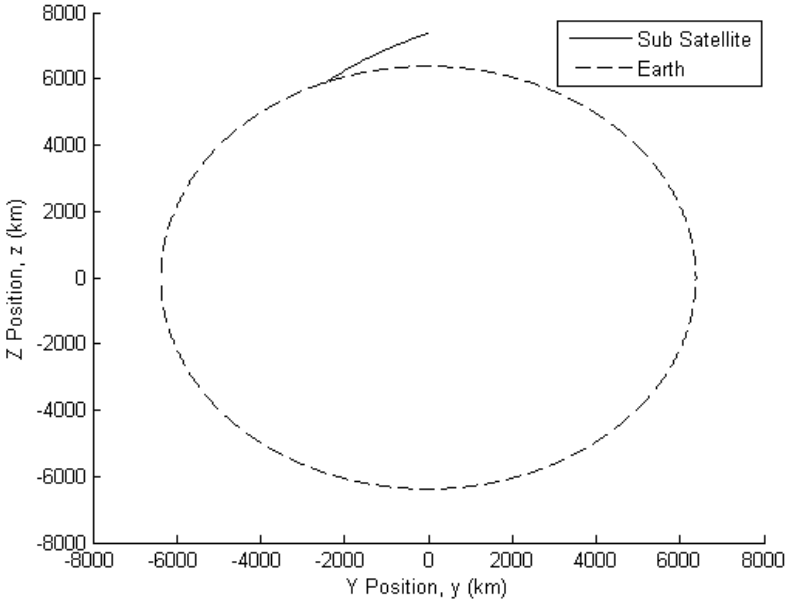

Figure 5.27 Trajectory at 1000 km Altitude for ΔV_{1z} = -3.0 km/s in Case 1

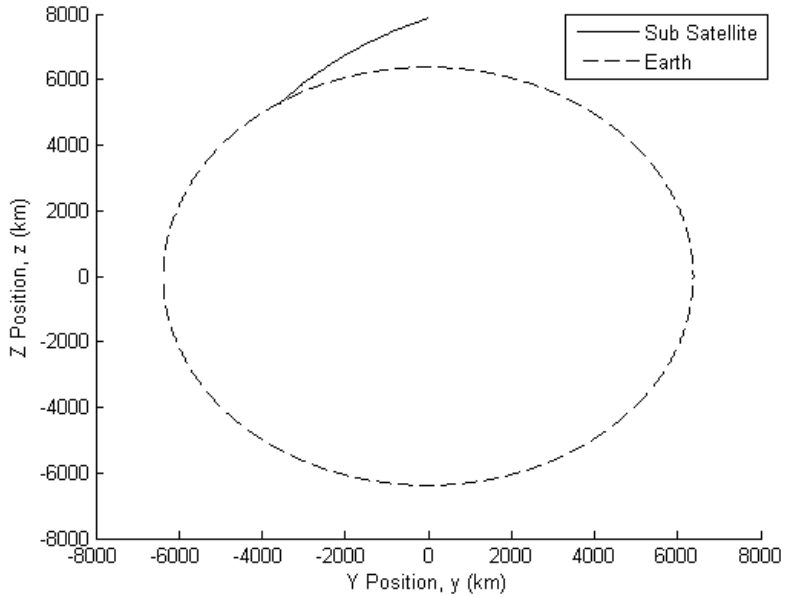

Figure 5.28 Trajectory at 1500 km Altitude for ΔV_{1z} = -3.0 km/s in Case 1

An impact is found for all values of the tether length from one kilometer to one hundred kilometers. As the tether length is increased for this impulsive change in velocity the ground

range and the time to impact decrease. These two trends can be seen in Figures 5.29 and 5.30. Table 5.9 gives specific values for three tether lengths.

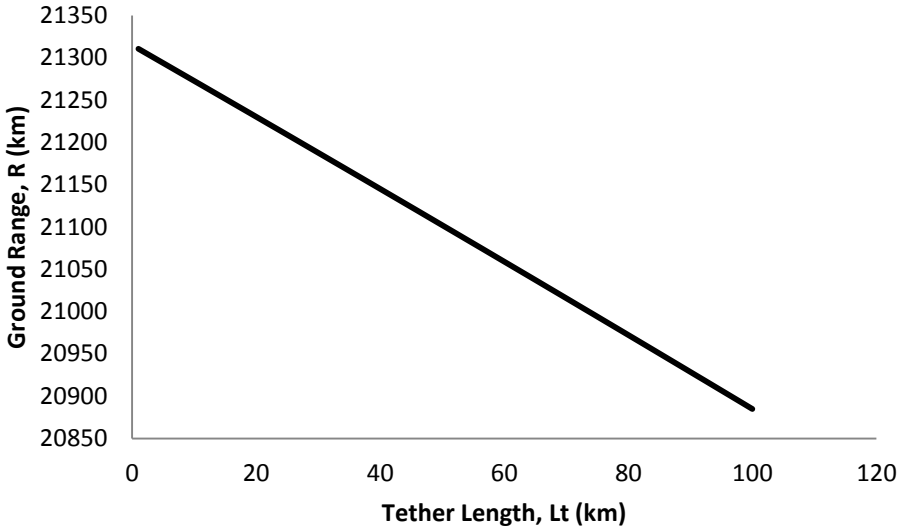

Figure 5.29 Ground Range vs. Tether Length for ΔV_{1z} = -3.0 km/s in Case 1

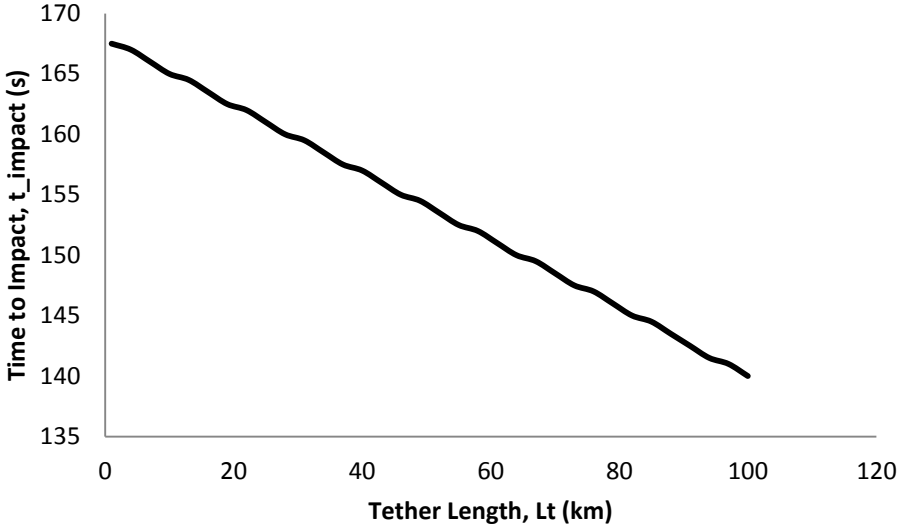

Figure 5.30 Time to Impact vs. Tether Length for ΔV_{1z} = -3.0 km/s in Case 1

Table 5.9 Range and Impact Time for $\Delta V_{1z} = -3.0$ km/s at Three Tether Lengths for Case 1

Tether Length (km)	Ground Range (km)	Time to Impact (s)
4	21297.8	167
55	21080.4	152.5
100	20884.8	140

The decrease in ground range and time to impact are caused by the impact trajectory of the sub-satellite after release. The impact point of the sub-satellite slowly moves closer to the release point; however, the impact trajectory becomes steeper as the tether length increases. This increase in the steepness of the impact trajectory leads to the decrease in time that is seen in figure 5.30. The impact trajectory of the sub-satellite with a four kilometer tether length is shown in figure 5.26. The impact trajectory for the sub-satellite with a fifty – five kilometer tether length and a one hundred kilometer tether length are shown in figure 5.31 and 5.32.

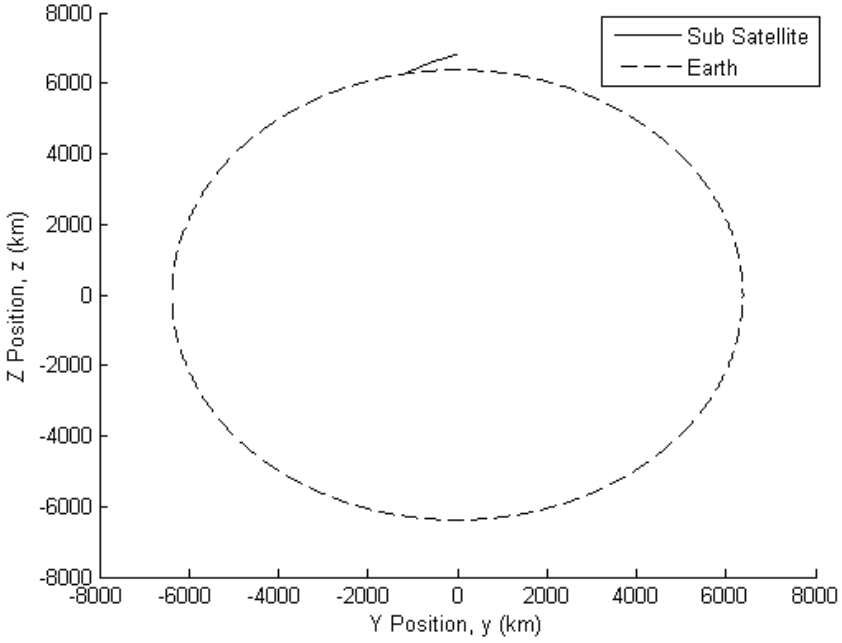

Figure 5.31 Trajectory at 55 km Tether Length for ΔV_{1z} = -3.0 km/s in Case 1

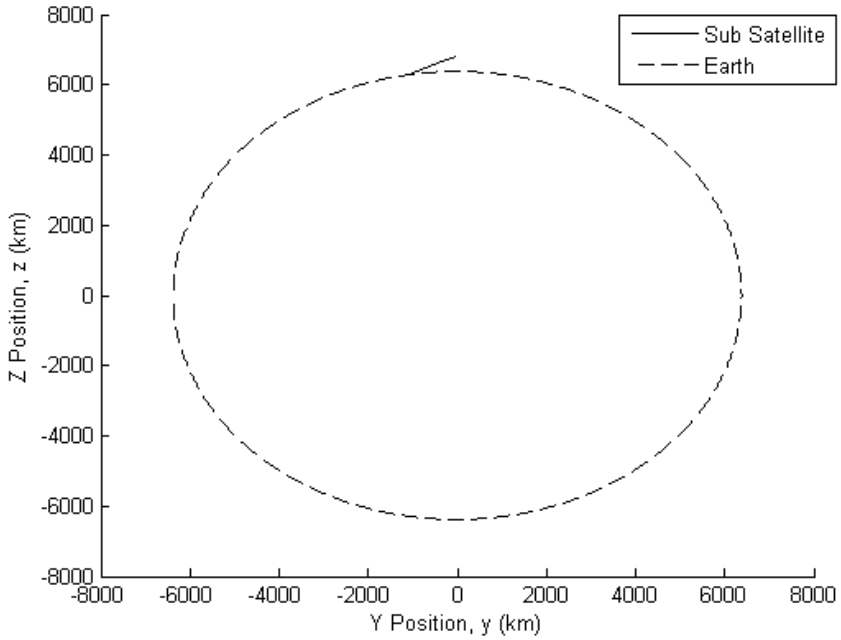

Figure 5.32 Trajectory at 100 km Tether Length for ΔV_{1z} = -3.0 km/s in Case 1

When the impulsive velocity change placed on the sub-satellite is increased in the negative Z – direction, the ground range and the time to impact are decreased. This decrease occurs because the impulsive velocity change increase results in a steeper descent toward the impact point and the movement of the impact point is toward the point of release. Figures 5.33 and 5.34 show ground range and time to impact as a function of the impulsive velocity change increase and are located on the next page.

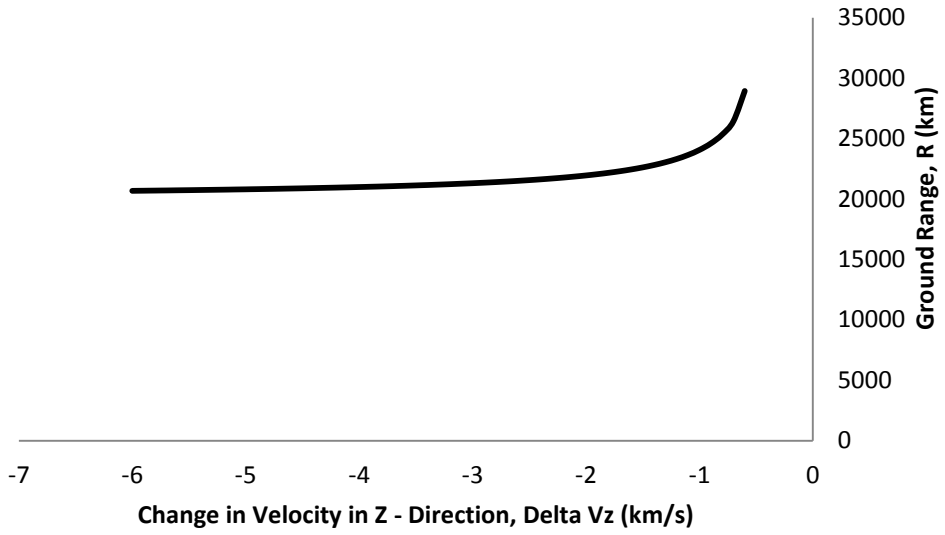

Figure 5.33 Ground Range vs. $-\Delta V_{1z}$ for Case 1

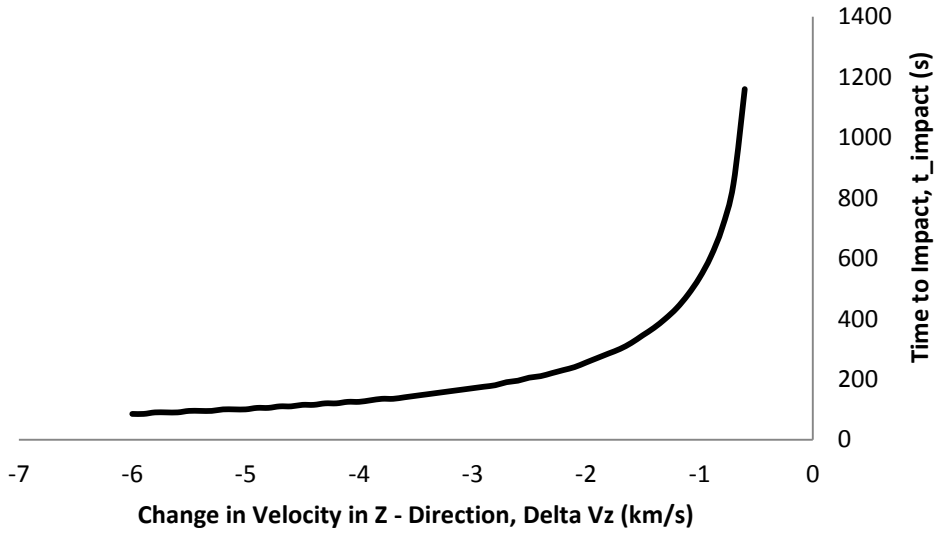

Figure 5.34 Time to Impact vs. $-\Delta V_{1z}$ for Case 1

The minimum impulsive velocity change required for an impact trajectory at a five hundred kilometer altitude and a tether length of four kilometers is 0.6 kilometers per second in the negative Z – direction. This impulsive velocity change is increased until it reaches 6.0

kilometers per second. The maximum and minimum values for the ground range and time to impact are shown in table 5.10.

Table 5.10: Maximum and Minimum Values as $-\Delta V_{1z}$ Increases for Case 1

Velocity Change (km/s)	Ground Range (km)	Time to Impact (s)
-0.6	28929.6	1160
-3	21297.8	170
-6	20667.6	85

5.1.4 Comparison between Velocity Changes for First Configuration

For the first configuration point a small impulsive velocity change in the positive Y and Z – directions leads to an impact trajectory; however, a minimum value of 0.6 kilometers per second in the negative Z – direction is needed to create the first impact point when the altitude is at five hundred kilometers and the tether length is at four kilometers. If the altitude is increased, the minimum impulsive velocity change needed in the positive Z – direction has to increase as well in order to achieve an impact at an altitude greater than eight hundred and fifty kilometers. The other two impulsive velocity changes do not require a further increase in order to achieve an impact trajectory for the altitudes tested in the simulation.

The impulsive velocity changes in the Y and Z – directions responded to changes in altitude and tether length in the same way. The range and time to impact increased for an increasing altitude and decreased for an increasing tether length. The tether length decreased the range in both cases by less than two hundred kilometers. An increase in the altitude for an impulsive velocity change in the positive Z – direction lead to a greater increase in the range when compared to the increase found in the range for an impulsive velocity change in the

positive Y – direction; therefore, if the objective is to have the longest range increasing the altitude and having an impulsive velocity change in the positive Z – direction will lead to the maximum range that can be achieved for this configuration. The minimum range can be achieved by increasing the tether length and implementing an impulsive velocity change in the positive Y – direction.

Another way to decrease the range in all three examples is to increase the impulsive velocity change. As the impulsive velocity change gets higher the range and time to impact decrease for a change in the positive Y – direction and for a change in the negative Z – direction. For the case when the impulsive velocity change is increased in the positive Z – direction, the range decreases but the time to impact starts to increase again after an impulsive velocity change of three kilometers per second. This occurs because the impact trajectory of the sub-satellite becomes lofted. As the sub-satellite is lofted into a higher orbit, the time it takes to impact the Earth will increase but the range may remain the same or slightly decrease. For this attempt in decreasing range, it is better to increase the impulsive velocity change in the positive Y – direction or in the negative Z – direction; however, having an impulsive velocity change of six kilometers in either direction will require a lot more fuel than changing the tether length or altitude of the TSS.

5.2 Results for Second Configuration or Case 2

For the second configuration, the sub-satellite is located above the main satellite. This is similar to case A for the analytical solutions. The three impulsive velocity changes that were applied to the sub-satellite in the second configuration are shown in table 5.11 on the next page.

Table 5.11: Impulsive Velocity Changes for Case 2

	Velocity Change (km/s)
ΔV_{1z}	1.0
ΔV_{1z}	-1.5
ΔV_{1y}	N/A
ΔV_{1y}	1.0

An impulsive velocity change in the positive Y – direction is not investigated because the velocity of the sub-satellite is in the positive Y – direction; therefore, an increase in the velocity in the positive Y – direction will only increase the size of the sub-satellite trajectory after release and its perigee point, which will not result in an impact of the sub-satellite.

5.2.1 Impulsive Velocity Change of 1.0 km/s in the Positive Z – Direction

For an increase in the altitude, the ground range covered by the impact trajectory and the time to impact increases; however, at altitudes greater than eight hundred and fifty kilometers the sub-satellite does not impact the Earth. This means that a greater impulsive velocity change in the positive Z – direction is needed in order to create an impact trajectory. The ground range and time to impact as a function of altitude are shown in figures 5.35 and 5.36. The figures are then followed by a table that lists the ground range and time to impact for an altitude of five hundred kilometers, six hundred and fifty kilometers, and eight hundred and fifty kilometers.

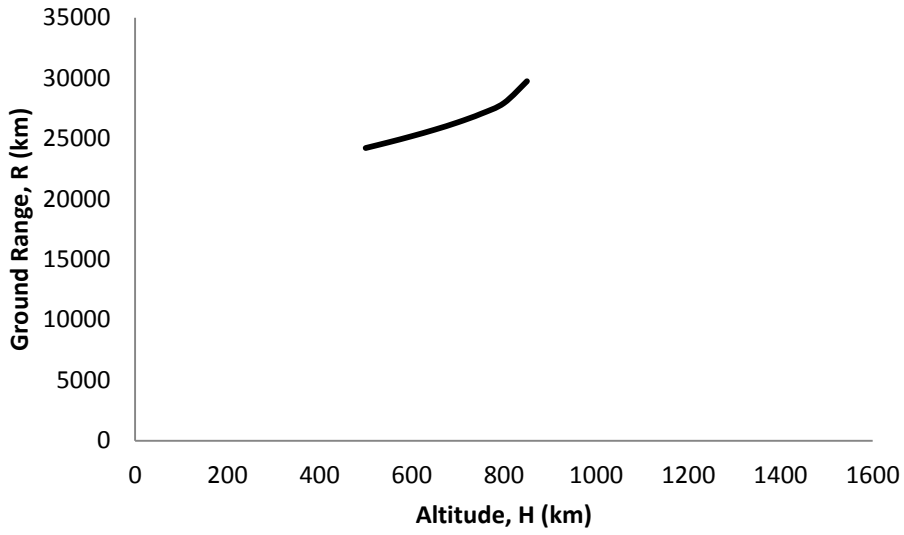

Figure 4.35 Ground Range vs. Altitude for ΔV_{1z} = 1.0 km/s in Case 2

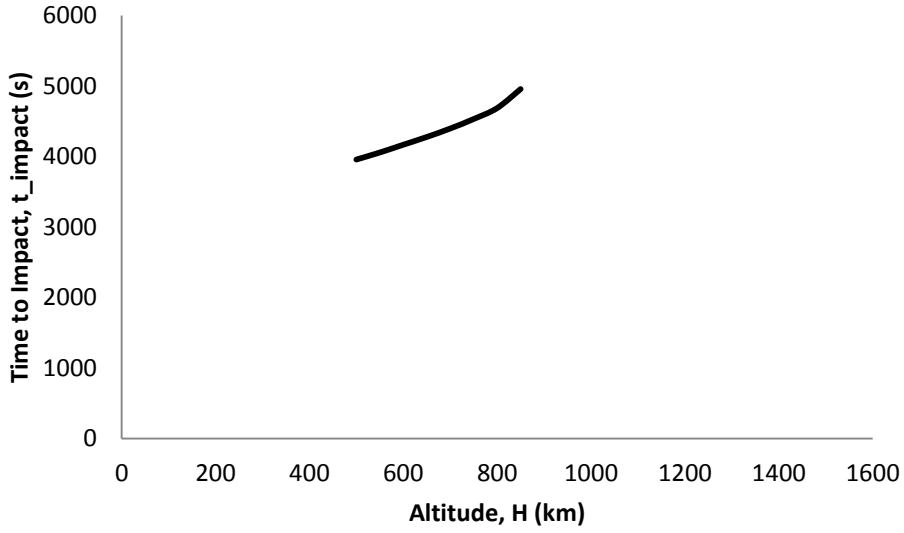

Figure 4.36 Time to Impact vs. Altitude for ΔV_{1z} = 1.0 km/s in Case 2

Table 5.12 Ground Range and Impact Time for ΔV_{1z} = 1.0 km/s at Three Altitudes for Case 2

Altitude (km)	Ground Range (km)	Time to Impact (s)
500	24210.6	3955
650	25730.4	4275
850	29736.1	4955

The impact trajectory of the sub-satellite is lofted until a maximum apogee is reached and then it begins its return toward the Earth. The increase in the ground range is caused by the movement of the impact point further away from the release point as the altitude increases. The increase in the time to impact is caused by the fact that as the altitude increases the area of the impact trajectory that is lofted increases as well. The impact trajectories for a five hundred kilometer altitude, a six hundred and fifty kilometer altitude, and an eight hundred and fifty kilometer altitude are shown below.

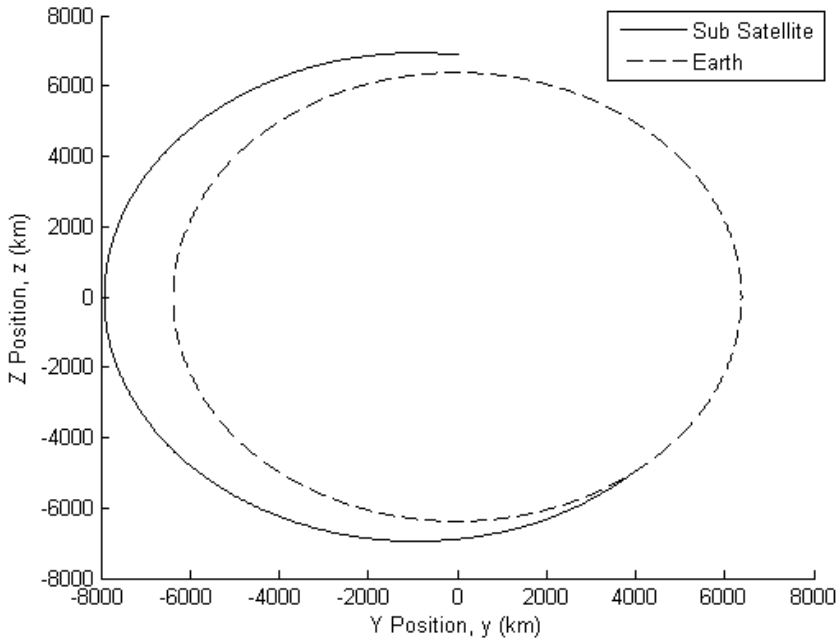

Figure 5.37 Trajectory at 500 km Altitude for ΔV_{1z} = 1.0 km/s in Case 2

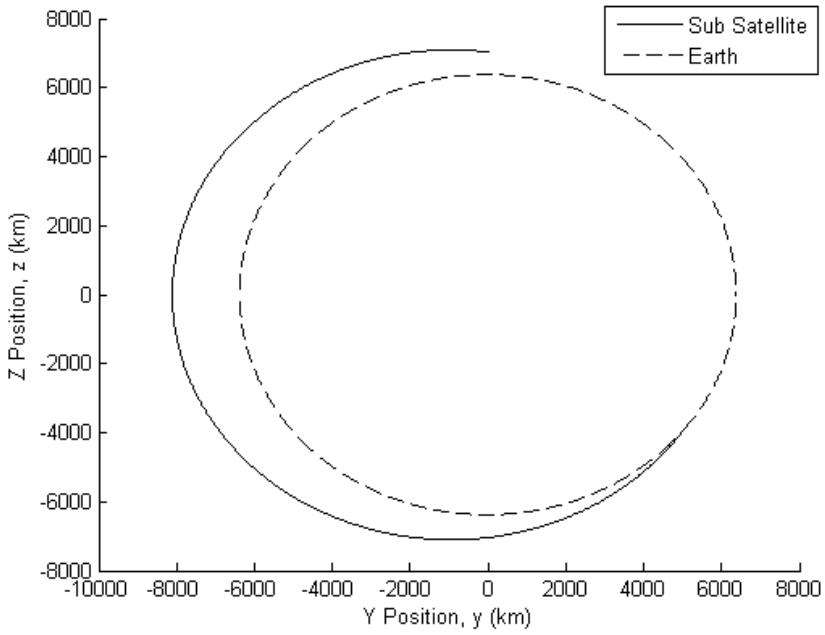

Figure 5.38 Trajectory at 650 km Altitude for ΔV_{1z} = 1.0 km/s in Case 2

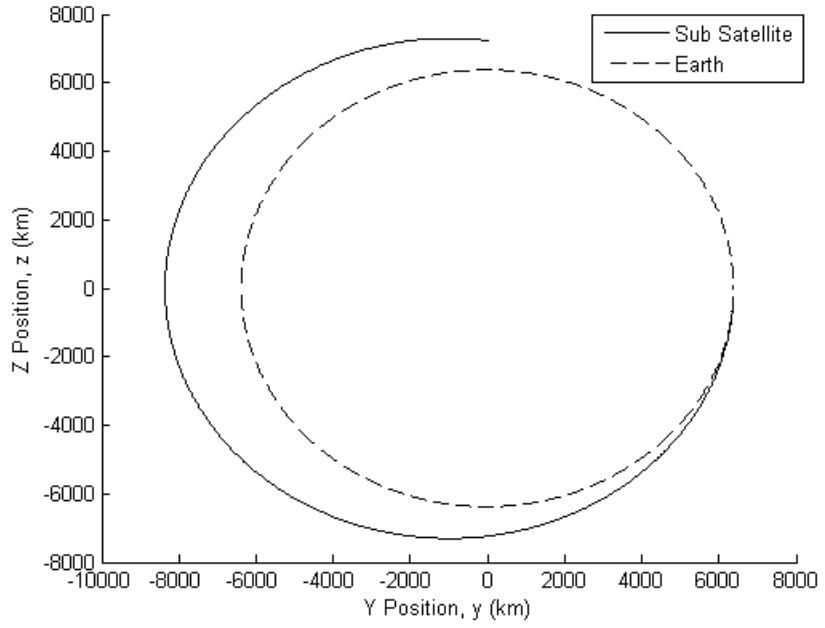

Figure 5.39 Trajectory at 850 km Altitude for ΔV_{1z} = 1.0 km/s in Case 2

The next change that is looked at for this impulsive velocity change is an increase in the tether length. The time to impact and the ground range increase as the tether length becomes longer. This means that the minimum range that can be achieved will occur at the shortest tether length, while the maximum range will occur at the longest length that the tether can reach. The increasing trends for the range and time to impact are shown in figures 5.40 and 5.41.

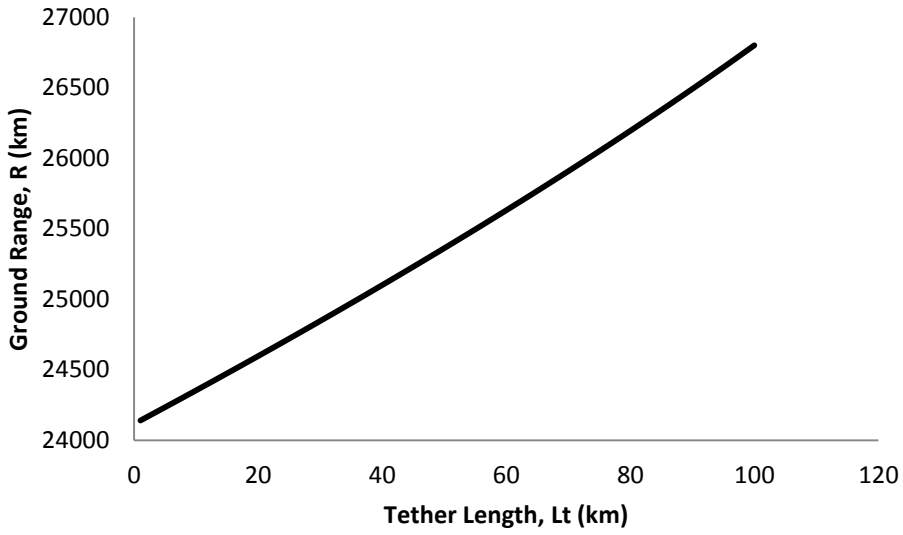

Figure 5.40 Ground Range vs. Tether Length for ΔV_{1z} = 1.0 km/s in Case 2

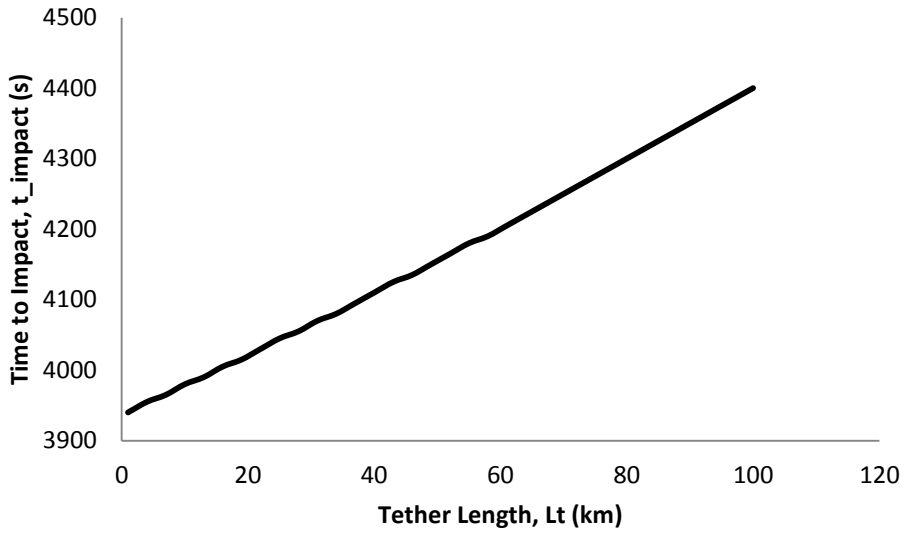

Figure 5.41 Time to Impact vs. Tether Length for ΔV_{1z} = 1.0 km/s in Case 2

A list of ground ranges and times to impact for a tether length of four kilometers, fifty-five kilometers, and one hundred kilometers is given in table 5.29.

Table 5.13 Range and Impact Time for ΔV_{1z} = 1.0 km/s at Three Tether Lengths for Case 3

Tether Length (km)	Ground Range (km)	Time to Impact (s)
4	24210.6	3955
55	25495.2	4180
100	26800.6	4400

The increase in tether length causes the ground range to increase because the point of impact moves further away from the point of release and the height of the sub-satellite is increasing. This same change in the impact point also causes an increase in the time to impact because if the impact point moves further away from the release point the time to get to an impact will increase. The impact trajectory at a four kilometer tether length is shown in figure 5.37. The other two impact trajectories are shown in the figures below.

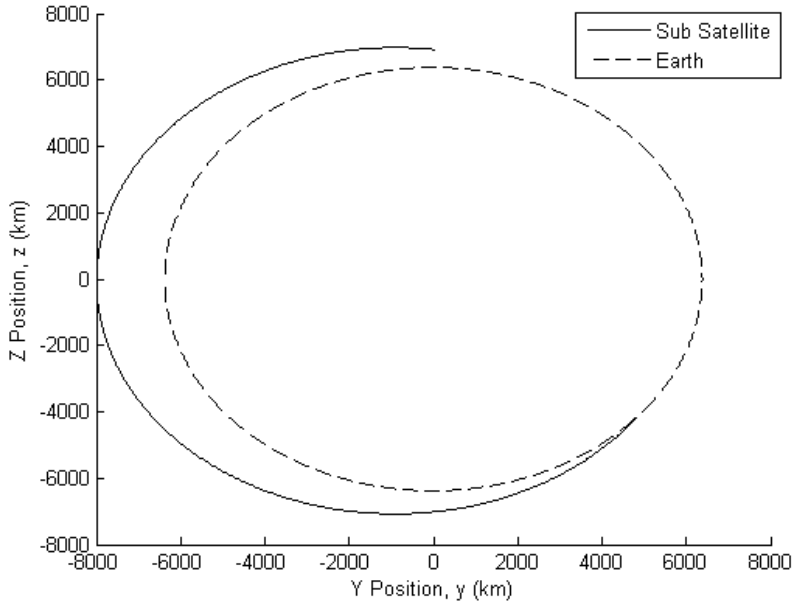

Figure 5.42 Trajectory at 55 km Tether Length for ΔV_{1z} = 1.0 km/s in Case 2

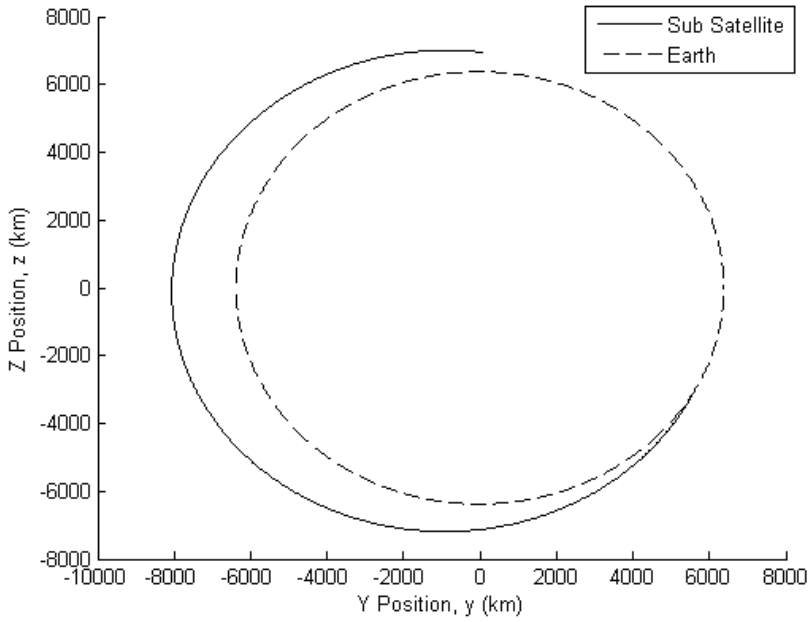

Figure 5.43 Trajectory at 100 km Tether Length for ΔV_{1z} = 1.0 km/s in Case 2

The last change that is looked at in order to cause an impact trajectory is the increase of the magnitude for the impulsive velocity change while keeping the altitude and tether length

constant at five hundred kilometers and four kilometers. The effect of the increase in the impulsive velocity change on the ground range and time to impact are shown in figures 5.44 to 5.45.

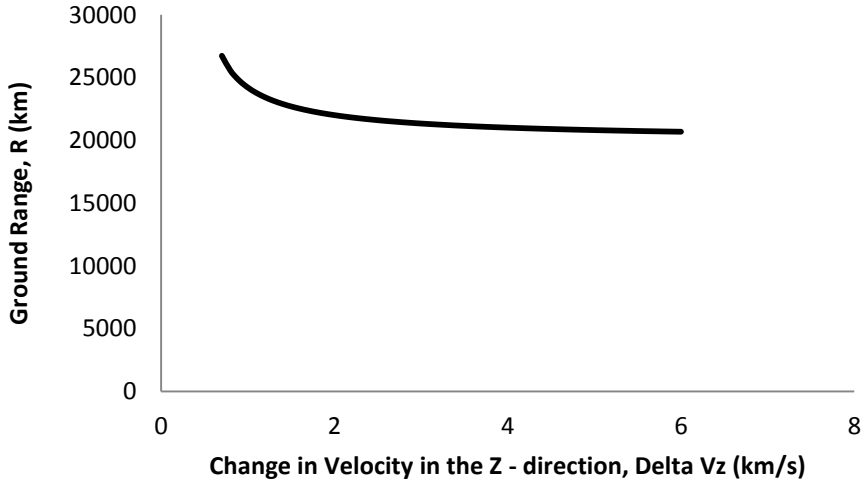

Figure 5.44 Ground Range vs. $+\Delta V_{1z}$ for Case 2

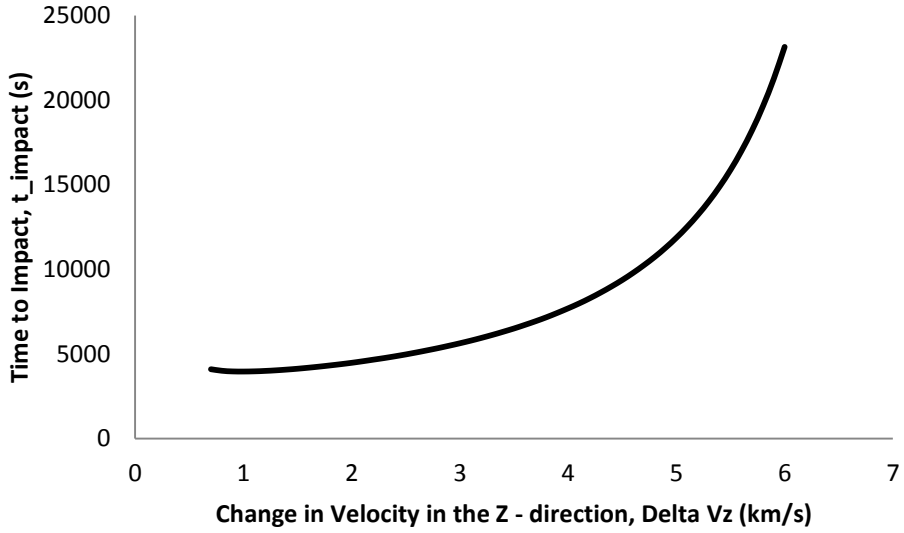

Figure 5.45 Time to Impact vs. $+\Delta V_{1z}$ for Case 2

The increase in the time to impact is caused by the lofted trajectory after the sub-satellite release. Figure 5.46 shows the lofted trajectory of the sub-satellite when an impulsive velocity change of three kilometers per second in the positive Z – direction is placed on the system.

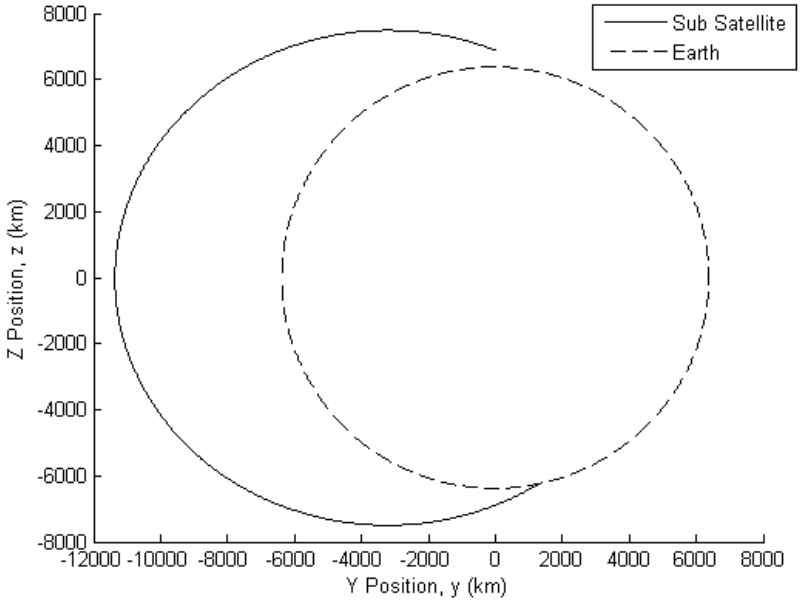

Figure 5.46 Lofted Trajectory at ΔV_{1z} = 1.0 km/s for Case 2

The ground range decreases because the impact point moves closer to the release point. The minimum impulsive velocity change in the positive Z – direction that was needed to cause an impact at a five hundred kilometer altitude and a tether length of four kilometers was 0.7 kilometers per second. The ground range and time to impact achieved during the minimum impulsive velocity change, a velocity change of 3.0 kilometers per second, and a velocity change of 6.0 kilometers per second are listed in table 5.14

Table 5.14 Maximum and Minimum Values as $+\Delta V_{1z}$ Increases for Case 3

Velocity Change (km/s)	Ground Range (km)	Time to Impact (s)
0.7	26743.1	4090
3	21344.7	5625
6	20690.8	23140

5.2.2 Impulsive Velocity Change of 1.5 km/s in the Negative Z – Direction

For an impulsive velocity change of 1.5 kilometers per second in the negative Z – direction an increase in the altitude leads to an increase in the range and time to impact; however, no impact trajectory is created at altitudes greater than thirteen hundred kilometers. A minimum impulsive velocity change of three kilometers per second in the negative Z – direction is required to have an impact at all altitudes that are tested. The increase in the range and time to impact as the altitude is increased for a velocity change of 1.5 kilometers per second our shown in figures 5.47 and 5.48.

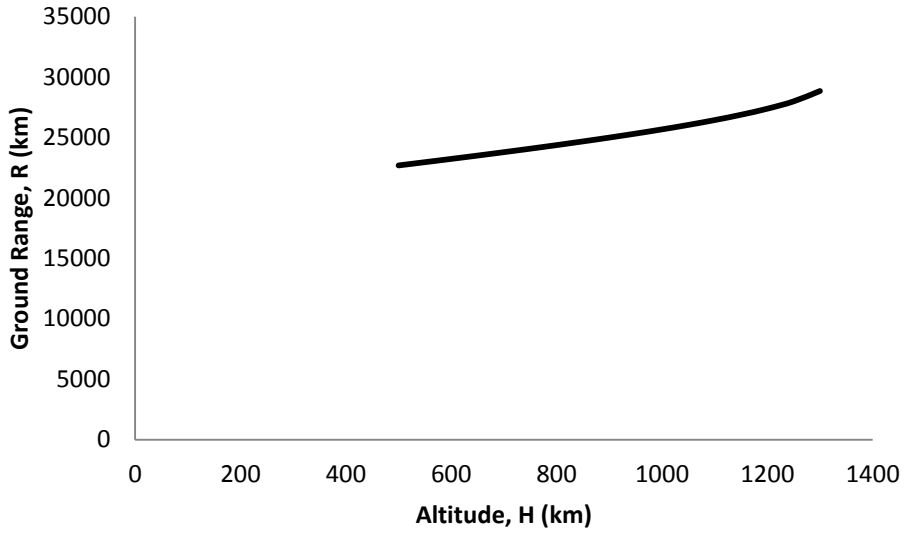

Figure 5.47 Ground Range vs. Altitude for ΔV_{1z} = -1.5 km/s in Case 2

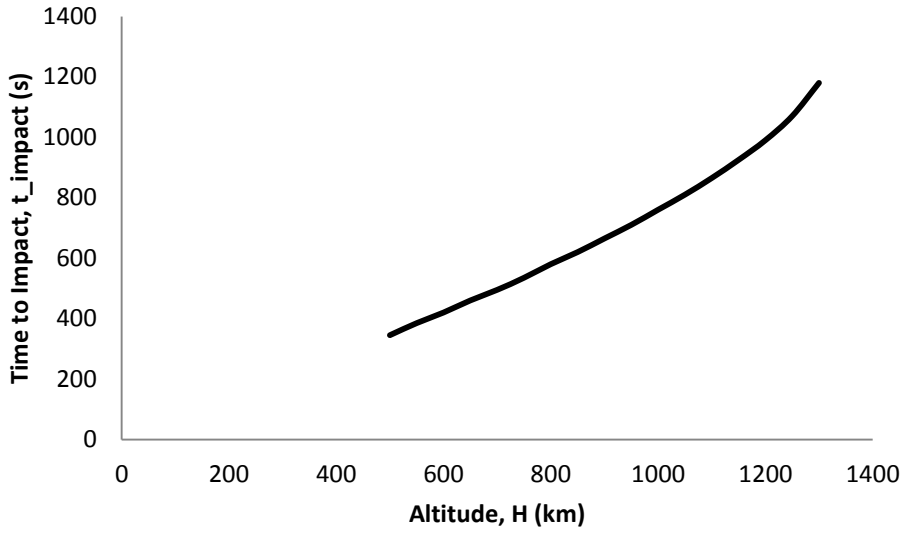

Figure 5.48 Time to Impact vs. Altitude for ΔV_{1z} = -1.5 km/s in Case 2

Since an impact trajectory does not occur at altitudes greater than thirteen hundred kilometers, the results for an impact trajectory at five hundred kilometers, one thousand kilometers, and thirteen hundred kilometers will be examined in more detail. A list of the ground range and time to impact achieved at these three altitude values are given in table 5.15.

Table 5.15 Range and Impact Time for ΔV_{1z} = -1.5 km/s at Three Altitudes for Case 2

Altitude (km)	**Ground Range (km)**	**Time to Impact (s)**
500	22683.8	345
650	25665.0	760
800	28841.2	1180

The small time to impact is caused by the steep impact trajectory of the sub-satellite after release. The impact trajectories of the sub-satellite at the three different altitudes are shown in figures 5.49 to 5.51.

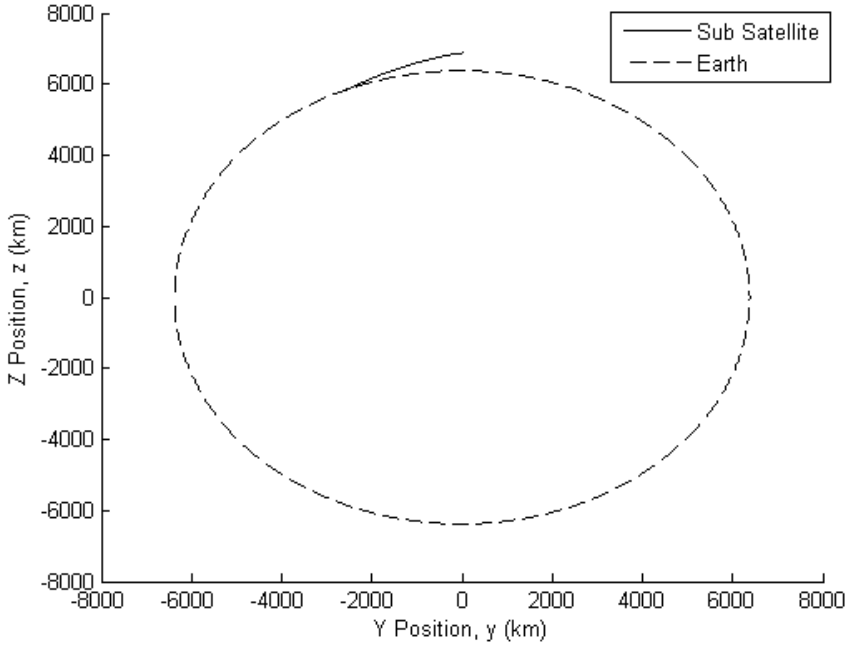

Figure 5.49 Trajectory at 500 km Altitude for ΔV_{1z} = -1.5 km/s in Case 2

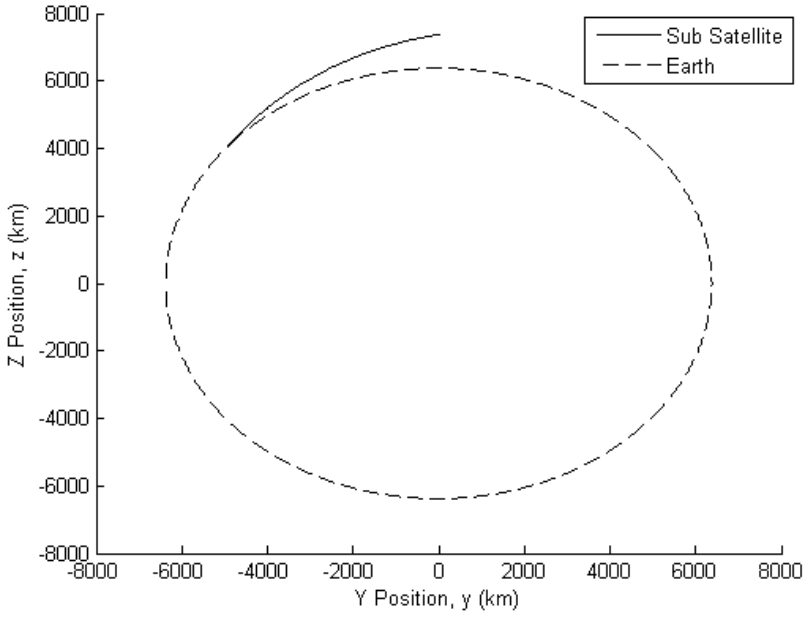

Figure 5.50 Trajectory at 1000 km Altitude for ΔV_{1z} = -1.5 km/s in Case 2

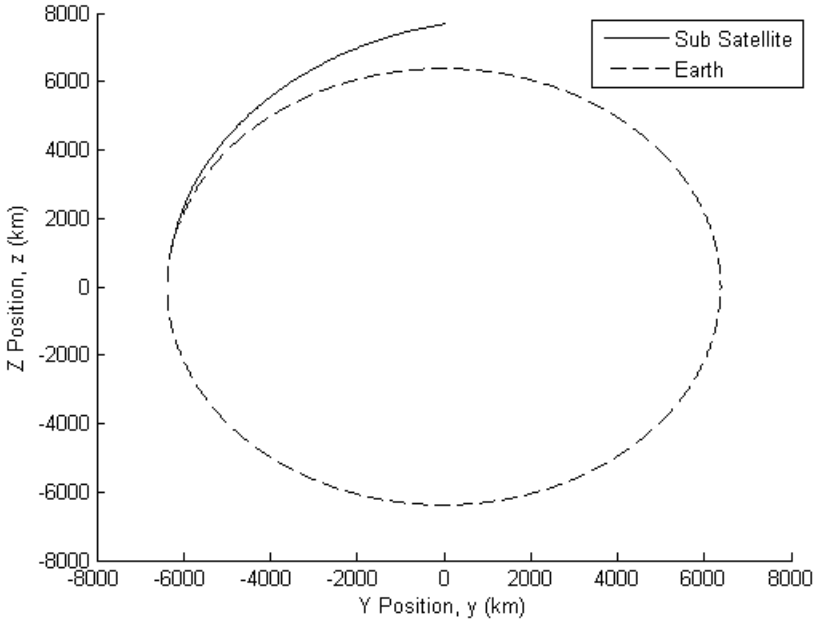

Figure 5.51 Trajectory at 1300 km Altitude for ΔV_{1z} = -1.5 km/s in Case 2

After inspecting the impact trajectory figures, it can be deduced that as the altitude increases the point of impact of the sub-satellite moves further along the surface of the Earth. This movement of the impact point results in an increase in the ground range. The increase of the time to impact is a direct result of the increase of the altitude of the TSS.

Even though an impact trajectory cannot be obtained for all altitudes, an impact trajectory can still be found for all the tested tether lengths. The trends for an impulsive velocity change of 1.5 kilometers per second in the negative Z – direction are shown in figures 5.52 and 5.53.

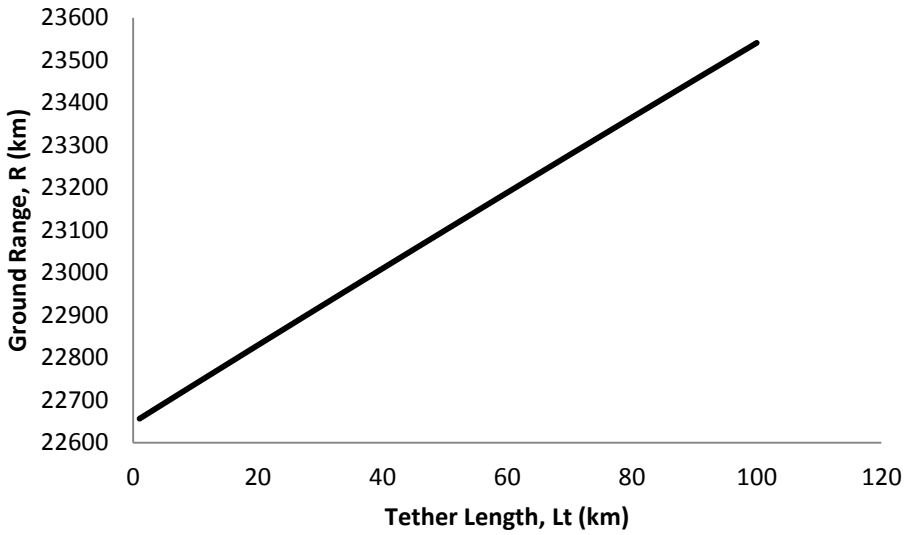

Figure 5.52 Ground Range vs. Tether Length for ΔV_{1z} = -1.5 km/s in Case 2

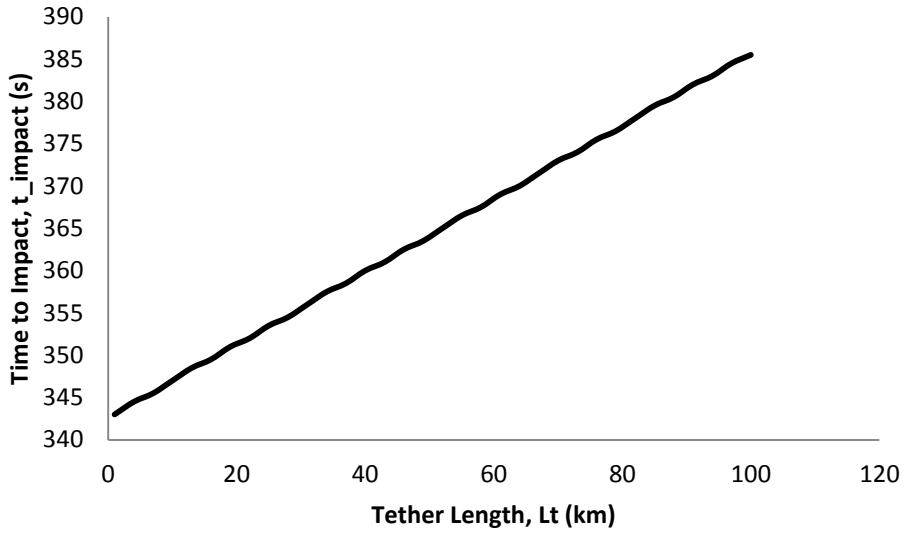

Figure 5.53 Time to Impact vs. Tether Length for ΔV_{1z} = -1.5 km/s in Case 2

Since the ground range and time to impact increase as the tether length increases, the maximum range and time to impact will result at the maximum tether length. The ground range, time to impact, and impact trajectories will be looked at in more detail for the same tether length values used in previous sections.

Table 5.16 Range and Impact Time for ΔV_{1z} = -1.5 km/s at Three Tether Lengths for Case 2

Tether Length (km)	Ground Range (km)	Time to Impact (s)
4	22683.8	344.5
55	23144.0	366.5
100	23540.6	385.5

The cause behind the increase in ground range and time to impact as the tether length increases can be found by examining the impact trajectories at each tether length. The impact trajectory for the four kilometer tether length and five hundred kilometer case is shown in figure 5.49. The other two impact trajectories also have an altitude of five hundred kilometers. The impact trajectories for these other two tether length values are shown below.

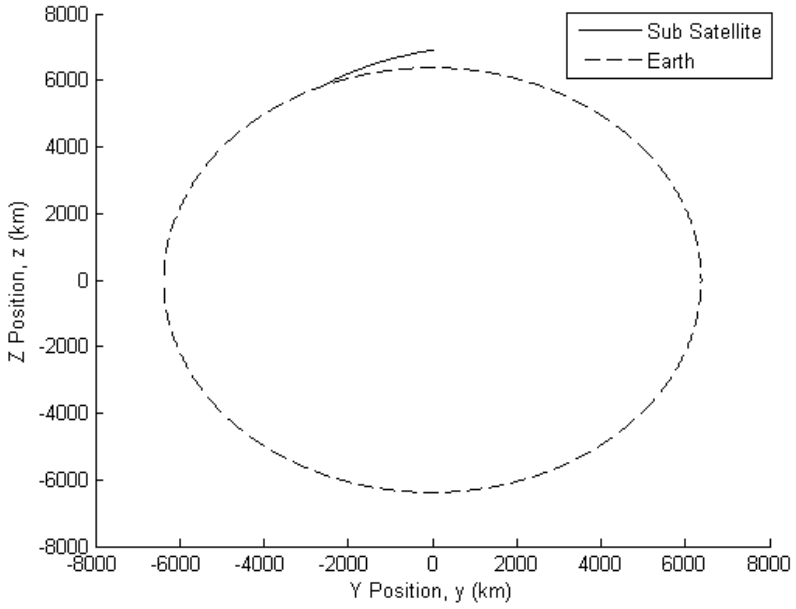

Figure 5.54 Trajectory at 55 km Tether Length for ΔV_{1z} = -1.5 km/s in Case 2

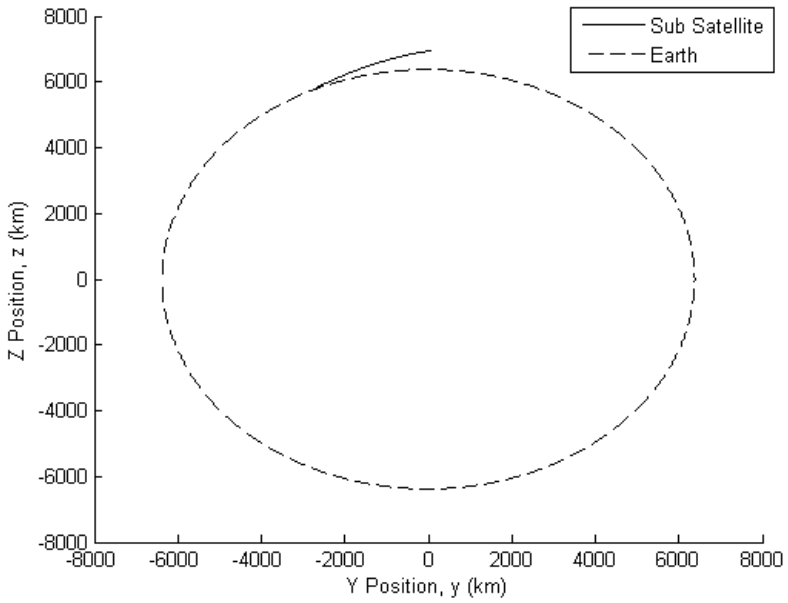

Figure 5.55 Trajectory at 100 km Tether Length for ΔV_{1z} = -1.5 km/s in Case 2

The increase in range is caused by the movement of the impact point further along the Earth's surface, while the time to impact is increased because the orbit is at a higher position. As the position or height of the orbit increases so will the time to impact.

The final change that is looked at in this section is an increase in the impulsive velocity change. The altitude and tether length are kept constant at five hundred kilometers and four kilometers, respectively. As the magnitude of the impulsive velocity change is increased in the negative Z – direction, the ground range and time to impact decrease. The decrease in the ground range and the time to impact can be seen in figures 5.56 through 5.57.

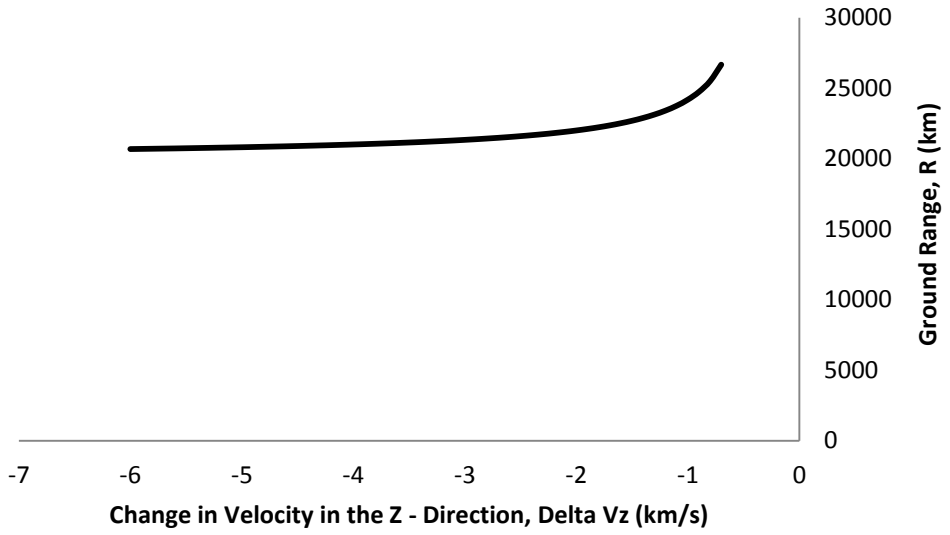

Figure 5.56 Ground Range vs. $-\Delta V_{1z}$ for Case 2

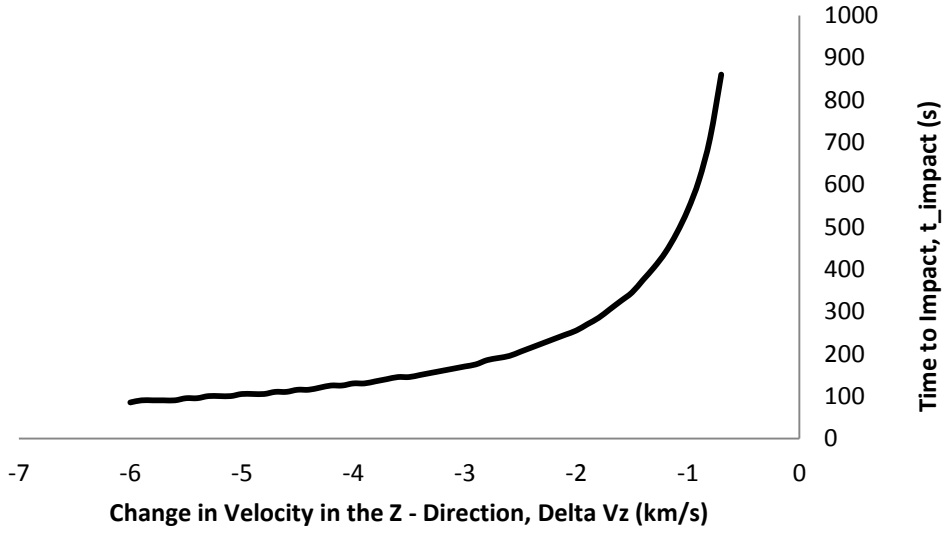

Figure 5.57 Time to Impact vs. $-\Delta V_{1z}$ for Case 2

The decrease in the ground range and the time to impact follows the trends displayed in the previous sections for different release points and impulsive velocity changes. In order to create an impact trajectory at this configuration a minimum impulsive velocity change value of

0.7 kilometers per second in the negative Z – direction is needed. Table 5.17 list values for the ground range and time to impact for three impulsive velocity changes.

Table 5.17 Maximum and Minimum Values as $-\Delta V_{1z}$ Increases for Case 2

Velocity Change (km/s)	Ground Range (km)	Time to Impact (s)
-0.7	26663.4	860
-3	21329.7	170
-6	20677.2	85

5.2.3 Impulsive Velocity Change of 1.0 km/s in the Positive Y – Direction

The ground range and time to impact increase as the altitude is increased and the tether length is kept constant at four kilometers with an impulsive velocity change of one kilometer per second in the positive Y – direction. The results for the ground range and time to impact as the altitude increases are shown below.

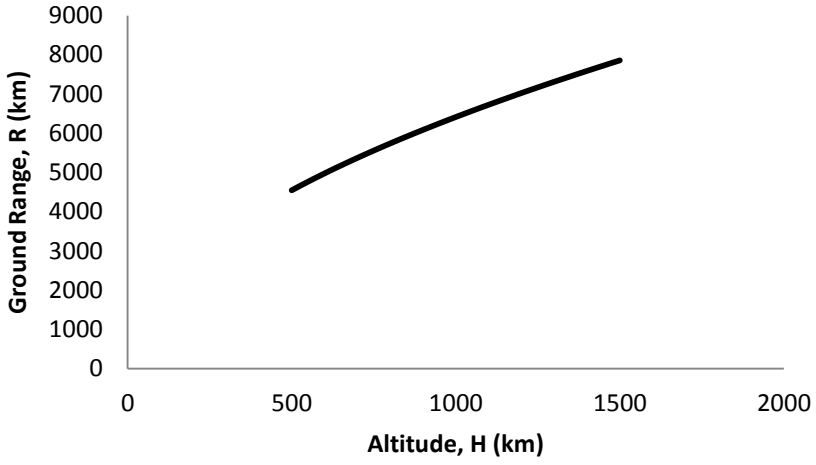

Figure 5.58 Ground Range vs. Altitude for ΔV_{1y} = 1.0 km/s in Case 2

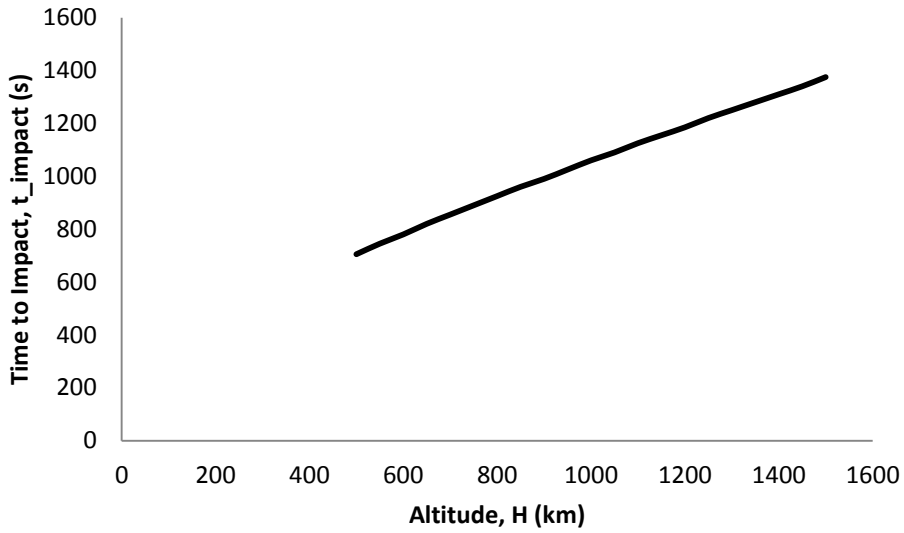

Figure 5.59 Time to Impact vs. Altitude for ΔV_{1y} = 1.0 km/s in Case 2

Altitudes of five hundred kilometers, one thousand kilometers, and fifteen hundred kilometers are examined in more detail. The values for the ground range and time to impact at these altitudes are listed in table 5.18.

Table 5.18: Range and Impact Time for ΔV_{1y} = 1.0 km/s at Three Altitudes for Case 2

Altitude (km)	**Ground Range (km)**	**Time to Impact (s)**
500	4544.8	705
1000	6412.0	1060
1500	7856.0	1375

The range and time to impact achieved with this impulsive velocity change are less than the ground range and time to impact calculated for different altitudes for the other two impulsive velocity changes. This is a result of the type of impact trajectory that is created after the velocity change is put into place and the sub-satellite is released from the TSS. The impact trajectory of the sub-satellite at each altitude is shown on the next two pages.

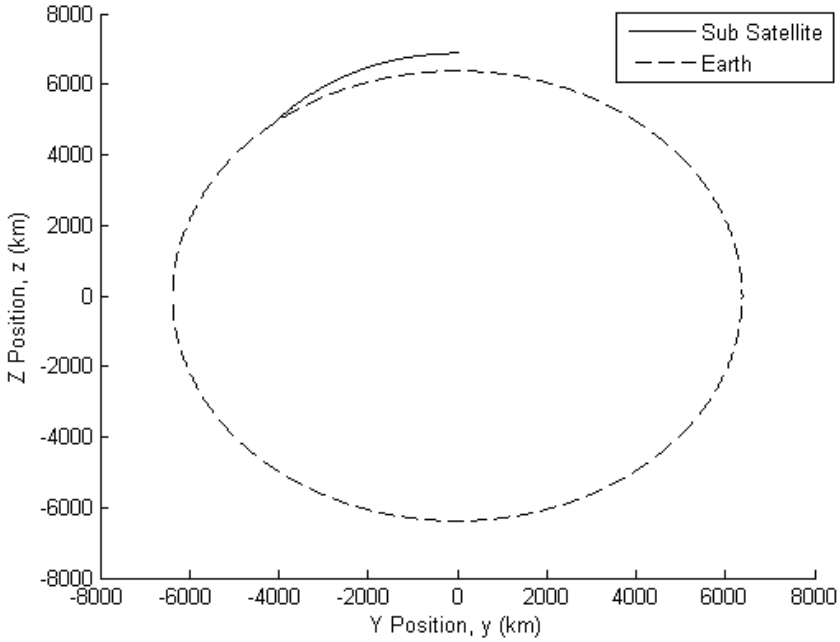

Figure 5.60 Trajectory at 500 km Altitude for ΔV_{1y} = 1.0 km/s in Case 2

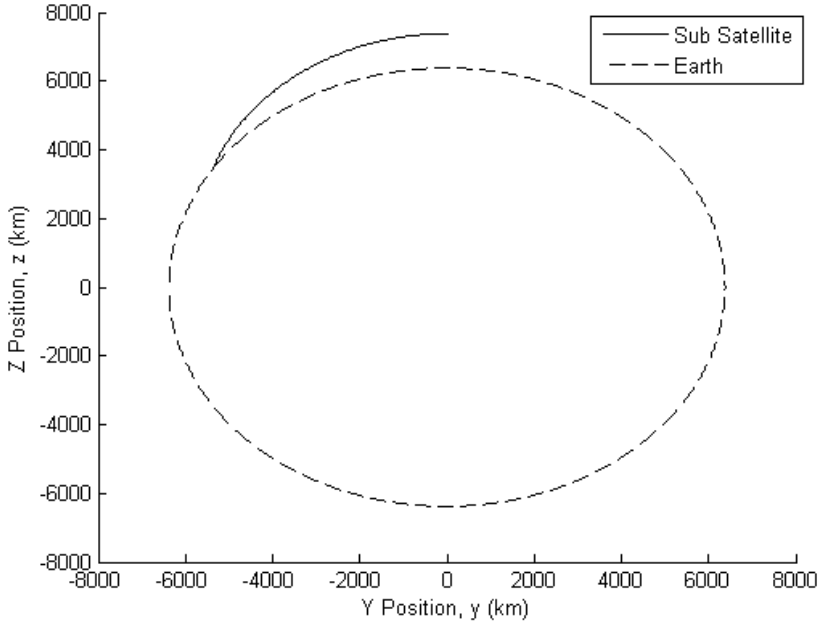

Figure 5.61 Trajectory at 1000 km Altitude for ΔV_{1y} = 1.0 km/s in Case 2

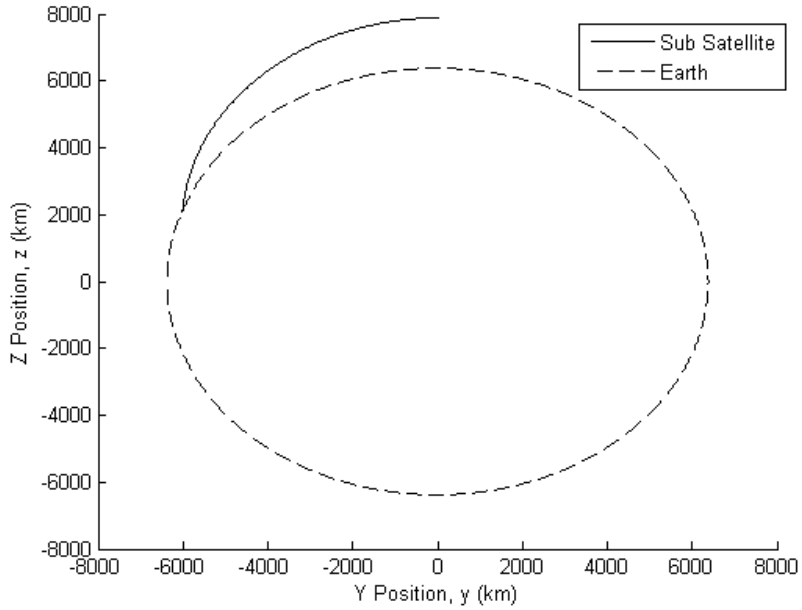

Figure 5.62 Trajectory at 1500 km Altitude for ΔV_{1y} = 1.0 km/s in Case 2

From the impact trajectories depicted in figure 5.60 through 5.62, it can be concluded that the ground range increases because as the altitude increases the release point occurs earlier in the TSS orbit and the impact point occurs further on the surface of the Earth. The increase in the time to impact happens because the impact trajectory is placed on a higher orbit that requires more time to travel around in order to get to the impact point.

An increase in the tether length of the TSS affects the ground range and time to impact of the impact trajectory after the sub-satellite is released from the system. For a constant impulsive velocity change of one kilometer per second in the positive Y – direction, an increase in tether length leads to an increase in the ground range and time to impact.

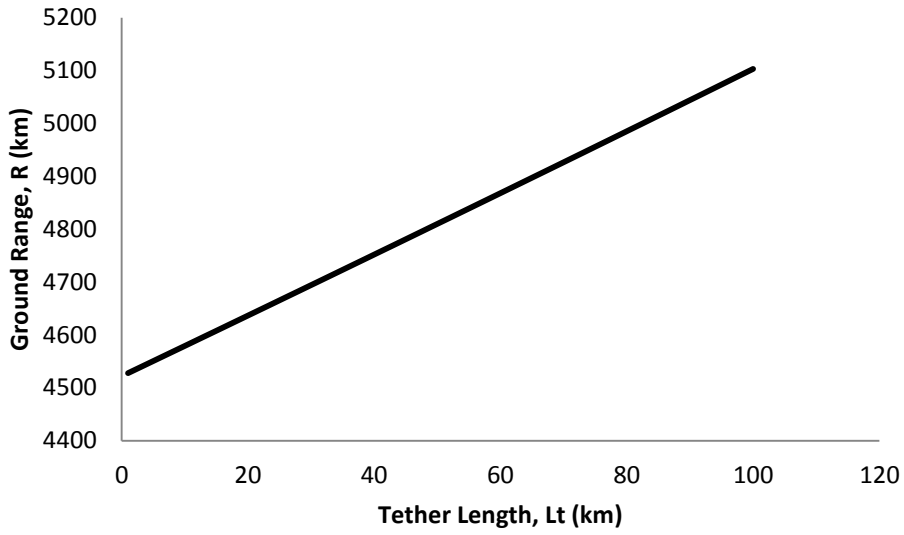

Figure 5.63 Ground Range vs. Tether Length for ΔV_{1y} = 1.0 km/s in Case 2

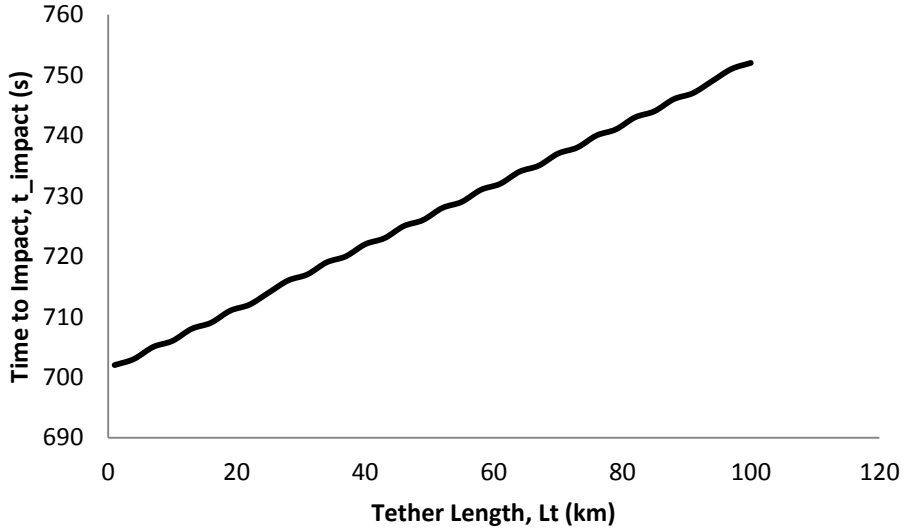

Figure 5.64 Time to Impact vs. Tether Length for ΔV_{1y} = 1.0 km/s in Case 2

The list of the ground range and the time to impact at three tether lengths are listed in table 5.19 on the next page.

Table 5.19 Range and Impact Time for ΔV_{1y} = 1.0 km/s at Three Tether Lengths for Case 2

Tether Length (km)	Ground Range (km)	Time to Impact (s)
4	4544.8	703
55	4839.0	729
100	5103.0	752

The ground range and time to impact are increased because an increase in the tether length causes the sub-satellite to be in a slightly higher orbit, which in turn causes the impact trajectory to start from a higher point and move the impact point further along the Earth's surface. In order to see if this is true the impact trajectories must be examined. The impact trajectory of the sub-satellite at a four kilometer tether length is shown in figure 5.60. The impact trajectories for the other two tether lengths are shown below. As the tether length increases the height in the impact trajectories are increased. This increase is what results in the increase in the time to impact shown in table 5.37. The plot of the impact trajectories also show that the impact point of the sub-satellite travels forward along the surface of the Earth. The movement of the impact point is not significantly large; therefore, a small increase in the ground range results from the increase of the tether length.

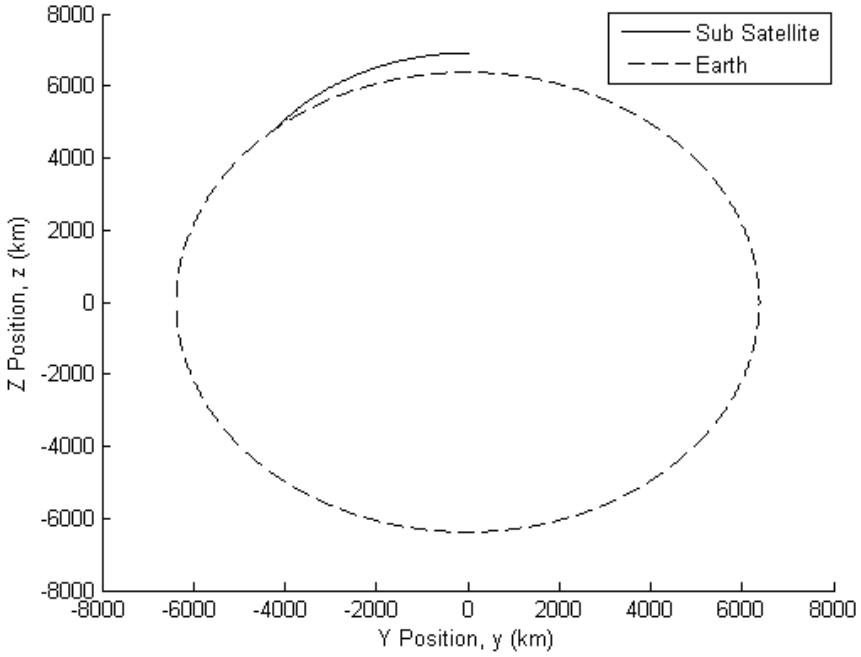

Figure 5.65 Trajectory at 55 km Tether Length for ΔV_{1y} = 1.0 km/s in Case 2

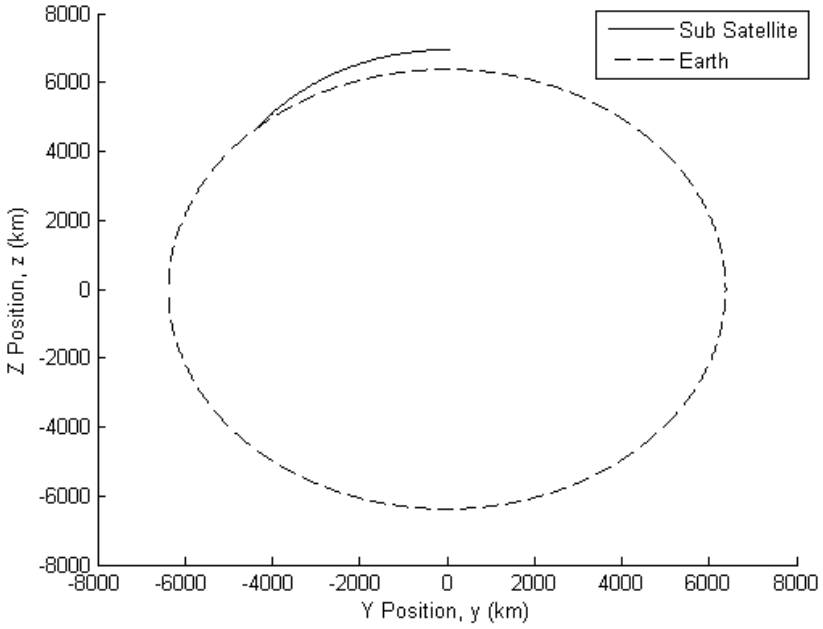

Figure 5.66 Trajectory at 100 km Tether Length for ΔV_{1y} = 1.0 km/s in Case 2

An increase of the magnitude of the impulsive velocity change in the positive Y – direction will also lead to a change in the ground range and time to impact. The increase in the impulsive velocity change results in a decrease of the ground range and the time to impact. This happens because the impact trajectory of the sub-satellite after release decreases in size as the impulsive velocity change increases; therefore, the sub-satellite will impact the Earth sooner at higher impulsive velocity changes. The effect of the impulsive velocity change on the ground range and time to impact values are shown in figures 5.67 through figures 5.68.

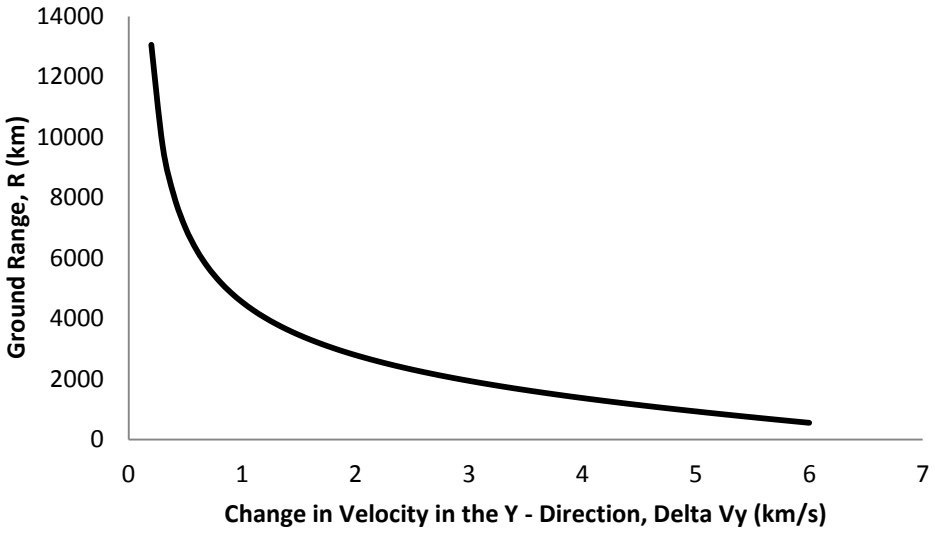

Figure 5.67 Ground Range vs. $+\Delta V_{1y}$ for Case 2

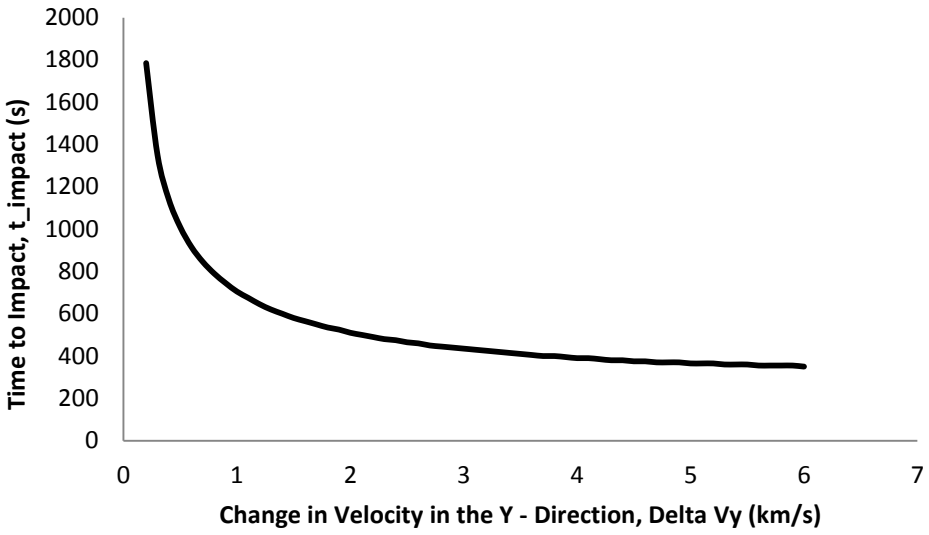

Figure 5.68 Time to Impact vs. $+\Delta V_{1y}$ for Case 2

The minimum impulsive velocity change in the positive Y – direction that is needed to create an impact trajectory for the second configuration is 0.2 kilometers per second. Note that this is the minimum impulsive velocity change needed when the altitude of the main satellite is five hundred kilometers and the tether length is kept at four kilometers. A maximum impulsive velocity change of six kilometers per second in the positive Y – direction is place on the system; therefore, the minimum time to impact and the minimum ground range will occur at this maximum impulsive velocity change. Values of the ground range and time to impact are listed in the table below.

Table 5.20: Maximum and Minimum Values at $+\Delta V_{1y}$ Increases for Case 2

Velocity Change (km/s)	**Ground Range (km)**	**Time to Impact (s)**
0.2	13058.2	1785
3	1938.1	435
6	549.4	350

5.2.4 Comparison between Velocity Changes For Second Configuration

The impulsive velocity changes that are placed on the sub-satellite result in different values for the ground range and the time to impact. For the second configuration an impulsive velocity change placed in the positive Z – direction will result in the maximum ground range and time to impact for the sub-satellite. These values for ground range and time to impact can be further increased by increasing the altitude and the tether length; however, a larger impulsive velocity change in the positive Z – direction will be needed to cause an impact trajectory at altitudes above eight hundred and fifty kilometers. For the case of an impulsive velocity change in the positive Z – direction, the tether length can be increased in order to increase the ground range without needing an increase in the magnitude of the impulsive velocity change. In order to save on fuel, the increase in tether length is the better way to achieve a longer ground range for this impulsive velocity change direction.

An impulsive velocity change in the positive Y – direction results in the minimum ground range and time to impact for the second configuration. The ground ranges achieved with this impulsive velocity change can be increased by placing the TSS in a higher altitude or by increases the tether length. The increase in altitude leads to a larger increase for the ground range, while the increase in tether length has a smaller effect on the ground range and time to impact. In this case, the method used to increase the ground range depends upon how big of an increase is needed in order to reach the desired impact point.

As at any release point, the magnitude of the impulsive velocity change can be increased in order to achieve a lower ground range. The time to impact will also decrease with the ground range when the impulsive velocity change is in the negative Z – direction or the positive Y – direction. When an impulsive velocity change is placed in the positive Z – direction, the time to

impact will increase because the sub-satellite is lofted into a higher orbit upon release. In other words, one has to consider the tradeoff of an increase in the time to impact in order to achieve a shorter ground range. Overall, impact trajectories will result at these impulsive velocity changes for the second configuration; however, which impulsive velocity change to be used depends upon if a maximum or minimum ground range is desired.

5.3 Comparison between the Analytical Results and the Simulation Results

In order to compare the analytical approach and the simulation results the algorithm to find the ground range and time to impact for the analytical calculation is used. The first configuration from the simulation is compared to case B from the analytical solution because both have the sub-satellite below the main satellite. Case A from the analytical solution is then compared to the second configuration from the simulation because both have the sub-satellite located above the main satellite. For each comparison an impulsive velocity change of one kilometer per second and six kilometers per second in the positive Y – direction will be placed on the sub-satellite.

The first comparison will be done using the first release configuration. The impulsive velocity change that is used for the simulation and the analytical calculations is one kilometer per second in the positive Y – direction. The ground range and time to impact calculated by the simulation and the analytical approach are listed in table 5.21.

Table 5.21: Results for Configuration 1 and Case B with ΔV_{1y} = 1.0 km/s

	Ground Range (km)	Time to Impact (s)
Simulation	4.5057232E+03	700
Analytical	4.4980330E+03	696.98

The percent error and the difference between the simulation value and the analytical value for the ground range and time to impact are calculated and listed below.

Table 5.22 Comparison of Results for Configuration 1 and Case B with ΔV_{1y} = 1.0 km/s

	Ground Range (km)	Time to Impact (s)
% Error	0.17068	0.43108
Difference	7.69028	3.01755

The percent error between the two ground ranges is less than one percent and the actual difference is about 7.7 kilometers. The percent error for the time to impact is also less than one percent but the actual difference between the two times is about 3.02 seconds with the time to impact from the simulation being the greater value.

The next comparison will be done at the second configuration with an impulsive velocity change of 6.0 kilometers per second in the positive Y – direction. The calculated values for the ground range and time to impact for both methods are listed below.

Table 5.23: Results for Configuration 1 and Case B with ΔV_{1y} = 6.0 km/s

	Ground Range (km)	Time to Impact (s)
Simulation	5.4562965E+02	350
Analytical	5.4529027E+02	346.72

The percent error and the direct difference between the ground ranges and times to impact are given in table 5.24 on the next page.

Table 5.24 Comparison of Results for Configuration 1 and Case B with ΔV_{1y} = 6.0 km/s

	Ground Range (km)	Time to Impact (s)
% Error	0.062201	0.936190
Difference	0.339384	3.276665

The percent error for the ground range and the time to impact are less than one. The difference between the ground ranges is 0.34 kilometers and the difference between the times is about 3.28 seconds. So far the analytical solution is giving similar results to those from the simulation.

The third comparison is done with the second configuration and an impulsive velocity change placed on the sub-satellite of one kilometer per second in the positive Y – direction. The simulation results and the analytical approach results are listed below in table 5.25.

Table 5.25: Results for Configuration 2 and Case A with ΔV_{1y} = 1.0 km/s

	Ground Range (km)	Time to Impact (s)
Simulation	4.5448026E+03	705
Analytical	4.5458193E+03	704.69

The analytical result for the ground range is greater than the ground range obtained from the simulation results. The time to impact calculated during the simulation is greater than the time to impact calculated by the analytical approach. The actual difference between the simulation values and the analytical values and the percent error are listed below.

Table 5.26: Comparison of Results for Configuration 2 and Case A with ΔV_{1y} = 1.0 km/s

	Ground Range (km)	Time to Impact (s)
% Error	0.02237	0.04446
Difference	1.01666	0.31343

The percent errors between the ground ranges and the times to impact are less than one percent. This is the same trend that has been seen in the past two comparisons. The difference between the ground range determined by the simulation and the ground range calculated using the analytical approach is about one kilometer. The difference between the times to impact is about 0.313 seconds.

The final comparison will be done with the second configuration and an impulsive velocity change of 6.0 kilometers per second in the positive Y – direction.

Table 5.27: Results for Configuration 2 and Case A with ΔV_{1y} = 6.0 km/s

	Ground Range (km)	Time to Impact (s)
Simulation	5.4939447E+02	350
Analytical	5.4986409E+02	349.86

The ground range calculated by the analytical approach is slightly larger than the ground range calculated by the simulation. The percent error and the actual difference between the two values are presented in table 5.28.

Table 5.28: Comparison of Results for Configuration 2 and Case A with ΔV_{1y} = 6.0 km/s

	Ground Range (km)	Time to Impact (s)
% Error	0.08548	0.04084
Difference	0.46964	0.14295

The percent error between the two ground ranges and the percent error between the two times to impact is less than one percent. The difference between the two ground ranges was about 0.45 kilometers. The time to impact calculated by the simulation is greater than the time to impact that was calculated using the simulation approach by almost 0.14 seconds.

More comparisons are not shown in this write up because the results have a percent error of less than one percent. The maximum difference between the times was found to be about 3.3 seconds, while the maximum difference for the ground ranges was 7.7 kilometers. The errors between the simulation and the analytical approach are caused by the rotation angle that is introduced into the simulation in order to keep the sub-satellite in a leading position. Overall the analytical approach provides a good estimate of what the time to impact and ground range will be after the sub-satellite release. A simulation should still be run in order to determine the impact trajectory after the sub-satellite is released and to place the impulsive velocity change in different directions on the sub-satellite.

Chapter 6: Conclusions and Future Work

The altitude, tether length, and the impulsive velocity change have been varied to determine the type of ground range and time to impact that can be achieved. The effects of the altitude, tether length, and impulsive velocity change on the ground range and time to impact were investigated using a numerical simulation approach and an analytical approach. The increase in altitude caused the ground range and time to impact to increase for all configurations and impulsive velocity changes. If the sub-satellite is located below the main satellite, an increase in tether length will cause the ground range and time to impact to decrease; however, if the sub-satellite is located above the main satellite, an increase in the tether length will result in an increase in the ground range and time to impact. An increase in the impulsive velocity change on the sub-satellite will always cause the ground range and the time to impact to decrease; however, there are a few occasions where the time to impact will increase because of the lofted impact trajectory. The changes in altitude and tether length are the better methods to increase or decrease the ground range and time to impact because an increase in an impulsive velocity change will result in a greater fuel usage. The analytical solutions were found to follow these exact same trends for a sub-satellite located above or below the main satellite. For the cases when a sub-satellite had the same altitude as the main satellite, the increase in altitude resulted in an increase in the ground range and time to impact, while an increase in the tether length resulted in an increase to the ground range and a decrease to the time to impact.

The final part of this research was to compare the analytical solution to the numerical simulation by comparing the ground range and the time to impact. The percent error between the ground ranges and times to impact for the analytical solution and the numerical solution was found to always be less than one percent. The percent errors and differences between the two approaches are caused by the fact that a rotation angle was introduced into the simulation in order to model the fact that the sub-satellite is leading the main satellite. The analytical approach can be used to provide an initial estimate of the ground range and time to impact; however, the numerical simulation should be used in order to track the trajectory of the sub-satellite before and after its release from the TSS.

In order to improve the ground range and time to impact calculated in the numerical simulation a more detailed model of the TSS should be put into place for future research. The effect of the Earth's oblateness and the aerodynamic drag on the satellites can be added to the simulation. The aerodynamic drag will impact the movement of the sub-satellite as it gets closer to the Earth's surface. The inclusion of the gravitational gradient in the model will keep the TSS in a natural orbital motion where the sub-satellite will remain in a lower orbit than the main satellite at all times. By adding the above three conditions to the model that is being used in the numerical simulation, the movement of the TSS will be model more accurately and the simulation will provide a more accurate result for the position of the sub-satellite at release. If the effects of the Earth's oblateness and the effects of the aerodynamic drag are placed on the sub-satellite after release, a more accurate model for the movement of the sub-satellite after release will be in place and more precise ground ranges and times to impact can be calculated.

References

1. Bate, Roger R., Mueller, Donald D., White, Jerry E., Fundamentals of Astrodynamics, Dover Publications, Inc., New York, 1971.

2. Beda, Peter B., "Anticipatory Computing in the Attitude Control of Satellites," Paper American Institute of Physics 0-7354-0012-1. 2001.

3. Beletsky, V. V., and Levin, E.V., *Advances in the Astronautical Sciences: Dynamics of Space Tether Systems*, Vol. 83, AAs, Sand Diego, CA, 1993, p. 7 – 9.

4. Chang, Insu, Park, Sang-Young, and Choi, Kyu-Hong, "Nonlinear Attitude Control of a Tether-Connected Multi-Satellite in Three-Dimensional Space," Paper IEEE Transactions on Aerospace and Electronic Systems, Vol. 46, No. 4, 2010.

5. Cho, Sungki, "Analysis of the Orbital Motion of a General Tethered Satellite System," Ph.D. Dissertation, Dept. of Aerospace Engineering, Auburn University, Auburn, AL, June 1999, p. 1 – 3, p. 10 – 23.

6. Cho, S., Cochran, Jr., J. E., and Cicci, D. A., "Identification and Orbit Determination of Tethered Satellite Systems."*Applied Mathematics and Computation*, Vol. 117, pp. 301 – 312, 2001.

7. Choe, Nammi J., "Detection and Orbit Determination of Tethered Satellite Systems," Ph.D. Dissertation, Dept. of Aerospace Engineering, Auburn University, Auburn, Al, August 2003, p. 1 – 8, p. 20 – 24.

8. Cicci, D. A., Qualls, C., and Lovell, T. A., "A look at Tethered Satellite Identification Using Ridge – Type Estimation Methods," *Applied Mathematics and Computation*, Vol. 119 pp. 297 – 316, 2001.

9. Cicci, D. A., Cochran, Jr., J. E., Qualls, C., and Lovell, T. A.,"Quick - Look Identification and Orbit Determination of a Tethered Satellite,"*The Journal of Astronautiacl Sciences*, Vol. 50, No. 3, pp. 339 – 353, July – September 2002.

10. Curtis, Howard D., Orbital Mechanics for Engineering Students, Elsevier, New York, 2005.

11. Ellis, Joshua R., and Hall, Christopher D. "Out-of-plane Librations of Spinning Tethered Satellite Systems,"*Celestial Mechanics and Dynamical Astronomy*, Vol. 106, No. 1, p. 39 – 67, 2009.

12. Ginsberg, Jerry, Engineering Dynamics, Cambridge University Press, New York, New York, 2008.

13. Hoots, F. R., Roehrich, R. L., and Szebehely, V. G., "Space Shuttle Tethered Satellite Analysis," Technical Report #83 – 5, Directorate of Astrodynamics, Peterson Air Force Base, CO, August 1983.

14. Hughes, Peter C., Spacecraft Attitude Dynamics, Dover Publications, Inc., Mineola, New York, 1984.

15. Ishimura, Kosei, and Higuchi, Ken, "Coupling among Pitch Motion, Axial Vibration, and Orbital Motion of Large Space Structures," *Journal of Aerospace Engineering*, Vol. 21, No. 2, April 1, 2008.

16. Kaplan, M. H., Modern Spacecraft Dynamics and Control. Ed. 1st, Wiley, John and Sons Incorporated, New Jersey, 1976, pp. 199.

17. Kulakowski, Bohdan T., Gardner, J. F., Shearer, J. L., Dynamic Modeling and Control of Engineering Systems, Cambridge University Press, New York, 2007. pg. 126 – 129.

18. Lovell, Thomas A., "State Estimation of Tethered Satellites Using Conventional and Intelligent Systems-Based Paradigms," Ph.D. Dissertation, Dept. of Aerospace Engineering, Auburn University, Auburn, AL, December 2001, p. 1 – 7, p. 16 – 38.

19. Lovell, T. A., Cho, S., Cochran, Jr., J. E., and Cicci, D. A., "A Study of the Re-Entry Orbit Discrepancy Involving Tethered Satellites," *Acta Astronautica*, Vol. 53, Issue 1, pp. 21 – 33, 2003.

20. Meriam, J. L., and Kraige, L. G., Engineering Mechanics: Dynamics, 6th Ed., John Wiley and Sons, Inc., New Jersey, 2007.

21. Misra, A.K., "Dynamics and Control of Tethered Satellite Systems," *Acta Astronautica*, Vol. 63, pp. 1169 – 1177, 2008.

22. Modi, V. J., Gilardi, G., Misra, A.K., "Attitude Control of Space Platform Based Tethered Satellite Systems."*Journal of Aerospace Engineering*, Vol. 11, No. 2, pp. 24 – 31, 1998.

23. Naigang, Cui, Dun, Liu, Yuhua, Liu, and Naiming Qi, "The Calculation of the Orbital Elements of a Tethered Satellite System after Release," Paper AIAA 94-3746-CP, 1994.

24. Qualls, C. and Cicci, D. A, "Preliminary Orbit Determination of a Tethered Satellite," *Applied Mathematics and Computation*, Vol. 188, pp. 462 – 471, 2007.

25. Rossi, E. V., Cicci, D. A., and Cochran Jr., J. E., "Existence of Periodic Motions of a Tether Trailing Satellite,"*Applied mathematics and Computation*. Vol. 155, pp. 269 – 281, 2004.

26. Schutte, Aaron D., and Dooley, Brian A., "Constrained Motion of Tethered Satellites," *Journal of Aerospace Engineering*, Vol. 18, No. 4, October 2005.

27. Space Dynamics Laboratory, "ProSEDS," Space Dynamics Laboratory Webpage, http://www.sdl.usu.edu/programs/proseds

28. Stanley, Curtis H., "Apparent Impacting Trajectories, Identification, and Orbit Determination of Tethered Satellite Systems," Master's Thesis, University of Colorado, Colorado Springs, CO, 2010.

29. Wen, Hao, Jin, Dongping P., and Hu, Haiyan Y., "Advances in Dynamics and Control of Tethered Satellite Systems,"*Acta Mechanica Sinica*, Vol. 24, p. 229 – 241, 2008.

Appendix A: Sample Results from Numerical Integration

Table A.1: Simulation Results as Altitude Increases for Case 1 at ΔV_{1y} = 1.0 km/s

Altitude (km)	**Time to Impact (s)**	**Ground Range (km)**
500	700	4505.723
550	740	4726.313
600	775	4937.022
650	815	5139.085
700	850	5333.504
750	885	5521.106
800	920	5702.580
850	955	5878.512
900	990	6049.402
950	1020	6215.682
1000	1055	6377.728
1050	1085	6535.871
1100	1120	6690.403
1150	1150	6841.584
1200	1180	6989.646
1250	1215	7134.797
1300	1245	7277.226
1350	1275	7417.105
1400	1305	7554.589
1450	1340	7689.820
1500	1370	7822.930

Table A.2: Simulation Results as Tether Length Increases for Case 1 at ΔV_{1y} = 1.0 km/s

Tether Length (km)	Time to Impact (s)	Ground Range (km)
1	701	4517.880
4	699	4505.723
7	697	4493.558
10	695	4481.383
13	693	4469.199
16	691	4457.006
19	689	4444.803
22	687	4432.590
25	685	4420.367
28	683	4408.133
31	681	4395.889
34	679	4383.634
37	677	4371.369
40	675	4359.092
43	673	4346.803
46	671	4334.502
49	669	4322.190
52	667	4309.865
55	665	4297.528
58	663	4285.178
61	661	4272.815
64	659	4260.439
67	657	4248.049
70	655	4235.645
73	653	4223.227
76	651	4210.795
79	649	4198.348
82	647	4185.886
85	645	4173.409
88	643	4160.917
91	641	4148.408
94	639	4135.884
97	637	4123.343
100	635	4110.786

Table A.3: Simulation Results as $+\Delta V_{1y}$ Increases for Case 1

Velocity Change (km/s)	**Time to Impact (s)**	**Ground Range (km)**
0		
0.1		
0.2	1755	12746.853
0.3	1335	9553.004
0.4	1130	7953.634
0.5	1000	6929.881
0.6	905	6197.195
0.7	840	5636.828
0.8	785	5188.739
0.9	740	4818.745
1	700	4505.723
1.1	670	4235.805
1.2	640	3999.452
1.3	620	3789.851
1.4	595	3601.989
1.5	580	3432.081
1.6	560	3277.210
1.7	545	3135.081
1.8	530	3003.864
1.9	520	2882.078
2	510	2768.509
2.1	500	2662.151
2.2	490	2562.160
2.3	480	2467.828
2.4	470	2378.548
2.5	465	2293.802
2.6	455	2213.141
2.7	450	2136.178
2.8	440	2062.572
2.9	435	1992.024
3	430	1924.271

Appendix B: Sample Results from Analytical Solutions

Table B.1: Analytical Results as Altitude Increases for Case A When R = 1500 km and θ_{imp} = 240°

Altitude (km)	**Velocity Change in the Y (km/s)**	**Angular Velocity (rads/s)**
500	0.60484	-0.16633
600	0.62511	-0.17191
700	0.62185	-0.17101
800	0.59824	-0.16452
900	0.55718	-0.15322
1000	0.50120	-0.13783
1100	0.43258	-0.11896
1200	0.35332	-0.09716
1300	0.26517	-0.07292
1400	0.16966	-0.04666
1500	0.06812	-0.01873

Table B.2: Analytical Results as Tether Length Increases for Case A When R = 1500 km and $\theta_{imp} = 240°$

Tether Length (km)	Velocity Change in the Y (km/s)	Angular Velocity (rads/s)
4	0.60484	-0.16633
14	0.61305	-0.04817
24	0.62098	-0.02846
34	0.62864	-0.02034
44	0.63602	-0.01590
54	0.64314	-0.01310
64	0.64999	-0.01117
74	0.65658	-0.00976
84	0.66292	-0.00868
94	0.66900	-0.00783
104	0.67483	-0.00714
114	0.68041	-0.00657

Table B.3: Analytical Results as ΔV_{1y} Increases for Case A When H = 500 km and L_t = 4 km

Velocity Change (km/s)	**Ground Range (km)**	**Time to Impact (s)**
0		
0.1		
0.2	13065.345	1793.531
0.3	9700.880	1355.315
0.4	8053.841	1142.390
0.5	7007.363	1008.651
0.6	6261.278	914.513
0.7	5692.005	843.645
0.8	5237.520	787.848
0.9	4862.674	742.480
1	4545.819	704.687
1.1	4272.780	672.600
1.2	4033.819	644.941
1.3	3821.997	620.798
1.4	3632.213	599.504
1.5	3460.618	580.556
1.6	3304.248	563.568
1.7	3160.775	548.237
1.8	3028.342	534.322
1.9	2905.447	521.628
2	2790.860	509.997
2.1	2683.561	499.298
2.2	2582.698	489.421
2.3	2487.551	480.274
2.4	2397.508	471.778
2.5	2312.045	463.867
2.6	2230.707	456.484
2.7	2153.102	449.579
2.8	2078.887	443.108
2.9	2007.758	437.034
3	1939.451	431.323